A FREQUENCY DOMAIN BASED TECHNIQUE FOR CONDITION MONITORING OF STRUCTURES USING LIMITED RANDOMLY MEASURED DYNAMIC RESPONSES

THESIS SUBMITTED FOR THE FULFILMENT OF
DOCTOR OF PHILOSOPHY DEGREE IN ENGINEERING

BY

JAFAR SADAK ALI

DEPARTMENT OF CONSTRUCTION ENGINEERING
FACULTY OF ENGINEERING AND TECHNOLOGY
JADAVPUR UNIVERSITY
KOLKATA
INDIA

2019

DEPARTMENT OF CONSTRUCTION ENGINEERING
FACULTY OF ENGINEERING AND TECHNOLOGY
JADAVPUR UNIVERSITY
KOLKATA
INDIA

CERTIFICATE

This is to certify that the thesis entitled **"A Frequency Domain Based Technique for Condition Monitoring of Structures Using Limited Randomly Measured Dynamic Responses",** submitted by Shri **Jafar Sadak Ali,** who got his name registered on **06.01.2012** for the award of **Ph.D (Engineering)** degree of Jadavpur University, is absolutely based upon his own work under the supervision of Prof. Dr. Debasish Bandyopadhyay and that neither this thesis nor any part of the thesis has been submitted for any degree/diploma or any other academic award anywhere before.

Date **(Signature of the Supervisor)**

Dr . Debasish Bandyopadhyay

Professor

(Office Seal)

REF NO. D-7/E/4/2012

Title of the Thesis:

A FREQUENCY DOMAIN BASED TECHNIQUE FOR CONDITION MONITORING OF STRUCTURES USING LIMITED RANDOMLY MEASURED DYNAMIC RESPONSES

Name, Designation & Institution of the Supervisor

Dr . Debasish Bandyopadhyay
Professor
Department of Construction Engineering,
Jadavpur University, Kolkata- 700098

List of Publications:

Book Chapter : (1 No)

1. **Bandyopadhyay D., Ali J.S. (2018)** "Modal Strain Energy Based Structural Parameter Identification from Limited Vibration Measurement". *Experimental Vibration Analysis for Civil Structures, Lecture Notes in Civil Engineering, vol 5*. **Springer** International Publishing AG 2018.(DOI 10.1007/978-3-319-67443-8_63)(pp. 714-724)

International Journal Publications: (4 Nos.)

. 1. **Jafar Sadak Ali** and **Debasish Bandyopadhyay** " Experimental Validation of the Proposed SHM Technique form Limited Extracted Dynamic Responses of a Steel Beam Adopting inverse Dynamic Approach" *International Journal of Technical Innovation in Modern Engineering & Science (IJTIMES)* (UGC Listed) ,e-ISSN: 2455-2585.

2. **Jafar Sadak Ali** and **Debasish Bandyopadhyay** " Numerical and Experimental Validation of the Proposed SHM Technique form Limited Static Responses Adopting Equation Error Approach" *Journal of Emerging Technologies and Innovative Research (JETIR)* (UGC Listed) ,ISSN: 2349 5162.

3. **J S Ali** and **D Bandyopadhyay** " Experimental Validation of the Proposed Technique for Condition Monitoring of Structure with Limited Noisy Modal Data" (Paper Accepted to International Journal of Structural Intigrity).

4. **J S Ali** and **D Bandyopadhyay** " Condition Monitoring of Structure using limied noisy data of modal slope and curvature of mode shapes" (Paper Accepted to International Journal of Structural Intigrity).

International Conference Publications: (3 Nos.)

1. **J S Ali and D Bandyopadhyay,** "Reliability based System Identification of Structures for Earthquake Damage considering Parameter Uncertainty" *Proceedings of ICTACEM 2014 International Conference on Theoretical, Applied, Computational and Experimental Mechanics* December 29-31, 2014, IIT Kharagpur, India

2. **D Bandyopadhyay, P Guha & J S Ali**, "Structural Health Monitoring of a Railway Truss Bridge from Limited Static & Dynamic Responses", *IABSE Symposiuum Kolkata 2013*

3. **D Bandyopadhyay, J S Ali and R Mitra,** "Structural Finite Element Model Updating Using Frequency Response Function Data" *Proceedings of ACECON,2015*

List of Patents : Nil

Dedicated to all my Family Members

Acknowledgement

After a wonderful journey has began with the imagination and objective in mind, kept on going with wide exposure of information, instrumentation, knowledge and application and finally reaching the destiny of completing my PhD thesis. It has become possible due to the direct and indirect contributions of many well wishers, who have provided me all the support to stand determined, motivated to move forward, strength to overcome the obstacles in reaching my goal.

I find no words to express my regards and gratitude to my supervisor professor Debasish Bandyopadhyay, for his continuous motivation, guidance and support in the investigation. He has inspired me and extended the necessary academic help in carrying out my research work. In spite of his busy schedule, he participated in each minute details of my progress of work. In the entire research tenure, his precious technical advice, in-depth interaction helped this journey to a fruitful end.

My sincere thanks are due to professor S. Majumdar, Ex. professor of IIT Kharagpur for his kind advice and encouragement.

I express my sincere thanks and regards to all the professors of Construction Engineering Department of Jadavpur University for their valuable suggestions at different stages of the investigation.

I also express my sincere thanks to all the professors of Civil Engineering Department of Aliah University for their kind cooperation during my research work .I am also thankful to the authority of Aliah University to allow me to continue the research work.

I take great pleasure to thank my co-research scholars, namely Kushal Ghosh, Siddhartha Sengupata, Suprateek Roy, Sayantan Basu Choudhury and all the staff

members specially Sibasish Banerjee of structural health monitoring laboratory for their kind support and co-operation.

I would like to convey my sincere thanks to Md Azizur Rahman, Sayed Hussain, and other post graduate students of Aliah University.

I would like to convey my sincere thanks to Arav and Johen for their help for completing the thesis.

This thanks giving part would remain incomplete, if I do not record my appreciation of understanding, inspiration and support I received from my parents and all family members, who have taken a lot of pain for this research venture.

Jafar Sadak Ali
Jadavpur University, Kolkata, India.

List of Figures

List of Tables

Abstract

Condition monitoring of structures is significantly important from the safety and durability consideration. Parameter identification and subsequent damage detection techniques, using inverse static or dynamic approaches, are important tools to improve the mathematical models for monitoring the condition of structure. However, noise in the measured data might lead to unreliable identification of damage in a structural system. The measurement of static and dynamic responses at all degrees of freedom of a structure is also not feasible in practice. Five different numerical models for damage detection of structures are developed for condition monitoring of truss, beam and framed structures in the framework of finite element model with limited static or dynamic responses. The structural properties viz. axial rigidity and bending rigidity are identified at the element level in the updated models of the structural system. Damage at the element level is identified, by comparing the identified structural parameters of the updated model of the system with those of the undamaged state. Proposed numerical models are suitable for practical problem, as it is able to identify the structural parameters with limited static and modal data of first few modes experimentally measured at selected degrees of freedom. Different numerical examples with various damage scenarios are explored to demonstrate the applicability of the proposed models. The models are able to identify the structural damage with greater accuracy from the noisy dynamic responses even if the extent of damage is small. Experimental validation on simple cantilever beams and portal frames, establish the potential of the proposed methods for its practical implementation.

Keywords: Condition Monitoring, Damage, Inverse Static and Dynamic Approach, Modal data, Noise

CONTENTS

5. Results and Discussion

6. Conclusion and Future Scope of Study

Chapter – 1

Introduction

1.0 General

Condition monitoring and damage detection in civil, mechanical and aerospace engineering communities has become one of the most important technique in maintaining the integrity and safety of structure. The objective of structural condition monitoring is to provide a continuous diagnosis of the state of the structure during its life span.

Distress of different forms occurs frequently within the life of structures due to its aging, action of the environment, improper design, inferior construction and accidental loading etc. Damage may also accumulate incrementally over a period of time such as that associated with fatigue or corrosion. Natural disasters such as earthquake, flood, cyclone etc. leaves behind their sign on structures in terms of damages. Damage in elements of some structures may also result from the scheduled discrete events such as aircraft landings. Monitoring of health for assessing the condition of age-old structures, disaster driven damaged structures has become an essential requirement for the safety of structures. Fast development of risk-based design and modern construction techniques inevitably invited some risks due to lack of adequate knowledge in understanding the structural behavior. Many a times the casual approach adopted in execution of a project is also responsible for occurrence of premature damage besides natural causes. Several existing structures may have inadequate capacities in compare to the demand with the latest provision of codal stipulations. Thus, the concern for assessment of structural health, repairing and maintenance of existing structures has gained tremendous impetus in recent times.

Condition monitoring (CM) of structure is useful in improving the safety and for better utilization of the structure, effective maintenance strategy and avoidance of catastrophic failure. The benefits of condition assessment include optimal

maintenance cost and constant reliability of the structure. Condition monitoring is a management issue of the structural system involving integration of sensors, smart materials, data transmission and computational cost with processing ability within the structure itself. But, in the present context considering the most important part, the diagnosis, CM may be stated as the improved version of Non-Ddestructive evaluation of structures for efficient diagnosis. It may be compared with the clinical monitoring of human body to diagnose illness, to assess the damage.

Various Non-Destructive techniques commonly adopted are based on experimental methods such as ultrasonic or acoustic testing, magnetic field procedure, radiography etc. which are local techniques, inspected in a piece-wise manner are most importantly location dependent. The accessibility criteria also pose difficulty in many situations. Condition monitoring technique based on dynamic responses seems to be a better proposition by addressing the global assessment. Rudimentary techniques of structural damage detection based on dynamic responses are a very old practice, such as practices of sounding of clay pots to reveal cracks and tapping along the surface of a material to detect voids. These methods are constrained with individual power of observation and seem to be subjective. However, the promising utility of these simple techniques are exploited by the researchers with more sophisticated inspection methods. Sophistication is provided in combination with sensitive & accurate instrumentation and detailed numerical modeling using acquired response data.

The existing techniques used in structural damage detection can be categorized into two main groups. Finite-element model (FEM) update algorithms are used in one group for damage detection, as a special case of the general model update problem. The goal of damage detection with FEM update method indicates those elements, and their material properties which vary independently from their desired values.

It is assumed that the damage will change the structural characteristics considerably and subsequently the static and dynamic responses which are influenced by these changed parameters. Therefore, the static and dynamic responses may be useful to identify the damage. The schematic diagram of the damage detection technique adopting both inverse static and dynamic approaches are used for condition monitoring, are shown below.

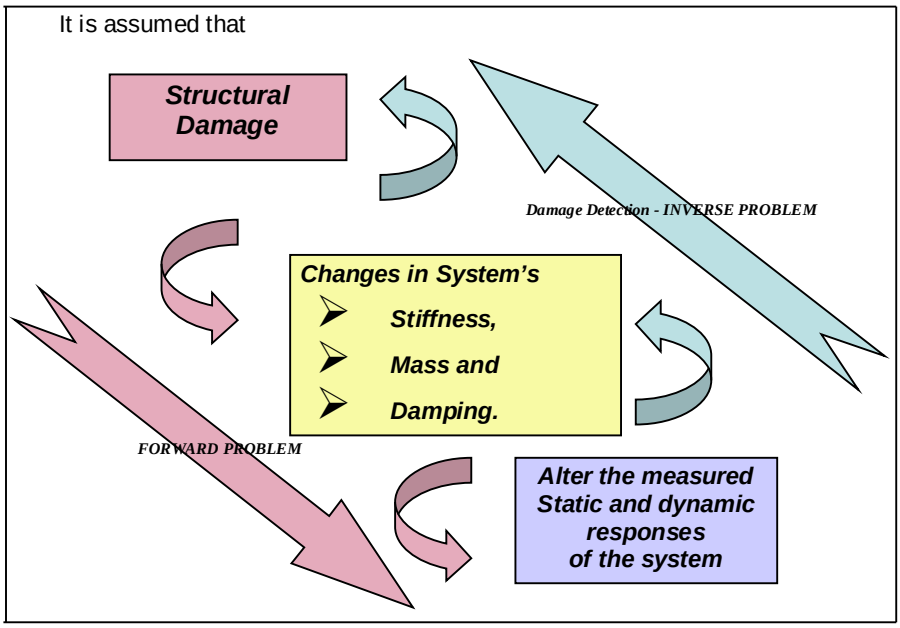

Fig 1.1: Schematic diagram of forward and inverse problem for condition monitoring

Structural damage detection algorithms are developed in this study based on the change of the elemental structural deflection and strain modal strain energy before and after the incorporation of damage in the structure. The degrees of freedom (DOFs) of the analytical model (FEM) of the structure are very large in practice and also only a limited number of the lower vibration modes of the structure can be measured accurately for damage detection. Moreover, it is known that the lower modes of a structure can be accurately modeled using the finite-element method, but substantial modeling errors exist in the higher modes. The proposed algorithm only uses few lower analytical and experimental modes in damage detection by the inclusion of the system stiffness. This improvement reduces significantly the

truncation and modeling errors in the higher modes with improvement in the convergence properties of the algorithm.

1.1 Objective of the present investigation

The objective of the present investigation is to monitor the condition of different types of structures using limited randomly measured dynamic responses adopting frequency domain techniques.

The detail of the objective of the present investigation to develop a numerical model using limited static and modal data measured at selected degrees of freedom for damage detection is represented schematically in Fig 1.2 and Fig 1.3

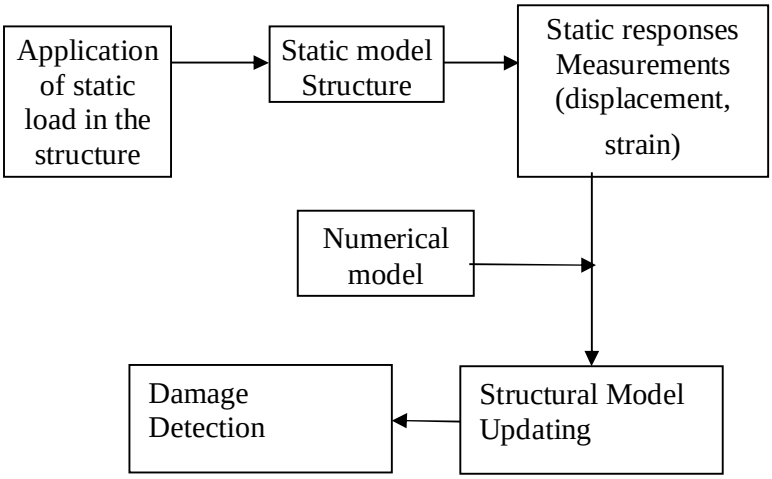

Fig 1.2: Inverse static approach with experimental test data

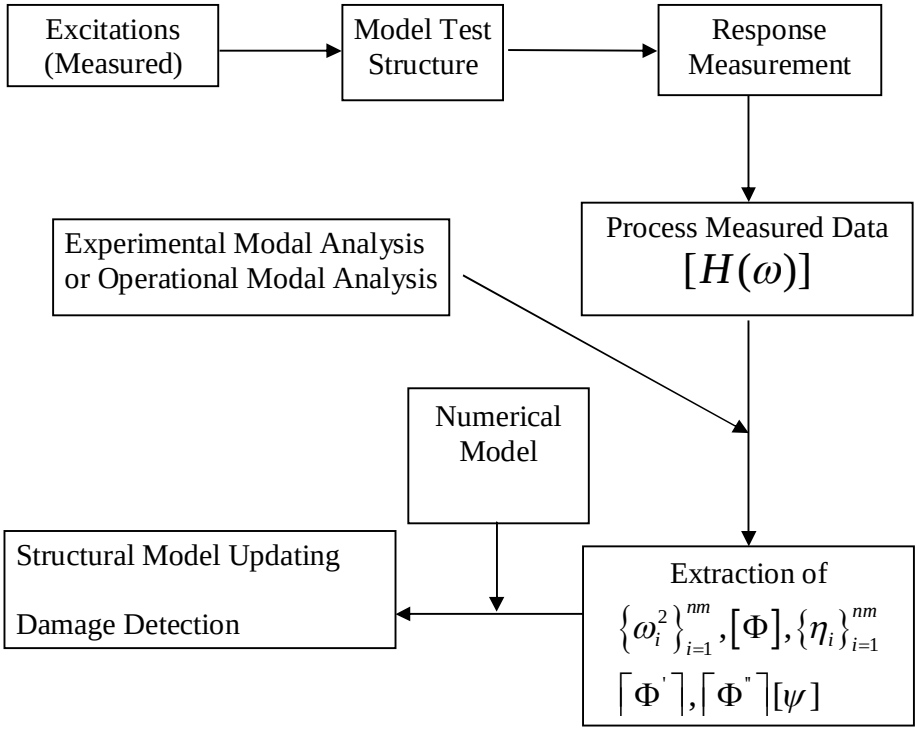

Fig 1.3: Inverse dynamic approach with experimental modal testing

1.2 Scope of work

To fulfill the objective of the present study the scope of work is categorized as:

a. Finite element model generation for beam, frame and plane truss structure.
b. Laboratory experiment to obtain the static displacement and bending strain data for different model structures.
c. Modal testing and subsequent extraction of modal parameters like natural frequencies, mode shapes and their derivatives, modal strain energy of different model structures.
d. Condition assessment of different structures using inverse approach both with static and dynamic responses.

1.3 Structure of the thesis

The thesis is subdivided into six chapters. In Chapter 1 discuss the introduction to structural condition monitoring and the objective & scope of

work of the present investigation. In Chapter 2 review of relevant literature and critical observations are discussed. Chapter 3 is devoted to the theoretical formulations for different developed numerical models of condition monitoring of structures. The details of the experimental study for the validation of the developed numerical techniques are presented in Chapter 4. Results of numerical examples as well as experimental studies are discussed in Chapter 5. The conclusions from the present investigations & future scope of work are outlined in Chapter 6. There are relevant referred papers, which are indexed subsequently.

Chapter – 2

Literature Review

2.0 General

Review of existing literature is quite important to understand the present state of art of the particular area of research. Various approaches have been attempted by different researchers to address the condition monitoring (CM) of structure based on static and dynamic responses.

More researchers are involved in developing efficient, reliable and low-cost damage diagnosis approaches using static and dynamic parameters measured from a structural system in aerospace, mechanical, and civil engineering disciplines According to the extent of acquirable damage information, the process of damage diagnosis can be broken down into four levels (*Rytter A.*, 1993)

- Level-1 Alarm of damage existence
- Level-2 Identification of damage location
- Level-3 Identification of damage severity and
- Level-4 Prediction of the remaining life of the structure

To detect damages in structural systems in terms of the structural parameters the measurement techniques that are adopted may be categorized into two groups e.g., measured excitation and ambient excitation. Similarly,there are two types of dynamic response data which are generally used for damage detection, namely, time domain response and frequency domain response.

Most of the condition monitoring approaches is based on the system identification technique adopting inverse dynamic methods. It is observed that the accurate and repeatable dynamic response measurements on complex structures are often difficult and thus pose a challenging problem to develop an efficient model for condition assessment. In addition, environmental and operational variations e.g., varying temperature, moisture, and loading conditions also affect the dynamic response of

structures and greatly influence the identification of damage or condition monitoring of the system. Thus, effect of noise of the system identification is important to address the condition assessment of structural system in more effective way to account for the uncertainties associated with the limited observations, data irregularities, model assumed and all other environmental and operational variations.

2.1 Damage detection using static response data

Sanayei et al. (1996**)** proposed a method for structural parameter identification utilizing elemental strain measurements. *Sanayei et al.* (1996) presented a method for the parameter estimation of structures using subsets of static applied forces and strain measurements and successfully identified structural stiffness in element level. It was also observed that in presence of measurements, the selection of these subsets drastically affects the accuracy of the parameter estimates. *Sanayei et al.* (1997) performed experiments on a small scale steel frame model to support the displacement based equation error function, displacement output error function, and strain output error function methods of structural parameter estimation using static nondestructive test data. Both static displacement and static strain measurements were used to successfully evaluate the unknown stiffness parameters of the structural components. On the other hand *Hjelmstad and Shin* (1997) developed a damage detection and assessment algorithm based on parameter estimation with an adaptive parameter grouping scheme. *Liu and Chian* (1997) proposed a method for identifying the element properties of a truss. The axial strains of the truss elements measured in static tests were used in the identification process. The finite-element method was used to derive the equilibrium equation of the truss. *Oh and Jung* (1998) developed an improved damage detection and assessment algorithm based on the method of system identification. *Yeo et al.* (2000) presented a damage assessment algorithm for framed structures based on a system identification scheme with a regularization technique. *Wang et al.* (2001) developed a structural damage identification algorithm using static test data and changes in natural frequencies. After obtaining the possible damage location, an iterative estimation scheme for solving non-linear optimization programming problems was used. *Jang et al.* (2002) examined damage assessment

algorithms based on the system identification (SI) method through laboratory experiments of static displacements from static loading and modal data from impact vibration were measured through laboratory experiments on a grid-type model bridge. Changes in the static response of a structure are characterized as a set of non-linear simultaneous equations that relate the changes in the static response to the location and severity of damage *Sanayei et al.* (2005*)* proposed a multi-response parameter estimation method, including an error function normalization procedure, to allow simultaneous estimation of stiffness and mass parameters for model updating. *Muthumani et al.* (2010) proposed a first stage condition monitoring methodology using natural frequencies and static deflections as damage indicators. The idea was that the first stage monitoring can be done for a large number of bridges and vulnerable structures in a remote manner and the features extracted from the data should help in determining whether any second stage detailed investigation may be warranted. *Kourehli et al.* (2012) presented an algorithm for damage detection and estimation in structures using incomplete static responses.

2.2. Damage detection using dynamic response data

*Lifshitz and Rotem (*1969*)* possibly published the first journal paper discussing damage detection using vibration measurements. Vibration based damage detection methods normally assume that structural vibration parameters are functions of its physical parameters. It is possible to identify the physical change of the structure due to damage by tracking its vibration parameters change (*Doebling et al.,* 1998). Unlike other disciplines, the damage detection problems for large civil structures such as bridges are complex. The main challenges and difficulty come from large scale of the structures, great degree of uncertainties, and inability for exciting higher order modes. Although much literature has proven that observing outliers in a continuously monitored vibration parameter may alarm the existence of damage, it is still difficult to locate and quantify, as further damage detection levels, the damage directly from these data (*Alampalli et al.* 1997). According to different analytical processes, the reviewed vibration-based damage detection methods in this chapter were reviewed in

two categories (*Hejll*, 2004). One category was the forward identification methods, and the other was the direct§ identification methods. The forward type methods attempt to solve the damage detection as an inverse problem; in this inverse problem, the identification is sought by error minimization between the predicted vibration parameter change and the measured vibration parameter change (*Zhang and Kumar*, 2011). Firstly, the theoretical vibration parameter of a structure is obtained by numerical modal analysis to its undamaged FE model. Secondly, a damage candidate is randomly introduced; and the change in the vibration parameter after this damage occurrence is calculated. Thirdly, comparing to the measured vibration parameter change, the analyst may decide whether the damage candidate tried in the numerical analysis matches the real damage in terms of the correlation of the theoretical parameter change and measured parameter change. In this manner, a damage detection process is seen as an optimization problem. The direct type methods as of another category are often developed being able to detect structural damage without optimization iterations. The relation between structural damage and natural frequency change, or in other words, the input, is explicitly described in the algorithm of a direct method. Therefore, an effective damage indicator in direct methods should be highly sensitive and robust to the damage-induced change in physical matrices of the underlying structure. The direct methods normally aim at identifying the location and/or severity of the damage at the same time after the existence of damage is certain. Therefore, they are expected to have the ability of solving Level-3 problems.

2.3. Damage detection using basic vibration parameters

Basic vibration parameters, including natural frequencies, mode shapes, and damping ratios, are deemed as a basic structural characteristic; they are to be identified in priority in most experimental or field modal tests. In this context, the techniques using these fundamental parameters are reviewed at first.

2.3.1 Natural frequency

Natural frequency is one of the most convenient characteristics in modal analysis; it has absorbed wide damage detection investigation (*Biswas et al.,* 1990; *Juneja et al.,* 1997; *Kanazawa,* 2006). This section highlighted the early leading work and the representative papers analyzing different structure cases, and publications considered as a key contribution to knowledge in this field. As pioneers in this area, *Cawley and Adams* (1979) developed an optimization based method by calculating similarity ratio of natural frequency change. It was found that the method is sensitive to damage in aluminum and carbon-fibre reinforced plastic plate. *Messina et al.* (1996) proposed damage localization assurance criterion (DLAC) that compared the normalized natural frequency change in theory before and after damage occurrence with regard to the normalized natural frequency change identified from measurement. The DLAC method was proven to have ability of damage location, but it is only applicable to the scenarios where damage happens at a single location. Later, *Messina et al.* (1998) differentiated a frequency-to-damage sensitivity matrix for the DLAC method in order to consider local element information. The revised method, namely multiple damage localization assurance criterions (MDLAC), enables the DLAC's applicability for multiple-damage cases. In addition, they investigated the second order sensitivity matrix for the MDLAC method but found no obvious improvement. Many applications of forward methods have been made; however, they mainly answered the 1st level problems, that is, the existence of structural damage. Still, very few of them have successfully solved higher level problems of multiple damage locations (*Hejll*, 2004). One of the possible restrictions prohibiting this is the sensitivity and reliability of natural frequency (*Doebling and Farrar*, 1996) as a global parameter in complicated damage detection cases. There were many other applications of natural frequencies, such as offshore structures (*Begg et al*., 1976; *Vandiver and Hole*, 1976), a concrete cantilever beam (*Gudmundson*, 1982), a concrete cantilever plate (*Friswell et al.*, 1998), a truss bridge (*Juneja et al*., 1997), and the steel girder of a highway bridge (*Biswas et al.*, 1990).Particularly, since the natural frequency-based damage indicators can hardly provide damage location information, therefore, the change of

natural frequencies in different multiple-damage cases can be the same. For example, *Farrar et al.* (1994) demonstrated insensitivity of the method using natural frequencies to detect damage on I-40 Bridge in the U.S. When the stiffness at the centre of a main span decreased by more than 90%, accordingly, the bridge's overall bending stiffness reduced by more than 20%, they did not observe significant change in the identified natural frequencies. In addition, to make structural damage detectable in practice by using these forward methods, the necessity of obtaining highly accurate modal measurement becomes another limit (*Doebling et al.*, 1998). For instance, the frequency change should be measured precisely and in a controlled environment

2.3.2 Mode shape

Mode shapes reflect the information of geometry, materials, mass, and stiffness. It is, therefore, another popular parameter incorporated in forward damage detection methods (*Li et al.*, 2005; *Ndambi et al.*, 2002). *West* (1984) and *Wolff and Richardson* (1989) presented early work making use of mode shapes in damage detection. The authors proposed modal assurance criterion (MAC) to detect the existence and the location of structural damage, defined as

$$\text{MAC (i,j)} = \frac{\left(\{\varphi_i^A\}^T\{\varphi_j^B\}\right)^2}{\left(\{\varphi_i^A\}^T\{\varphi_j^A\}\right)\left(\{\varphi_j^B\}^T\{\varphi_j^B\}\right)} \tag{2.1}$$

Where φ_i^A is the i^{th} mode safe of a structure before damage whilst φ_j^B is the j^{th} mode shape of the structure after damage. MAC is a scale factor from zero to one. Bigger the MAC values closer the relation between the two evaluated mode shape vectors. In addition, *Fox* (1992) found that, if the MAC value at a measurement point of one mode is close to the node points, the MAC indicator is sensitive to damage. In their findings, graphical comparison between the mode shapes before and after damage occurrence is perhaps a better way where only the natural frequencies and mode shapes are available to use. Another issue for MAC evaluation is that, as it only uses one pair of mode shape vectors in judgement, how to choose the appropriate mode for MAC calculation becomes determinant. To overcome this, *Lieven and Ewins* (1988)

proposed a coordinate modal assurance criterion (COMAC) (that was later used by many other scholars. The COMAC coefficient is defined as

$$\text{COMAC}(i) = \frac{\left(\sum_{r=1}^{md} \{\varphi_i^A\}_r^T \{\varphi_i^B\}_r\right)^2}{\left(\sum_{r=1}^{md} \{\varphi_i^A\}_r^T \{\varphi_i^A\}_r\right)\left(\sum_{r=1}^{md} \{\varphi_i^B\}_r^T \{\varphi_i^B\}_r\right)} \qquad (2.2)$$

Where $\{\varphi_i^A\}_r$ is the i^{th} component of the r_{th} undamaged mode shape; $\{\varphi_i^B\}_r$ is the i_{th} component of the r^{th} damaged mode shape; *md* is the highest mode number of interest. Structural damage can be possibly identified at the location where the COMAC is close to zero. *Ko et al.* (1994) combined MAC and COMAC-based sensitivity in damage detection for steel-framed structures and argued that the performance of the combined method still depends on the selection of most sensitive mode pairs. *Shi et al.* (2000) extended the MDLAC method by using incomplete noisy mode shapes in damage localization assurance criterion. With incorporating the derived mode shape sensitivity matrix, they found that the index of mode shape correlation has considerable potential in damage detection for a truss model. Similarly, *Koh and Dyke* (2007) also presented a method, noted as stacked mode shape correlation (SMSC), to report structural damage using mode shapes but without using mode shape sensitivity. In this method, the mode shapes evaluated in the correlation criterion is stacked together as a column vector. The feasibility of SMSC method was validated through simulations on a flexible cable-stayed bridge model where some errors were found in damage severity prediction. *Skjaerbaek et al.* (1996) studied the issues of optimal sensor location for damage detection based on the change in mode shapes and natural frequencies using a substructure iteration method. *Cobb and Liebst* (1997) demonstrated their work on optimal sensor locations based on an eigenvector (mode shapes) sensitivity analysis. *Ratcliffe* (1997) presented a technique for locating beam damage using the finite difference approximation of a Laplacian operator on mode shape data. *Rahai et al.* (2006) characterized the mode shapes of a structure as a function of stiffness, where the mode shapes are divided into measured and unmeasured sets in equations. From the simulations on a truss and

frame, they evidenced the capability of the proposed optimization criterion of locating, quantifying the damage by solving few sets of equations. Apparently, the downside of a forward method using mode shapes is that the mode shapes are more uncertain and can be contaminated by environmental noise in practical testing comparing to natural frequency-based methods. For large structures, on the other hand, it is hard to capture accurate and reliable mode shapes using a limited number of sensors, especially when it comes to meet the belief in some literature (*Cempel et al.*, 1992) that the higher modes are deemed more favorable in damage detection than the lower modes.

2.3.3 Modal flexibility

There is also plenty of literature studying other modal derivatives: for example, modal flexibility, mode shape curvatures, modal strain energy and strain mode shapes. The damage indicator using modal flexibility matrix, which is made up of natural frequencies and mode shapes, is defined as

$$F = \Phi A^{-1} \Phi^T = \sum_{i=1}^{m} \frac{1}{\omega_i^2} \Phi_i \Phi_i^T \tag{2.3}$$

Where ω_i is the i^{th} natural frequency and Φ_i is the i^{th} mode shape vector.

The motivation of using modal flexibility in damage detection is that it does not require complete vibration parameters in damage detection (*Pandey and Biswas*, 1994, 1995) and this feature is welcomed in practical measurement since only the parameters of limited modes can be captured. *Reich and Park* (2000) investigated a local flexibility method using substructure techniques. Their experimental comparison of the proposed damage indicator on a bridge column before and after damage showed the method's ability of damage localization. *Bernal* (2002) concluded by two numerical examples that the change in a flexibility-based damage locating vector (DLV) can reflect damage; also, the DLV indicator is independent on the model or sensor availability. *Wang et al.* (2000) examined the modal sensitivity indices of different vibration parameters to detect simulated damage scenarios on Tsing Ma Bridge and found that the modal flexibility has better performance than natural frequencies and mode shapes. *Gao and Spencer* (2006) studied an extended modal

flexibility-based DLV method for long-term monitoring purpose. They conducted ambient and forced vibration tests on a 14-bay truss; it was proven that the improved method is useful to detect damage with limited sensor information. However, the feasibility of the flexibility-based methods was doubted by *Huth et al.* (2005), from the analysis of a prestressed concrete bridge, they argued the parameter's difficulty of locating early stage damage because of the stiffness recovery after cracks close in prestressed concrete, and also the environmental influence on vibration parameters.

2.3.4 Mode shape curvature

Mode shape curvatures have a direct relation with bending strains. *Pandey et al.* (1991) proposed a curvature-based method in damage detection for a cantilever beam and a simply-supported beam model. The curvature is calculated by central difference approximation to mode shapes

$$\upsilon'' = \frac{(\upsilon_{i+1} - 2\upsilon_i + \upsilon_{i-1})}{h^2} \tag{2.4}$$

Where υ the mode shape component at two adjacent elements and h is is the length of the element. They found that the curvature change is a useful indicator for damage.

Chance et al. (1994) investigated the relation of the measured strain time-series with curvature used for neural network training purpose. They found that, in this way, the inaccuracy problems in traditional curvature approximation can be overcome.

Maeck and De Roeck (1999) applied a direct stiffness approach to damage detection, location, and quantification for the prestressed concrete bridge Z24 in Switzerland. They found that the curvature change is rather small for the side spans.

Wang et al. (2000) presented a numerical damage detection simulation on Tsing Ma Bridge in Hong Kong; and they concluded that the mode shape sensitivity (curvature) is less sensitive to damage than modal flexibility. In a comparison investigation, *Maia et al.* (2003) compared various methods by the raw data measured in an operational test. As all tested methods were frequency response function (FRF)-based, they do not require modal identification. Simulation results on a numerical beam showed that the curvature-based method outperforms the others. However, some false damage alarms

still need attention. *Hamey et al*. (2004) examined four methods on a carbon/epoxy composite model: they are the absolute difference of curvature mode shape method (ADM), the curvature damage factor method (CDF), the damage index method (DIM), and the FRF curvature method (FCM). In contrary to most existing curvature-based damage detection methods, the curvature used in their study was directly measured by piezoelectric sensors. The DIM method was proclaimed to be the best method. *Lestari and Qiao* (2005) demonstrated that using curvature mode shapes can be useful in damage quantification of fibre reinforced polymer (FRP) honeycomb sandwich structures. Other scholars, such as *Doebling et al.* (1997); *Wahab and Roeck* (1999); *Lestari et al.* (2006); *Xu and Wu* (2007); *Qiao et al*. (2007); *Tomaszewska* (2010), and *Yoon et al.* (2009), also attempted mode shape curvature in damage detection indices, but most of these applications only referred to basic laboratory models.

2.3.5 Slope of mode shapes

Most of the existing methods using this parameter in damage detection still focused on simple structures, such as beams or plates. *Abdo and Hori* (2002) used slope of the mode shape in damage detection. Through their numerical analysis on a simple steel plate model, it was found that, comparing to traditional mode shapes, the change in absolute values of mode shape rotations (slopes) is useful to locate damage efficiently. *Kim and Kwak* (2001) compared various crack detection criteria using COMAC, Enhanced COMAC (ECOMAC), and Absolute Difference of Strain Mode Shape (ADSM), along with their newly proposed method using strain mode shapes. They proved the superiority of the proposed method in most simulations.

Sazonov et al. (2003) also justified the feasibility of using the change of strain energy mode shapes in damage detection activity for a complex bridge structure without using baseline data.

2.3.6 Modal Strain Energy

Modal strain energy (MSE) is acknowledged as sensitive variable to element location and has been widely used in investigating modal participation of structural elements (*Lim and Kashangaki*, 1994) and *Stubbs et al.* (1992) presented a pioneering work of using modal strain energy for damage localization. The MSE of a structure on the r_{th} mode can be demonstrated as

$$MSR_r = \frac{1}{2}\Phi_r^T K \Phi_r \tag{2.5}$$

Where, K is the stiffness matrix of a structure.

Stubbs and Kim (1996) verified the feasibility of a practical modal strain energy method for damage localization and severity estimation with only the post-damage information available. Carrasco et al. (1997) discussed using modal strain energy change to find damage location and extent for a space truss model and claimed that the magnitude change of the indicator is related with the damage's overall magnitude. Result of the test showed that this method works well at locating damaged elements. Also, *Park et al.* (2001) examined another damage index using modal strain energy. The index was extracted from the periodical measurement data of the prior visually inspected cracks on a concrete box-girder bridge. They found that the environmental factors are likely to affect the accuracy of the proposed. *Wang et al.* (2010) studied MSE as a correlation indicator, called modal strain energy correlation (MSEC) to identify damage for truss bridge structures. The MSE based damage sensitivity was derived from theory. The capacity of MSEC was verified through several damage scenarios. It was found that the method has high computational efficiency, however, when measurement noise is considered, the method may report false alarms. *Cornwell* (1999) examined the application of a modal strain energy method on a plate-like model. The method only requires mode shape data before and after damage. From the experimental validation, the method is effective even for the damage whose extent is as low as 10%.*Shi et al.* (1998) proposed a method based on modal strain energy for locating damage in a Structure. This method makes use of the change of modal strain energy in each structural element before and after the occurrence of damage. Some

properties of this Modal Strain Energy Change are given to illustrate its sensitivity in locating the structural damage. Information required in the identification is the measured mode shapes and elemental stiffness matrix only without knowledge of the complete stiffness and mass matrices of the structure. *Shi et al.* (2000) derived the sensitivity of the MSE with respect to damage is derived. The sensitivity is not based on any series expansion and is a function of the analytical mode shape changes and the stiffness matrix. Only incomplete measured mode shapes and analytical system matrices are required in this damage localization and quantification approach. Damage quantification of two damages is successful with a maximum of 14% error under a 5% measurement noise.

2.3.7 Damping Ratios

Damping ratio is a significant vibration characteristic that is directly related to how the vibration energy can be dissipated along a structure. Unlike the extensively researched natural frequencies or mode shapes-based parameters, very few dynamic parameter based condition monitoring methods employing modal damping as damage indicators were found in the literature. The main reason denouncing modal damping being adopted as damage indicators is probably the uncertainties and errors in experimental damping estimation. One of the early studies making use of modal damping as damage indicator was done by *Tsai et al.* (1985). The authors investigated a cross random decrement method for early damage detection. The change in modal damping ratios was used to identify damage in an offshore platform structure. They found that, under random excitation, the proposed method is related with progressive damage severity. *Williams and Salawu* (1997) suggested that damping ratios maybe advantageous and feasible in some damage detection scenarios, particularly when both natural frequencies and mode shapes are found to be insensitive. *Kawiecki* (2001) used surface-bonded piezo elements to determine modal damping characteristics of a beam and found that structural or material damage is frequently associated with damping change. However, the author suggested that the proposed method is only practically useful for damage detection of light-weight or small scale structures. *Kyriazoglou et al.* (2004) measured the specific damping capacity (SDC)

of a composite flexural beam. They applied quasi-static loading to test a beam under the undamaged/damaged state and observed that the SDC is a promising damage indicator for the similar structures.

2.3.8 Frequency response function (FRF)

Frequency response function (FRF) quantitatively measures a system's output spectrum in response to its imposed excitation. Therefore, it is popularly used in dynamic characterization for time-invariant systems. As a traditional and well-studied parameter, nowadays FRF can be readily obtained in many ways. There are quite a few researchers who have proposed frequency domain-based damage detection methods using FRF. *Lew* (1995) used a coherence algorithm to exploit the change of transfer functions of a nine-bay truss example and successfully detected the damage type and location. *Wang et al.* (1997) validated a FRF-based damage indicator that is useful to locate and quantify damage on a 3-bay frame model using incomplete measurement. *Zang and Imregun* (2001) employed the size-reduced FRF data to train an ANN in the damage detection of a rail wheel. The outcomes showed the potential of this method in damage detection with noise contaminated data. *Wu and Xu* (2006) proposed a new acceleration response energy method by relating the FRF of the structural acceleration responses with mode shape data. The simulations on a long-span cablestayed bridge indicated the accuracy advantages of the method by comparison to the mode shape curvature method. *Yoon et al.* (2010) derived another parameter called operating deflection shape from the measured FRF from a plate. By comparing the experimental analysis using global fitting method and directing subtracting method, they found that the proposed method is more accurate and less sensitive to noise in the damage detection case of a notched beam. *Hsu et al.* (2011) developed a FRF change method supported by the wireless sensing system; the method was then verified to detect the damage of a six-story laboratory frame. The experimental casestudy demonstrated the proposed method's efficiency improvement and the capability of locating and quantifying damage when no environmental factors are considered.

On the other hand, the applicability and robustness of FRF-based indices for detecting damage is still suspected by some researchers. For example, *Mares et al.* (1999) simulated a crack damage in a cantilever beam and found that if the load is applied right on the damaged elements, there is no observable difference of FRF for the damaged element from its intact state; if the load is applied on the damage-free elements, the FRF will change. A later argument is from *Agneni* (2000) who investigated the influence of the truncation in measured time-series data that are to be transferred to frequency domain on FRF. He found that the truncation can cause significant FRF change even there is no damage at all. Moreover, *Crema and Mastroddi* (1998) correlated the FRF measurement with physical parameters of the structure and found that the noise can corrupt the frequency resolution of the FRF when it is used for damage inspection. Based on these facts, therefore, using FRF to derive damage identification methods requires attention. The use of FRF curvature was also studied by *Maia et al.* (1997) *and Sampaio* (1999). Rather than just using resonant frequencies as done in *Pandey et al.* (1991), their methods were an extension work to consider all the identified frequency range. Also, the mode shape has been replaced by FRF data. The FRF curvature is defined as

$$\alpha''(\omega)_{I,J} = \frac{\alpha(\omega)_{i+1,j} - 2\alpha(\omega)_{i,j} + \alpha(\omega)_{i-1,j}}{h^2} \tag{2.6}$$

Where $\alpha_{i,j}$ is the receptance FRF measured at the i^{th} location excited by an input force at location *j.α"* is the second-order derivation of α. Then the summation of the difference between the undamaged and damaged FRF curvatures along the frequency range at all exciting locations becomes a damage indication for the i^{th} location

$$S_i = \sum_j \Delta\alpha''_{i,j} = \sum_j \left(\sum_\omega \left| \alpha''_d(\omega)_{i,j} - \alpha''_{ud}(\omega)_{i,j} \right| \right) \tag{2.7}$$

Where, *d* and *ud* denote damaged and undamaged states, respectively.

Experimental data from the American I-40 Bridge showed considerable potential of using FRF curvature for its simplicity. Also, this damage indicator does not require natural frequencies or mode shape to be identified. As already been mentioned in

Section 2.2.3, FRF-based mode shape damage indices were investigated by *Maia et al.* (2003).

2.3.9 Operational modal analysis

Operational modal analysis (OMA) simply known as output-only modal analysis, has recently prevailed in structural vibration test and monitoring. OMA technique use unmeasured ambient excitations, such as moving traffic, wind, and other natural loads. Therefore, these methods overcome the difficulties of applying a traditional artificial excitation-based modal testing method in the real world civil structures. Since an engineer only needs to record output time-series in OMA techniques, the testing procedure is more affordable and feasible in practical civil structure applications. *R.B. Randall et al., (*2004*)* compared several curve-fitting methods for extraction of the modal parameters from response vibration measurements, and in particular the best damping estimates. *De-Wen Zhang and Fu-Shang Wei (*2007*)* shown that the dynamic flexibility (DF) and improved dynamic flexibility (IDF) methods can be applied to extract constrained structural modes from free-free modal test data. An analytical comparison between three techniques for the identification of modal properties of structures when subjected to ambient vibrations is performed by *Diego F. Giraldo et al., (*2011*)* explained that an accurate estimation of the modal parameters of a structure, including modal frequency and damping ratio, is crucial for many practical engineering problems. *Rune Brincker and Palle Andersen* have done some further work following the idea introduced by *Parloo et al.* where they proposed that the scaling factor should be estimated by repeated testing introducing mass changes in different points on the structure.

2.3.9.1 Study of time domain techniques

Zhang et al. (2002) established a common mathematical framework for a unified two-stage time domain (TD) modal identification, based on a formula of modal decomposition of the time response function (TRF), represented as impulse response function, free decay response, or correlation function, as well as data correlation of

the TRF. The Structural Time Domain Identification (STDI) toolbox for use with MATLAB^{TM} is developed by *P.H. Kirkegaard; P. Andersen and R. Brincker (*1997*)* at Aalborg University, Denmark, based on the system identification research performed during recent years. *Reza D. Nayeri et al., (*2009*)* explained that while numerous studies have been published concerning the application of a variety of system identification techniques in conjunction with vibration measurements from civil infrastructure systems.

2.3.9.2 Modal Parameter extraction by Frequency Domain Decomposition

R. Brincker and P.Andersen introduced a new frequency domain technique for the modal identification from ambient responses *Jorge Rodrigues, Rune Brincker and Palle Andersen* explored the idea of estimating the spectral densities as the Fourier Transform of the random decrement functions for the application of frequency domain output-only modal identification methods. *Brincker et al.* (2001) did their research on identification and damage detection of a highway bridge by Frequency Domain Decomposition method.

2.3.9.3 Modal Parameter extraction by Empirical Mode Decomposition

*Xingyu Song et al. (*2017*)* developed modal parameter identification method based on empirical mode decomposition and Natural Excitation Technique (NEXT) .A methodology is presented by *Paul J. Fanning and E. Peter Carden (2004)* for detecting added mass in structural systems maintaining a linear response. A single frequency response function measured at several frequencies along with a correlated analytical model of the structure in its original state are used to detect and quantify the added mass. *J.C. Asmussen and R. Brincker (*1996*)* discussed a method for estimating frequency response functions by the Random Decrement technique. *R. Brincker et al., (*1996*)* discussed that the dynamic analysis of Queensboro Bridge data recorded by EDI Ltd., based in Vancouver (Canada), under environmental excitation, is a chance to involve a few different research groups already working in this field. *Moller*

*N. et al (*2001*)* performed modal testing of mechanical structures subject to operational excitation forces. For operational modal analysis two different estimation techniques are used: a non-parametric technique based on frequency domain decomposition (FDD), and a parametric technique working on the raw data in time domain, a data driven Stochastic Subspace Identification (SSI) algorithm. *Carlos E. Ventura et al (*2001*)* in their paper describes results of a model updating study conducted on a 15-storey reinforced concrete shear core building. The output-only modal identification results obtained from ambient vibration measurements of the building were used to update a finite element model of the structure. Experimentally identifying vibration characteristics of a structure has been widely studied in engineering disciplines in the past half century. As one of the earliest milestones made in this area, *Kennedy and Pancu* (1947) introduced the accurate identification of natural frequencies and damping levels for aircraft structures and even their methods had not been out-dated for many years (*Ewins*, 2000). Traditionally, the experimental modal analysis approaches are developed on the basis of forced vibration test (FVT). FVT requires both the excitation force and the structural response are required to be measured simultaneously. The theory and application of the traditional methods have been well-established and extensively investigated in the aerospace and automotive communities (*He and Fu*, 2001; *Maia and Silva*, 1997). However, the methods employing FVT encounter many challenges when they are applied to identifying modal characteristics of civil structures. For instance, a large dimension bridge will require an appropriate equipment to produce adequately large, but non-destructive excitations. Furthermore, the normal traffic on the bridge has to be closed in the duration of a FVT session. These limitations have obviously made the traditional modal identification methods inconvenient and inappropriate in modern long-term continuous SHM tasks. *Shama et al.* (2001) conducted an ambient vibration test for North Grand Island Bridge in West New York. The identified modal properties were utilised for FE model validation. *Jaishi et al.* (2003) applied an ambient vibration test to identify the modal properties of a historic structure in Nepal and evaluated the seismic safety of the structure using an updated FE model.

2.3.10 Time-frequency analysis

The time-frequency analysis is based on spectrogram, which is the basic short term Fourier transform, Wigner-Wille transform, wavelet and empirical mode decomposition. Various wavelets such as coifet, daubechies, symmlet and vaidyanathan were used by the researchers to decompose an impact-type waveform and the wavelet coefficients were compared. *Staszewski* (1998) reported a summary of advances and applications of wavelet analysis for damage detection. It included time-frequency analysis, wavelet spectrum, orthogonal or discrete wavelet decomposition, wavelet-based data compression, de-noising and feature extraction, linear and nonlinear system identification and image processing. The wavelet analysis provides new insight in non-stationary signal analysis with respect to classical time-invariant approaches and seems to be promising of its wider range of applications. *Kitada* (1998) also adopted wavelet technique for the non-linear identification of the dynamic system. *Zabel* (2005) presented an algorithm for the parameter identification of a finite element model. The author utilised wavelet coefficient of the measured data and their integrals or derivatives respectively. The application of discrete wavelet analysis and correction coefficient to parametric system identification was demonstrated with numerical and experimental investigations.

2.3.11 Singular value decomposition (SVD)

Ruotolo and Surace (1997) reported that the structures under test could be subjected to alterations during normal operating conditions, such as changes in mass. Damage detection method based on singular value decomposition (SVD) can able to distinguish between changes in the undamaged and damaged conditions. Initially it was able to detect and analyze the stress waves, but could not dissociate the stress waves generated from damage and those from the acoustic emissions of the test apparatus. Thus the results were inconclusive for damage detection at that time.

2.3.12 Principal component analysis (PCA)

Principal component analysis (PCA) is a method of multivariate statistics which was adopted to overcome many limitations. *Kullaa* (2003) studied the condition monitoring of Z24 Bridge in Switzerland for three types of damage configurations.

Stochastic subspace identification technique and stabilization diagram were used for automated modal parameter identification. Principal Component Analysis (PCA) was also incorporated to reduce the computational cost. *Yan et al.* (2005) proposed a damage detection method based on Principal Component Analysis (PCA) for condition monitoring under varying environmental and operational condition.

2.3.13 Soft computing tools for SHM

Tee et al. (1990) studied the application of Fuzzy logic for assessing the condition of concrete slab bridges. *Pande and Barai* (2000) presented an application of multilayer perceptron in the damage detection of steel bridge structures adopting Artificial Neural Network (ANN). The Author reported that the performance of the network with two hidden layers was better than that of single-layer architecture in general. *Barai and Pande* (1997) adopted Traditional neural networks (TNN) and the time-delay neural networks (TDNN) for detecting the damage in bridge structure using vibration signature analysis. The authors carried out a comparative study for the various cases of complete and incomplete measurement data. It is reported that TDNN performed better than TNN. *Routolo and Surace* (1997) presented a method for non-destructive detection of cracks in beam employing genetic algorithm. *Bani-Hani et al.* (1999) presented an experimental study of identification and control charts using neural network. Further, *Barai and Pande* (2000) presented damage assessment paradigms integrated on *blackboard* platforms with special reference to steel bridge structures.

2.3.14 Artificial neural networks

There are development of mathematical models with new technologies. ANN is the system inspired from the operations of biological neural networks, in other words, it emulates biological neural system.

One of the important applications of ANN is pattern recognition, with which many researchers have proposed statistical damage detection methods. After an ANN is trained by sample data, the network can associate output patterns with input patterns. Therefore, a basic idea of employing ANN in damage detection activities is to train a

network being able to recognize assorted damage scenarios resulting from various inputs, such as the reviewed dynamic parameters that can found in prior subheadings. Therefore, a promising potential of ANN techniques in structural damage detection is that, by adapting the network to highly complex relations between the input and output patterns (namely supervised learning), an ANN is expected to correctly or nearly correctly predict damage information for future incomplete or even partially incorrect inputs. Such highly non-linear capability is normally not available in the traditional techniques (*Balageas et al.,* 2006).*Worden* (1997)'s feed-forward network with multi-layer perceptron is a representative application of ANN in structural damage detection. An important benefit of this network is the use of bottleneck, where the patterns can be transferred from the bottom input layer through the hidden layers and reach higher layers that have fewer nodes than input layer. The scheme drives the network to learn the significant features of the corresponding patterns efficiently. Although Worden's work only responded to Level-1 diagnosis problems, there are still attractive novelties. Theoretically, the model not only fits any global damage detection problems, but also does not depend on the structure or damage type. In addition, it can feature with any excitations; this is especially welcome for real structures where usually only ambient vibration is available. *Besides Worden, Wu et al.* (1992) studied another ANN to detect member damage in a 3-storey frame model; *Pande and Barai* (1997) built up a detailed ANN architecture in their study to identify damage in a 21-bar bridge truss. *Zhao et al.* (1998) investigated a counter-propagation neural; *Zapico et al.* (2001) developed an ANN-based procedure for damage assessment of steel structures. *Xu and Humar* (2005, 2006) studied the feasibility of a multi-step ANN approach for Level-3 damage detection problem of a girder bridge using energy-based damage indices. Recently, some new ANN types, such as fuzzy neural networks, were incorporated in numerical damage detection study for multi-storey structures (*Wen et al.,* 2007; *Jiang et al.,* 2011).Most of the studies proved that ANN can provide correct damage information in the numerically simulated structural damage scenarios without considering error. The research in ANN techniques that are predominantly driven by experimental data is still desirable. In addition, the experimental measurement error should be considered in ANN-based methods.

2.3.15 Genetic algorithm in structural damage detection

The damage detection is an inverse problem, the solution of which is normally sought by various optimization algorithms. Apart from the methods that have been used in the model updating methods mentioned in the previous section, other optimization techniques that have been involved in damage detection include the following: constrained least-squares (*Luber,* 1997; *Pothisiri and Hjelmstad,* 2003), linear matrix inequality (*Abdalla et al.,* 2003), multi-criteria non-linear optimization (*Hassiotis and Jeong,* 1993, 1995; *Hassiotis,* 2000), and most popularly, genetic algorithms (GA). The popularity of GA in damage detection realm lies in the fact that, most often, the damage detection problem for a practical structure associates with a large number of damage candidate elements. Therefore, directly applying conventional optimization algorithms for damage detection becomes inefficient and inaccurate. As a widely investigated optimization process, GA is a search heuristic that imitates the mechanisms of biological evolution by the repetitive process of encoding, selection, crossover and mutation (*Goldberg,* 1989). The optimization strategy of the algorithm borrows the ideas from the biological evolution principle 'survival of the fittest'. The advantage of GA over the traditional optimization algorithms is that it does not require knowledge of the relation between the objective function and design variables. This feature gives a higher chance to explore the entire design space (*Erbatur et al.,* 2000; *Lagaros et al.,* 2002). To date, many studies have applied GA successfully in the realm of structural damage identification.

Guo and Li (2009) investigated a two-stage approach using the information fusion technique with micro-search genetic algorithm (MSGA) and included both the natural frequencies and mode shapes. The results from simulations on a cantilever beam showed validity and effectiveness of the two-stage approach. Other representative publications on this topic were made by *Chou and Ghaboussi* (2001), Friswell et al. (1998), *Perera et al.* (2009), and *Lingmi Zhang et al.* (2002).

Among these investigations, it seems that few researchers have discussed in detail the effect of using different setting-up parameters in GA for damage detection applications. *Carlin and Garcia* (1996) published the work particularly on parameter

setting issues of GA, but the recommendations were made with a three-DOF springmass system example. Their conclusions still need verifications by practical complicated structures.

2.4 Critical observation

Based on the extensive review of the existing literature the following are observed.

1. Different approaches have attempted by several researchers to address the problem of condition monitoring based on static and dynamic responses.
2. Most of the researches show that damage is the change in stiffness mainly. However, other researchers have considered damage as the changes in mass and / or damping also, in addition to the changes in stiffness. However, material non-linearity and geometric non-linearity were not considered in most of the approaches.
3. Damage is typically a local phenomenon and may not significantly influence the lower-frequency global response of a structure that is normally measured during vibration tests. Thus, measurement of natural frequency alone for the first few modes may not be sufficient to identify the structural parameters with great accuracy.
4. It is noted that among the identification techniques using measured data in frequency domain, The model using derivatives of modal parameters performed better in many situations.
5. Frequency domain and time domain analyses both have been employed for condition monitoring with specific advantages and limitations. Truly, time-domain and frequency-domain mathematical models complement each other and describe the structural behaviour from different perspective.
6. The deterministic models are able to accurately predict the structural parameter provided sufficient accurate measured data are available. However, the noisy data decreases the accuracy of the numerical model.
7. A few numerical models have limitations of the requirement of measured responses at all nodal degrees of freedom. However, for practical feasibility

damage detection is required to be performed where all data from damaged systems are not available.

8. In addition, lack of accurate and repeatable static and dynamic responses measurement on complex structures in real life situation is a challenging problem to develop an efficient model for condition assessment.
9. It has been observed that the environmental and operational variations such as varying temperature, moisture, and loading conditions affect the dynamic response of the structures and subsequent accuracy of the models.
10. Damage detection is required to be performed where all data from damaged systems are not available. The formulation with noise limited data seems to be practically feasible.
11. It is noted that lack of accurate and repeatable dynamic response measurements on complex structures in real life situation is a challenging problem to develop an efficient model.

Chapter – 3

Theoretical Formulation

3.0 General

Different approaches have been attempted by several researchers to address condition monitoring of structures based on both static and dynamic responses. Structural condition monitoring is a management issue of the structural system involving integration of sensors, smart materials, data acquisition and computational cost etc. In most of the damage detection methods, it is assumed that the damage may alter the stiffness, mass or energy dissipation properties of the structural elements, which in turn alter the measured dynamic response of the system. The objective is, therefore to detect the location and the extent of damage in structure by observing the changes in the static and dynamic responses. In the proposed models, least square method is used to optimize the equation error in a finite element platform. In static models measured static displacement and static strain at few locations are used to detect damage using inverse static approach .Natural frequencies with corresponding modal vectors and their derivatives of first few modes are used to identify the damage in terms of reduction in bending rigidity at the element level in the proposed dynamic models.

3.1 Damage Identification

In general, damage may be defined as the changes developed in a structure that adversely affects the current or future performance of the structure. Therefore, this definition of damage is not meaningful without a comparison between two different states of a system, one of which is assumed to represent the initial and often undamaged state. Damages are limited to changes to the material and/or geometric properties of the structural systems, including changes of the boundary conditions and system connectivity, which adversely affect the current or future performance of these systems. The proposed model is assumed that accurate modal data are available to predict the structural parameters in the initial model. But in practice, the presence of

noise in the measured data is inevitable. Thus, the effect of the noise in measured modal data on the identified structural properties is also studied. The applicability of the proposed model for multiple damage scenario are also examined. The availability of large number of modal data is difficult in real situation. Thus, the effect of number of measured mode data on the accuracy of the identified properties is also studied.

3.2 Mathematical models

3.2.1 Generation of mathematical model of beam

The two dimensional beam element has a total of two possible nodal displacements at each unconstrained joint: one translation components along the Y axes and one rotational component about these axes. The elemental stiffness matrix [K] of two noded beam element in the finite element framework is

$$[K]=\frac{2EI}{L^3}\begin{pmatrix} 6 & 3L & -6 & 3L \\ 3L & 2L^2 & -3L & L^2 \\ -6 & -3L & 6 & -3L \\ 3L & L^2 & -3L & 2L^2 \end{pmatrix} \tag{3.1}$$

where E: Modulus of elasticity: Length of element; I: Moment of inertia of element

Also the elemental consistent mass matrix $[M]$ is

$$[M]=\frac{\overline{m}L}{420}\begin{pmatrix} 156 & 22L & 54 & -13L \\ 22L & 4L^2 & 13L & -3L^2 \\ 54 & 13L & 156 & -22L \\ -13L & -3L^2 & -22L & 4L^2 \end{pmatrix} \tag{3.2}$$

where $\overline{m}$ = mass per unit length.

The local coordinate of stiffness matrix and mass matrix can be converted to the global coordinate stiffness matrix and mass matrix by using the transformation matrix $[T]$. Here the transformation matrix is

$$[T]=\begin{pmatrix} \cos\theta & \sin\theta & 0 & 0 \\ -\sin\theta & \cos\theta & 0 & 0 \\ 0 & 0 & \cos\theta & \sin\theta \\ 0 & 0 & -\sin\theta & \cos\theta \end{pmatrix} \tag{3.3}$$

So the global stiffness matrix $[\bar{K}]$ and the global mass matrix $[\bar{M}]$ can be calculated by the following equation.

$$[\bar{K}]=[T]^T[K][T]$$
$$[\bar{M}]=[T]^T[M][T] \tag{3.4}$$

3.2.2 Generation of mathematical model of frames

The stiffness matrix corresponding to the nodal coordinates for the frame segment is obtained by combining the stiffness matrix for axial effects with the beam and final elemental stiffness matrix is formed as shown below.

$$[K]=\frac{EI}{L^3}\begin{bmatrix} \frac{AL^2}{I} & 0 & 0 & -\frac{AL^2}{I} & 0 & 0 \\ 0 & 12 & 6L & 0 & -12 & 6L \\ 0 & 6L & 4L^2 & 0 & -6L & 2L^2 \\ -\frac{AL^2}{I} & 0 & 0 & \frac{AL^2}{I} & 0 & 0 \\ 0 & -12 & -6L & 0 & 12 & -6L \\ 0 & 6L & 2L^2 & 0 & -6L & 4L^2 \end{bmatrix} \tag{3.5}$$

where A: Cross-sectional Area; E: Modulus of Elasticity: Length of the element

Also the lumped mass matrix at element level is

$$[m]=\frac{\bar{m}L}{2}\begin{bmatrix} 1 & 0 & 0 & 0 & 0 & 0 \\ 0 & 1 & 0 & 0 & 0 & 0 \\ 0 & 0 & 0 & 0 & 0 & 0 \\ 0 & 0 & 0 & 1 & 0 & 0 \\ 0 & 0 & 0 & 0 & 1 & 0 \\ 0 & 0 & 0 & 0 & 0 & 0 \end{bmatrix} \tag{3.6}$$

where $\bar{m}$ is the mass per unit of length.

Combining the mass matrix for flexural effects with axial effects, we obtain the consistent mass matrix for a uniform frame element in reference to the nodal coordinates as

$$[M]=\frac{\bar{m}L}{420}\begin{bmatrix} 140 & 0 & 0 & 70 & 0 & 0 \\ 0 & 156 & 22L & 0 & 54 & -13L \\ 0 & 22L & 4L^2 & 0 & 13L & -3L^2 \\ 70 & 0 & 0 & 140 & 0 & 0 \\ 0 & 54 & 13L & 0 & 156 & -22L \\ 0 & -13L & -3L^2 & 0 & -22L & 4L^2 \end{bmatrix} \tag{3.7}$$

3.2.3 Generation of mathematical model of plane truss

The elemental stiffness matrix [K] of two noded truss element as

$$[K]=\frac{EA}{L}\begin{pmatrix} 1 & 0 & -1 & 0 \\ 0 & 0 & 0 & 0 \\ -1 & 0 & 1 & 0 \\ 0 & 0 & 0 & 0 \end{pmatrix} \tag{3.8}$$

where E: Modulus of elasticity: Length of element and elemental consistent mass matrix $[M]$ is

$$[M]=\frac{\bar{m}L}{6}\begin{pmatrix} 2 & 0 & 1 & 0 \\ 0 & 2 & 0 & 1 \\ 1 & 0 & 2 & 0 \\ 0 & 1 & 0 & 2 \end{pmatrix} \tag{3.9}$$

Where $\bar{m}$ = mass per unit length.

3.3 Damage detection models

The inverse damage detection approaches are classified into the following groups in compliance with the sequence of model development.

a) Static approach with limited deflection data (SLD)

b) Static approach with limited strain data (SSD)

c) Dynamic approach with limited natural frequencies and mode shape data (DFS)

d) Dynamic approach with limited natural frequencies, slope and curvature of mode shape data (DFC)

e) Dynamic approach with modal strain energy data (DMS)

3.3.1 Static approach with limited deflection data (SLD)

The static condensation technique can be adopted to identify the damage of a structure as proposed by *Sanayei and Onepede (1991)*.

$$\begin{bmatrix} f_m \\ f_u \end{bmatrix} = \begin{bmatrix} K_{mm} & K_{mu} \\ K_{um} & K_{uu} \end{bmatrix} \begin{bmatrix} U_m \\ U_u \end{bmatrix} \tag{3.10}$$

where f_m is force sub vector at measured d.o.f.

f_u is force sub vector at unmeasured d.o.f.

U_m is displacement sub vector at measured d.o.f.

U_u is displacement sub vector at unmeasured d.o.f.

K_{mm}, K_{mn}, K_{um} and K_{uu} are the partitioned stiffness matrices with respect to different combination of measured and unmeasured d.o.f . For example K_{mm} stands for a sub matrix corresponding to measured d.o.f with respect to force and response.

Then,

$$\begin{aligned} [f_m] &= [K_{mm}][U_m] + [K_{mu}][U_u] \\ [f_u] &= [K_{um}][U_m] + [K_{uu}][U_u] \\ [f_m] &= [[K_{mm}] - [K_{mu}][K_{uu}]^{-1}[K_{um}]][U_m] + [K_{mu}][K_{uu}]^{-1}[f_u] \end{aligned} \tag{3.11}$$

$[f_m], [f_u], [U_m]$ are known from the static test data and $[K_{mm}], [K_{mu}], [K_{um}], [K_{uu}]$

are stiffness sub matrices which are the functions of the sectional properties assumed primarily. The input force error matrix, [*E*(p)] can be formed with the difference between the [f_m], evaluated from the Eqn. (3.10)

$$[E(p)] = [[K_{mm}] - [K_{mu}][K_{uu}]^{-1}[K_{um}]][U_m] + [K_{mu}][K_{uu}]^{-1}[f_u] - [f_u] \tag{3.12}$$

If the structure is undamaged, then the global stiffness matrix, [*K*] remains unchanged. In that case, the error matrix should be a null matrix. Otherwise, it must not be a null matrix. The error matrix [*E*(p)] can be converted into an error vector {*E*(*p*)} of size NM (Number of Measurements) by 1. The {*p*} is a vector containing the unknown parameter's values. The size of {*p*} is NUP (Number of unknown parameters) by 1. For adjusting the parameters {*p*} in [*E*(*p*)], a first order Taylor Series expansion have been applied. It is necessary for the linearization of the vector as follows:

$$\{E(p+\Delta p)\} \approx \{E(p)\} + [S(p)]\{\Delta p\} \tag{3.13}$$

$$\text{Where, } [S(p)] = \left[\frac{\delta\{E(p)\}}{\delta\{p\}}\right] \tag{3.14}$$

Which is termed as sensitivity matrix.

For the analytical evaluation of the sensitivity matrix [*S*(*p*)], [*E*(*p*)] is differentiated with respect to each parameter as follows

$$[\bar{S}(p_j)] = \left[\frac{\partial[K_{mm}]}{\partial p_j} - \frac{\partial[K_{mu}]}{\partial p_j}[K_{uu}]^{-1}[K_{um}] - [K_{mu}][K_{uu}]^{-1}\frac{\partial[K_{mu}]}{\partial p_j} + [K_{mu}][K_{uu}]^{-1}\frac{\partial[K_{uu}]}{\partial p_j}[K_{uu}]^{-1}[K_{um}]\right][U_m]$$
$$+\left[\frac{\partial[K_{mu}]}{\partial p_j}[K_{uu}]^{-1} - [K_{mu}][K_{uu}]^{-1}\frac{\partial[K_{uu}]}{\partial p_j}[K_{uu}]^{-1}\right][f_u] \tag{3.15}$$

The sensitivity coefficient, $[\bar{S}(p_j)]$ is evaluated for j=1 to NUP. Similar to [*E(p)*], the elements of $[\bar{S}(p_j)]$ are assembled into a vector of size NM by 1. These vectors are horizontally concatenated for j=1 to NSF to form the sensitivity matrix [*S*(*p*)] of size NM by NUP. In most of the cases this formulation for determination of sensitivity coefficient gives a consistent and acceptable result. But a different formulation using displacement as the measured response instead of force can give a more feasible and practical solution for the problem of system identification since measurement of displacement at different d.o.f is relatively easier than the measurement of force responses at those locations. Subsequently an alternative formulation is given below which takes displacement as the measured response during the static condensation.

Linear Minimization

The scalar performance error function, $J(p+\Delta p)$ can be defined as,

$$J(p+\Delta p)=\{E(p+\Delta p)\}^T\{E(p+\Delta p)\} \tag{3.16}$$

Least square technique is applied by minimizing the scalar performance error function with respect to stiffness parameter of each element to identify the change on stiffness.

$$\frac{\delta J(p+\Delta p)}{\delta\{p\}}=\{0\} \tag{3.17}$$

From this it can be derived that

$$[[S(p)]^T[E(p)]-[S(p)]\{\Delta p\}]=\{0\} \tag{3.18}$$

The different sets of forces are applied to the feasible nodes & the measurements are taken for each sets of force at sensitive d.o.f with the information gathered from the sensitivity analysis. The number of independent measurements may be lesser than or equal to or greater than the number of unknown parameters. For the first case, there is no unique solution. For the next case, the direct inversion method can be used as

$$\{\Delta p\}=-[S(p)]^{-1}\{E(p)\} \tag{3.19}$$

For the last case, the sensitivity matrix $[S(p)]$ is a rectangular matrix. So, the following pseudo inverse technique is adopted for the determination of $\{\Delta p\}$.

$$\{\Delta p\}=[[S(p)]^T[S(p)]]^{-1}[S(p)]^T\{E(p)\} \tag{3.20}$$

After evaluating the vector $\{\Delta p\}$, the change in structural properties an iterative process is used to identify the damaged parameter as,

$$\{p\}^{r+1}=\{p\}^r+\{\Delta p\} \tag{3.21}$$

3.3.2 Static approach with limited strain data (SSD)

Strain displacement relationship

The finite element model is based on the stiffness relationship between forces and displacements. To utilize strain measurements, a mapping between displacements and strains is developed as suggested by *Sanayei a*nd *Salentik (1996).*A relationship is developed in the form of an element mapping vector $\{B_n\}$ in the global co-ordinate

system. At first the mapping vector $\{B_n\}$ is formulated in the local co-ordinate system, such that the following relationship is satisfied for the elemental strain ε_n and displacement $\{\overline{U_n}\}$.

$$\varepsilon_n = \{\overline{B_n}\}\{\overline{U_n}\} \tag{3.22}$$

Then $\{U_n\}$ is transformed from the local coordinates to the global coordinates as

$$\{\overline{U_n}\} = [T_n]\{U_n\} \tag{3.23}$$

And finally the global strain displacement relationship is developed as

$$\{\varepsilon\} = [B]\{U\} \tag{3.24}$$

Finite-Element Model

The static element equation for a constrained structural system is

$$\{F\} = [K(p)]\{U\} \tag{3.25}$$

By substituting Eqn. 3.23 in Eqn. 3.24 it gives

$$\{\varepsilon\} = [B][K(p)]^{-1}\{F\} \tag{3.26}$$

$$[\varepsilon] = [B][K(p)]^{-1}[F] \tag{3.27}$$

It is not require all the strain of a system; therefore Eqn. 3.27 is first partitioned based of measured strains (subscript "*a*") and unmeasured strains (subscript "*b*")

$$\begin{bmatrix} \varepsilon_a \\ \varepsilon_b \end{bmatrix} = \begin{bmatrix} B_a \\ B_b \end{bmatrix}[K(p)]^{-1}[F] \tag{3.28}$$

Since there is no need of unmeasured strain s, $\{\varepsilon_b\}$ is eliminated as

$$[\varepsilon_a] = [B_a][K(p)]^{-1}[F] \tag{3.29}$$

Output Strain Error Function

To measure the difference between analytical strain and measured strain an error function is formed. The output strain error function is defined as

$$[e(p)] = [e_a(p)]^a - [e_a]^m \tag{3.30}$$

"a" subscript implies analytical values; and "m" implies measured values. On substituting Eqn. 3.29 in Eqn. 3.30.

$$[e(p)] = [B_a][K(p)]^{-1}[F] - [e_a]^m \tag{3.31}$$

Finally the error is expanded using Taylor Series expansion to develop the sensitivity matrix

$$\left[\overline{S}(p_j)\right] = -[B_a][K(p)]^{-1}\frac{\partial}{\partial p_j}([K(p)])[K(p)]^{-1}[F] \tag{3.32}$$

3.3.3 Dynamic approach with limited natural frequencies and mode shape data (DFS)

The dynamic equilibrium equation of motion of finite element model can be expresses as,

$$[\mathrm{m}]\{\ddot{\mathrm{u}}\} + [\mathrm{k}]\{\mathrm{u}\} = \{\mathrm{f}\} \tag{3.33}$$

Where, [k] and [m] are the stiffness and consistent mass matrices of the element respectively. {u} and {f} are the nodal displacements and force vectors. Assembling the element equations and applying boundary conditions, one can obtain the following equilibrium equation for damped forced vibration

$$[M]\{\ddot{U}\} + [C]\{\dot{U}\} + [K]\{U\} = \{F(t)\} \tag{3.34}$$

The same equation for the undamped forced vibration shall be

$$[M]\{\ddot{U}\} + [K]\{U\} = \{F(t)\} \tag{3.35}$$

Where $[M], [K]$, $[C], \{U\}$ and $\{F(t)\}$ indicates the global mass matrix, global stiffness matrix, global damping matrix, nodal displacement and force vector respectively.

For free vibration, substitution of $\{F(t)\} = 0$ and $\{\mathrm{U}\} = \{\varphi \exp(i\omega t\}$ in equation (3.35) gives,

$$\left([K]-\omega^2[M]\right)\{\varphi\}=\{0\} \text{ i.e. } [K]\{\varphi\}=\lambda[M]\{\varphi\} \text{ where } \lambda=\omega^2. \qquad (3.36)$$

Equation (3.36) is a generalized eigenvalue problem that can be solved for λ and $\{\varphi\}$. The eigenvector $\{\varphi\}$ is the mode shape and eigenvalue λ is the square of the associated natural frequency in radians per seconds. The identification of the structural parameters can be formulated as minimization of a nonnegative error function ε which is defined according to *Hajela, and Soeiro (1990*),

$$\text{Minimize, } \varepsilon=\sum_{k=1}^{p}\left([K]\{\varphi_k\}-\lambda_k[M]\{\varphi_k\}\right)^2 \qquad (3.37)$$

Where, λ_k and $\{\varphi k\}$ are the k^{th} measured modal data; p is the total number of measured modes. The characteristics equation for the motion can be partitioned in terms of mode shapes at measured and unmeasured d.o.f for each measured frequency as shown below as suggested by *Hajela and Soeiro(1990).*

$$\left[\begin{array}{c|c}K_{aa} & K_{ab}\\ \hline K_{ba} & K_{bb}\end{array}\right]\left\{\begin{array}{c}\phi_a\\ \hline \phi_b\end{array}\right\}_i=\lambda_i\left[\begin{array}{c|c}M_{aa} & M_{ab}\\ \hline M_{ba} & M_{bb}\end{array}\right]\left\{\begin{array}{c}\phi_a\\ \hline \phi_b\end{array}\right\}_i \qquad (3.38)$$

By condensing out the unmeasured mode shapes the following equation can be obtained.

$$\begin{aligned}&[K_{aa}]\{\phi_a\}_i-[K_{ab}]\left([K_{bb}]-\lambda_i[M_{bb}]\right)^{-1}\left([K_{ba}]-\lambda_i[M_{ba}]\right)\{\phi_a\}_i\\&=\lambda_i[M_{aa}]\{\phi_a\}_i-\lambda_i[M_{ab}]\left([K_{bb}]-\lambda_i[M_{bb}]\right)^{-1}\left([K_{ba}]-\lambda_i[M_{ba}]\right)\{\phi_a\}_i\end{aligned} \qquad (3.39)$$

The modal stiffness based error function $\{e(p)\}$ is defined as the residual of the equation no (3.39) for each mode, where p is the unknown parameter.

$$\{e(p)\}=\begin{pmatrix}\left([K_{aa}]-\lambda_i[M_{aa}]\right)-\left([K_{ab}]-\lambda_i[M_{ab}]\right).\\ \left([K_{bb}]-\lambda_i[M_{bb}]\right)^{-1}\left([K_{ba}]-\lambda_i[M_{ba}]\right)\end{pmatrix}\{\phi_a\} \qquad (3.40)$$

The modal error function is inverse of stiffness and the mass matrix and therefore it is non-linear. Using Taylor Series expansion it has been approximated to linear function.

The analytical sensitivity coefficients $\bar{S}(p_j)$ associated with the "modal stiffness – based error function" are derivative of Eqn. (3.40) for each unknown parameter p_j.

$$\left[\bar{S}(p_j)\right]=\begin{pmatrix}\left(\frac{\partial[K_{aa}]}{\partial p_j}-\lambda\frac{\partial[M_{aa}]}{\partial p_j}\right)-\left(\frac{\partial[K_{ab}]}{\partial p_j}-\lambda\frac{\partial[M_{ab}]}{\partial p_j}\right)\\ *\left([K_{bb}]-\lambda[M_{bb}]\right)^{-1}\left([K_{ba}]-\lambda[M_{ba}]\right)\\ +\left([K_{ab}]-\lambda[M_{ab}]\right)\left([K_{bb}]-\lambda[M_{bb}]\right)^{-1}*\left(\frac{\partial[K_{bb}]}{\partial p_j}-\lambda\frac{\partial[M_{bb}]}{\partial p_j}\right).\left([K_{bb}]-\lambda[M_{bb}]\right)^{-1}.\left([K_{ba}]-\lambda[M_{ba}]\right)\\ -\left([K_{bb}]-\lambda[M_{bb}]\right)^{-1}.\left([K_{ab}]-\lambda[M_{ab}]\right)\left(\frac{\partial[K_{ba}]}{\partial p_j}-\lambda\frac{\partial[M_{ba}]}{\partial p_j}\right)\end{pmatrix}\{\phi_a\} \quad (3.41)$$

A Gauss -Newton method is used to find the change of the parameters $\{\Delta p\}$ for each iteration k. $\{p_{k+1}\}=\{p_k\}+\{\Delta p\}$ Iteration continues till estimation of the parameters is found. The convergence is specified by the desired tolerance level with the relative change in $\{\Delta p\}$ on the order of $10^{-3}, 10^{-6}$ etc.

3.3.4 Dynamic approach with limited natural frequencies, modal slope and curvature mode shape data (DFC)

From this model error is formed based on mode shpaes and slopes and curvature of mode shapes as suggested by *Pandey and Biswas(1991), Pandey and Biswas(1994).*Generalized eigenvalue equation is to be differentiated two times successively to develop an equation consisting of slope and the curvature of the mode shapes and subsequently a non negative error function is developed for the identification of damages in structural properties.

$$([k''] - \lambda[M'']\{\Phi\}_i + 2([k'] - \lambda[M']\{\Psi\}_i + ([k] - \lambda[M])\{\xi\}_i) = 0 \quad (3.42)$$

where $[k]$ and $[M]$ are stifness and mass matrices of the structure $[k']$ and $[M']$ are the first order differential and

$[k'']$ and $[M'']$ are the second order differential

$\{\xi\}$ and $\{\psi\}$ are mode shape curvature and modal slope respectively

Also λ is the eigen value vctor and $\{\phi\}$ is mode shape vector

Similarly the error function shall be divided into three parts as shown in equation

$$\{e(p)\}_i = \{e(p)_1\}_i + \{e(p)_2\}_i + \{e(p)_3\}_i \quad (3.43)$$

The mode shapes, slope and modal curvature of mode shapes based error function $\{e(p)\}_i$ is defined as the residual of each mode, where {p} is the vector of the unknown parameters. Unknown parameters are the axial, bending, and torsional rigidities of the structure.

$$\{e(p)_1\}_i = (([k''_{aa}] - \lambda[M''_{aa}]) + [k''_{ab}] - \lambda[M''_{ab}]).([k''_{bb}] - \lambda[M''_{bb}])^{-1}.(\lambda[M''_{ba}] - [k''_{ba}]))\{\Phi_a\}_i \quad (3.44)$$

$$\{e(p)_2\}_i\} = (([k'_{aa}] - \lambda[M'_{aa}]) + ([k'_{ab}] - \lambda[M'_{ab}]).([k'_{bb}] - \lambda[M'_{bb}])^{-1}.(\lambda[M'_{ba}] - [k'_{ba}]))2\{\Psi_a\}_i \quad (3.45)$$

And

$$\{e(p)_3\}_i = (([k_{aa}] - \lambda([M_{aa}]) + ([k_{ab}] - \lambda([M_{ab}]).[k_{bb}] - \lambda([M_{bb}])^{-1}(\lambda[M_{ba}] - [k_{ba}]) \quad (3.46)$$

Using the Taylor Series expansion, the mode shape and modal slope and curvature of mode shapes based error function is approximated linearly by

$$[S(p)_1]_i = (([(\frac{\delta}{\partial p}[k''_{aa}] - \lambda\frac{\partial}{\partial I}[M''_{aa}]) + (\frac{\partial}{\partial p}[k''_{ab}] - \lambda\frac{\partial}{\partial p}[M'_{ab}])](\left[(\lambda[M''_{ba}] - [k''_{ba}])([k'_{bb}] - \lambda[M'_{bb}])^{-1}\right]) - [(\frac{\partial}{\partial_x}[k''_{bb}] - \lambda\frac{\partial}{\partial A}[M''_{hh}])([k''_{hh}] - \lambda[M''_{hh}])^{-2}(\lambda\frac{\partial}{\partial p}[M''_{ba}] - \frac{\partial}{\partial A}[k''_{ba}])].([k''_{aa}] - \lambda[M''_{aa}] + [k''_{ab}] - \lambda[M''_{ab}]))\{\Phi_a\}_i \quad (3.47)$$

$$[S(p)_2]_i=([(\frac{\partial}{\partial p}[k'_{aa}]-\lambda\frac{\partial}{\partial p}[M'_{aa}])+(\frac{\partial}{\partial p}[k'_{ab}]-\lambda\frac{\partial}{\partial p}[M'_{ab}])].($$
$$\left[(\lambda[M'_{ba}]-[k'_{ba}])([k'_{bb}]-\lambda[M'_{bb}])^{-1}\right])-[(\frac{\delta}{\partial p}[k'_{bb}]-$$
$$\lambda\frac{\partial}{\partial p}[M'_{bb}])([k'_{bb}]-\lambda[M'_{bb}])^{-2}($$
$$\lambda\frac{\partial}{\partial p}[M'_{ba}]-\frac{\partial}{\partial p}[k'_{ba}])].([k'_{aa}]-\lambda[M'_{aa}]+[k'_{ab}]-\lambda[M'_{ab}]) \quad (3.48)$$

$$[S(p)_3]_i=([(\frac{\partial}{\partial p}[k_{aa}]-\lambda\frac{\partial}{\partial p}[M_{aa}])+(\frac{\partial}{\partial p}[k_{ab}]-\lambda\frac{\partial}{\partial p}[M_{ab}])].($$
$$[(\lambda[M_{ba}]-[k_{ba}])([k_{bb}]-\lambda[M_{bb}])^{-1}])-[(\frac{\partial}{\partial p}[k_{bb}]-$$
$$\lambda\frac{\partial}{\partial p}[M_{bb}])([k_{bb}]-\lambda[M_{bb}])^{-2}($$
$$\lambda\frac{\partial}{\partial p}[M_{ba}]-\frac{\partial}{\partial p}[k_{ba}])].([k_{aa}]-\lambda[M_{aa}]+[k_{ab}]-\lambda[M_{ab}])\{\xi_a\}_i \quad (3.49)$$

Finally the sensitivity matrix shall be developed considering contribution of all three sensitivity matrices.

$$[S(p)]_i=[S(p)_1]_i+[S(p)_2]_i+[S(p)_3]_i=([($$
$$\frac{\partial}{\partial p}[k''_{aa}]-\lambda\frac{\partial}{\partial p}[M''_{aa}])+(\frac{\partial}{\partial I}[k''_{ab}]-\lambda\frac{\partial}{\partial p}[M'_{ab}])].($$
$$\left[(\lambda[M''_{ba}]-[k''_{ba}])([k'_{bb}]-\lambda[M'_{bb}])^{-1}\right])-[(\frac{\partial}{\partial p}[k''_{bb}]-$$
$$\lambda\frac{\partial}{\partial p}[M''_{bb}])([k''_{bb}]-\lambda[M''_{bb}])^{-2}($$
$$\lambda\frac{\partial}{\partial p}[M''_{ba}]-\frac{\partial}{\partial p}[k''_{ba}])].([k''_{aa}]-\lambda[M''_{aa}]+[k''_{ab}]-\lambda[M''_{ab}])\{\Psi_a\}_i+([($$
$$\frac{\partial}{\partial p}[k'_{aa}]-\lambda\frac{\partial}{\partial p}[M'_{aa}])+(\frac{\partial}{\partial p}[k'_{ab}]-\lambda\frac{\partial}{\partial v}[M'_{ab}])].($$
$$\left[(\lambda[M'_{ba}]-[k'_{ba}])([k'_{bb}]-\lambda[M'_{bb}])^{-1}\right])-[(\frac{\delta}{\partial p}[k'_{bb}]-$$
$$\lambda\frac{\partial}{\partial p}[M'_{bb}])([k'_{bb}]-\lambda[M'_{bb}])^{-2}($$
$$\lambda\frac{\partial}{\partial p}[M'_{ba}]-\frac{\partial}{\partial p}[k'_{ba}])].([k'_{aa}]-\lambda[M'_{aa}]+[k'_{ab}]-\lambda[M'_{ab}])2\{\Psi_a\}_i+([($$
$$\frac{\partial}{\partial p}[k_{aa}]-\lambda\frac{\partial}{\partial I}[M_{aa}])+(\frac{\partial}{\partial A}[k_{ab}]-\lambda\frac{\partial}{\partial p}[M_{ab}])].($$
$$[(\lambda[M_{ba}]-[k_{ba}])([k_{bb}]-\lambda[M_{bb}])^{-1}])-[(\frac{\partial}{\partial p}[k_{bb}]-$$
$$\lambda\frac{\partial}{\partial A}[M_{bb}])([k_{bb}]-\lambda[M_{bb}])^{-2}($$
$$\lambda\frac{\partial}{\partial r}[M_{ba}]-\frac{\partial}{\partial p}[k_{ba}])].([k_{aa}]-\lambda[M_{aa}]+[k_{ab}]-\lambda[M_{ab}])\{\xi_a\}_i \quad (3.50)$$

Similar optimization technique is adopted as described in chapter 3.3.1 to minimize the error developed and also for the updating the structural parameter of each element in each iteration.

3.3.5 Dynamic Approach with Modal Strain Energy data (DMS)

Elemental modal strain energy (MSE) is defined as the product of the elemental stiffness matrix and the second power of its mode shape component (*Shi et al.* 1998). For the j^{th} element and i^{th} mode, the elemental MSE before and after the occurrence of damage are given as

$$MSE_{ij} = \Phi_i^T K_j \Phi_i \quad , \quad MSE_{ij}^d = \Phi_i^{dT} \mathrm{K}_j \Phi_i^d \tag{3.51}$$

Where MSE_{ij} and MSE_{ij}^d= j^{th} elemental modal strain energy corresponding to the i^{th} mode shape for the undamaged and damaged states, respectively; K_j is the j^{th} elemental stiffness matrix, and ϕ =the i^{th} mode shape. The superscript *d* denotes the damaged state. Since the damage elements are not known, the undamaged elemental stiffness matrix K_j is used instead of the damaged one as an approximation in MSE_{ij}^d. The elemental modal strain energy change ratio (MSECR) has been verified to be a good indicator for damage localization and is defined as (*Shi et al.*1998).

$$MSECR_{ij} = \frac{\left| MSE_{ij}^d - MSE_{ij} \right|}{MSE_{ij}} \tag{3.52}$$

A structural damage often causes a loss of stiffness in one or more elements of a structure but not a loss in the mass. In the theoretical development that follows, damage is assumed to affect only the stiffness matrix of the system. When damage occurs in a skeletal structure, it can be represented by a small perturbation in the original system. Thus, the stiffness matrix K^d, the i^{th} modal eigenvalue λ_i^d, and the i^{th} mode shapes ϕ_i d.o.f the damaged system can be expressed as follows:

$$\mathrm{K}^{\mathrm{d}} = \mathrm{K} + \sum_{\mathrm{j}=1}^{\mathrm{L}} \Delta \mathrm{K}_{\mathrm{j}} = \mathrm{K} + \sum_{\mathrm{j}=1}^{\mathrm{L}} \alpha_{\mathrm{j}} \mathrm{K}_{\mathrm{j}}, (-1 < \alpha_{\mathrm{j}} << 0) \tag{3.53}$$

$$\lambda_i^d = \lambda_i + \Delta\lambda_i \tag{3.54}$$

$$\Phi_i^d = \Phi_i + \Delta\Phi_i \tag{3.55}$$

Where α_j= coefficient defining a fractional reduction in the j^{th} elemental stiffness matrices; and L=total number of elements in the system.

The elemental modal strain energy change (MSEC) for the j^{th} element in the i^{th} mode is expressed as

$$MSEC_{ij} = \Phi_i^{d^T} K_j \Phi_i^d - \Phi_i^T K_j \Phi_i \tag{3.56}$$

Substituting Eqn. (3.53) into Eqn. (3.56) and neglecting the second-order terms, the $MSEC_{ij}$ becomes

$$MSEC_{ij} = 2\Phi_i^T K_j \Delta\Phi_i \tag{3.57}$$

For a small perturbation in an undamped d.o.f dynamic system, the equation of motion becomes

$$[(K + \Delta K) - (\lambda_i + \Delta\lambda_i)M](\Phi_i + \Delta\Phi_i) = 0 \tag{3.58}$$

Neglecting second-order terms, Eqn. (3.58) leads to

$$(K - \lambda_i M)\Delta\Phi_i = \Delta\lambda_i M\Phi_i - \Delta K\Phi_i \tag{3.59}$$

$\Delta\Phi_i$ in Eqn. (3.59) can be expressed as a linear combination of mode shapes of the original system (*Fox and Kapoor* 1968)

$$\Delta\Phi_i = \sum_{k=1}^{n} d_{ik}\Phi_k \tag{3.60}$$

Where d_{ik} =scalar factors and n=total number of modes of the original system.

Substituting Eqn. (3.59) into Eqn. (3.60), and pre multiplying Φ_r^T to both sides of Eqn. (3.59), it can be modified as

$$\sum_{k=1}^{n} d_{ik}\Phi_r^T(K-\lambda_i M)\Phi_k = \Delta\lambda_i\Phi_r^T M\Phi_i - \Phi_r^T\Delta K\Phi_i \tag{3.61}$$

With the orthogonal relationship, it can be simplified into the following when *r* is not equal to *i*:

$$d_{ir} = -\frac{\Phi_r^T\Delta K\Phi_i}{\lambda_r-\lambda_i}, where, r\neq i \tag{3.62}$$

For the case of $r=i$, d_{ir} equals 0.0 from the orthogonal relationship $\Phi_i^T M\Phi_i=I$. Therefore, Eqn. (3.60) can be written as

$$\Delta\Phi_i = \sum_{r=1}^{n} -\frac{\Phi_r^T\Delta K\Phi_i}{\lambda_r-\lambda_i}\Phi_r, where, r\neq i \tag{3.63}$$

Substituting Eqn. (3.63) into Eqn. (3.57), the $MSEC_{ij}$ becomes

$$MSEC_{ij} = 2\Phi_r^T K_j\left(\sum_{r=1}^{n} -\frac{\Phi_r^T\Delta K\Phi_i}{\lambda_r-\lambda_i}\Phi_r\right), where, r\neq i \tag{3.64}$$

Substituting Eqn. (3.53) into Eqn. (3.64), one can obtain

$$MSEC_{ij} = \sum_{p=1}^{L} -2\alpha_p\Phi_i^T K_j\sum_{r=1}^{n}\frac{\Phi_r^T K_p\Phi_i}{\lambda_r-\lambda_i}\Phi_r, where, r\neq i \tag{3.65}$$

The term on the left-hand side of Eqn. (3.65) is the elemental modal strain energy change of the *j*th element in the *i*th mode, which can be calculated from Eqn. (3.56) by using the experimental mode shape of the undamaged and damaged states. And all the terms on the right-hand side of Eqn. (3.65) except $\alpha_p$are all known information of the undamaged system. Solving Eqn. (3.65) can be used to quantify the damage magnitude.

If we assume the number of damaged elements to be identified is *q*, and the number of the measured elements for the computation of MSEC in Eqn. (3.56) is *J*, Eqn. (3.65) can be expressed in the following form for the *i*th mode:

$$\begin{Bmatrix} MSEC_{i1} \\ MSEC_{i2} \\ \cdots \\ MSEC_{iJ} \end{Bmatrix} = \begin{bmatrix} \beta_{11} & \beta_{12} & \cdots & \beta_{1q} \\ \beta_{21} & \beta_{22} & \cdots & \beta_{2q} \\ \cdots & \cdots & \cdots & \cdots \\ \beta_{J1} & \beta_{J2} & \cdots & \beta_{Jq} \end{bmatrix} \begin{Bmatrix} \alpha_1 \\ \alpha_2 \\ \cdots \\ \alpha_J \end{Bmatrix} \tag{3.65}$$

in which the element β_{st} (s=1,2,...,J; t=1,2,...,q)=the sensitivity coefficient of MSEC for the suspected damaged element, and it is given by

$$\beta_{st} = -2\sum_{r=1}^{n} \Phi_r^T K_s \frac{\Phi_r^T K_t \Phi_i}{\lambda_r - \lambda_i} \Phi_r, where, r \neq i \tag{3.67}$$

3.4 Application Technique

Several examples are considered for the validation of different models adopted. The summary of the examples are given below. However, the details of these examples are described in Chapter 5.

Example I: Acrylic cantilever beam

Example II: Steel cantilever beam

Example III: Steel fixed-fixed beam

Example IV: 13 member steel pratt truss

Example V: RCC gable frame

Example VI: Steel portal frame.

A. Static approach with limited deflection data (SLD)

i) Numerically generation of static deflection data of first few d.o.f of rigid frame structure based on finite element method.

ii) Identification of structural parameters with analytical and experimentally measured deflection data of the structure with different damage conditions
(Example II as mentioned in chapter 5.2 and Example IV as mentioned in chapter 5.4).

B. Static approach with limited strain data (SSD)

i) Numerically and experimentally generation of static strain data of few d.o.f of rigid frame structure based on finite element method.
ii) Identification of structural parameters with analytical and experimentally measured strain and deflection data of the structure with different damage conditions. (Example II as mentioned in chapter 5.2 , Example IV as mentioned in chapter 5.4).

C. Dynamic approach with limited natural frequencies and mode shape data (DFS)

i) Numerically generation of set of modal data for rigid framed structure of first few modes mixed with random noises of specified level.
ii) Identification of structural parameters with analytical and experimentally measured modal data of the structure with different damage conditions.
iii) Various degrees of damaged states to study the effect of damage severity on the modal parameters and identification (Example II as mentioned in chapter 5.2 ,Example IV as mentioned in chapter 5.4).

D. Dynamic approach with limited natural frequencies, modal slope and curvature mode shape data (DFC)

i) Numerically generation of set of modal data for rigid framed structure of first few modes mixed with random noises of specified level.
ii) Identification of structural parameters with analytical modal data of the structure with different damage condition. (Example III as mentioned in chapter 5.3).

E. Dynamic approach with modal strain energy data (DMS)

i) Numerically and experimentally generation of set of modal data for rigid framed structure of first few modes mixed with random noises of specified level.

ii) Identification of structural parameters with analytical and experimentally measured modal data of the structure with different damage conditions. (Example V as mentioned in chapter 5.5 and Example VI as mentioned in chapter 5.6).

Chapter – 4

Experimental Study

4.0 General

Experimental studies are essential and helpful to understand the effect of various uncertainties, inherently present in real situations. It is also important for validation of the proposed numerical model. In the present study experimentation on simple structure has been performed. Most importantly, the feasibility of the developed numerical model for the structural condition monitoring is studied using experimentally obtained data. The experimental investigation may be divided into four parts as follows.

A. Static testing to measure the static deflection and bending strain at selected d.o.f. developed in the structure.
B. Dynamic testing of structures to acquire vibrational responses in time domain with the impact hammer loading and with the response only data using one directional shake table.
C. Extraction of the modal data from phase change of FRF in case of experiment modal analysis or by singular value decomposition in case of operational modal testing
D. Validation of the proposed numerical model on condition monitoring with the experimentally obtained from both static and dynamic data.

4.1 Experiment for static data:

Two no of experiments are performed for the collection of static test data. Displacements and static strains are measured at limited degrees of freedom.

4.1.1 Different instruments for static testing:

a) Strain gauges and strain indicator:

To record the bending strain data at specified nodes strain gauges are attached with the test specimen. Strain gauges are attached properly and then applied soldering

process for connection with wire & strain gauges. Single strand wires are connected with the strain gauges very carefully. All wire connections are checked by multi-meter. To record the strain data at specified nodes strain gauges are satisfactorily bonded to almost any solid material with the test material by adhesive. The soldering point has to be homogeneous, smooth and shiny. Gauge factor is defined as unit change in resistance per unit change in length of strain wire. The gauge factor of the strain gauges which are used for the experiment purpose is 2.1.

The digital strain indicator and the different Wheatstone Bridges diagrams are shown in Fig. 4.1.1 and Fig. 4.1.2.

Fig 4.1.1: Digital strain indicator, Kristech Automation, India

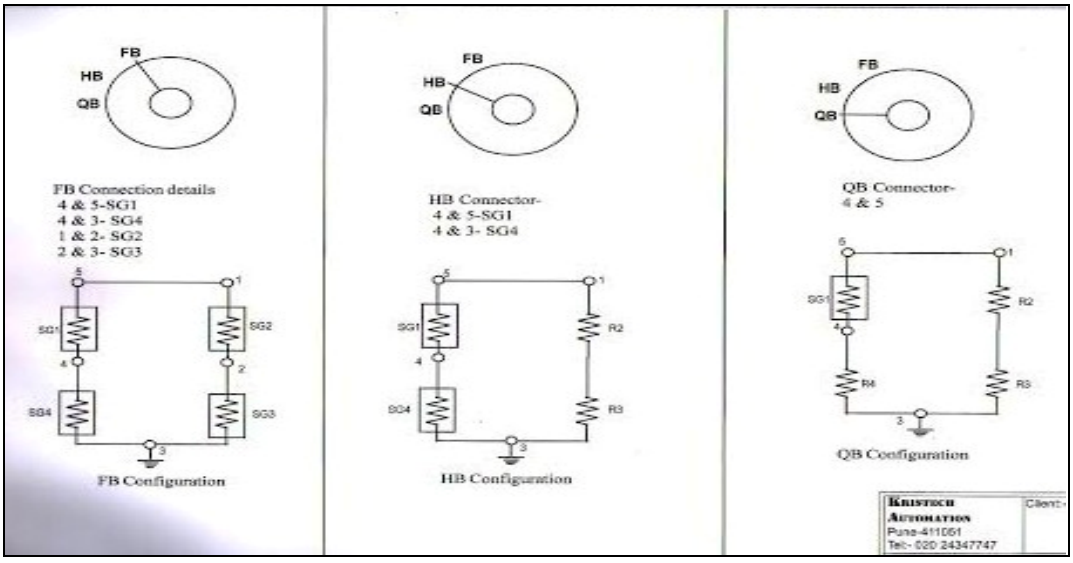

Fig 4.1.2: Different Wheatstone Bridge configurations used for the static bending strain measurement

b) Dial gauge and Magnetic stand

A dial gauge is a precision measurement commonly used to measure machined parts for production tolerances or displacement. Dial gauges are capable of producing extremely fine measurement values; increments of 0.00005 inch (0.001mm) are possible with some gauges. Measurement inputs are transferred to the gauge via a plunger, hinged lever, or the jaws of a veneer. Plunger instruments are generally used in conjunction with a clamp or stand which holds the gauge in a fixed position in relation to the work piece. The work piece is then rotated or moved to take the measurements. The dial gauge used for the experiment is shown in Fig. 4.1.3.

A magnetic base is a magnetic fixture based on a magnet that can effectively be turned "on" and "off" at will; they are often used to hold a dial indicator. A magnetic base can therefore be attached in a variety of positions to any attractive surface, allowing the base to be positioned in the best orientation for the part to be tested. Combine this with the flexibility of movement allowed by the arms gives the operator a large range of options in positioning the dial indicator. The magnetic base stand used for the experiment is shown in Fig. 4.1.4.

Fig 4.1.3: Dial gauge

Fig 4.1.4: Magnetic base stand

Several other instruments used for the experiment like multimeter, clamps, scale, different weights etc. are shown in Fig 4.1.5.

Fig 4.1.5: Different instruments used for the experiment

4.1.2 Example I (Acrylic cantilever beam)

A cantilever beam of 350 mm span length is prepared from 25 mm wide and 8 mm thick rectangular acrylic strip. Edge of the beam is rigidly fixed with three numbers of clamps to the supporting frame. The clamps are tightened to the maximum extent to ensure adequate rigidity. The statistical variations in length, width and thicknesses are measured. The specimens are intentionally not machined perfectly to have the variations as expected in the structures in practice. Firstly the damage was introduced with 5% reduction of thickness in element no 9 and subsequently thickness reduction was increased to 10%, 20%, 30%, and 50% in the element no 9 to perform different single damage cases (1D9). After performing the experiment on single damage cases, the double damage case (2D9,17) have been created by reducing the thickness by 5%,10%, 20%, 30%, and 50% in the element no 17 keeping a fixed reduction(50%) of thickness in the element no 9 . The schematic diagram of the undamaged beam is shown in Fig.4.1.6 and also single damage and double damage states of the beams are shown in Fig.4.1.7 and Fig. 4.1.8.

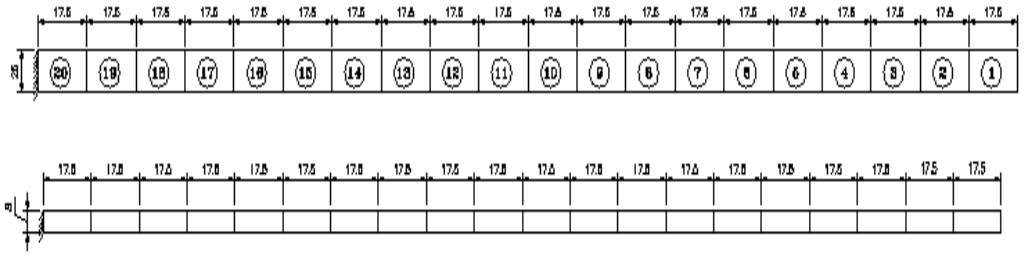

Fig 4.1.6: Plan and elevation of the undamaged cantilever beam

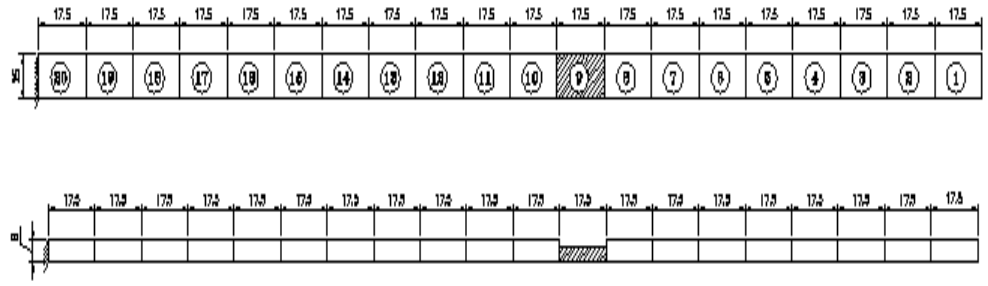

Fig 4.1.7: Plan and elevation of damaged (single element-1D9) cantilever beam.

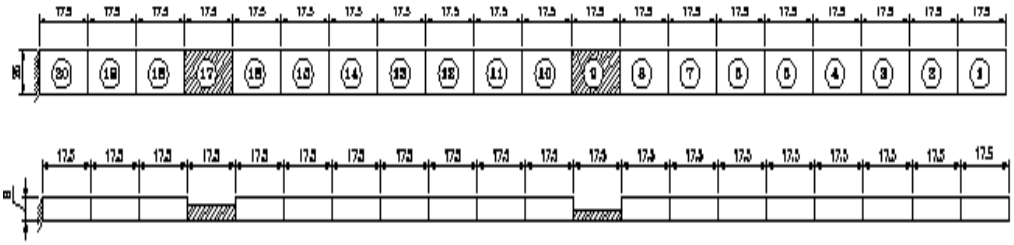

Fig 4.1.8: Plan and elevation of damaged (double element-2D9, 17) cantilever beam.

4.1.2.1 Mechanical properties of the specimen

The mechanical properties of the test specimen are evaluated based on the tensile test and bending test in accordance to IS: 1608 (1995). The tensile test of the material is conducted by the load controlled, 600 KN capacity universal testing machine (Model AMT-60 Remote Display and Control System), ASI Sales Pvt. Ltd, India make to evaluate the modulus of elasticity, yield stress, ultimate stress, percentage elongation. The

test specimen for the tensile test is shown in Fig. 4.1.9 and setup for test during bending test is shown in Fig. 4.1.10.

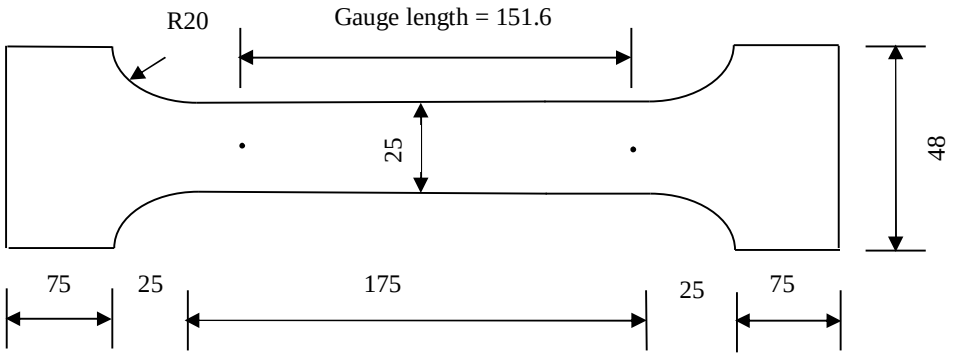

Fig 4.1.9: Different dimensions for the test specimen (all dimensions are in mm)

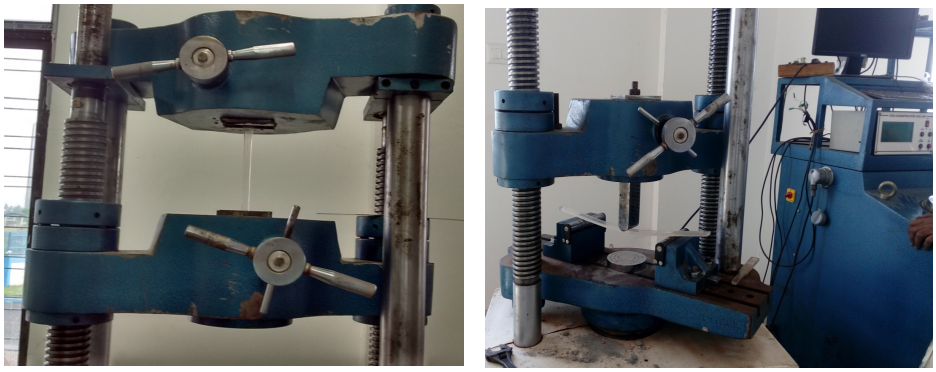

Fig 4.1.10: Setup for tensile test and bending test in universal testing machine

The dimensions are made in accordance with IS: 1608, 1995. The gauge length is kept as 151.60 mm. The Poisson Ratio of the acrylic material which is used for test purpose is 0.35 and mass density of the material is 1.18 g/cm^3.

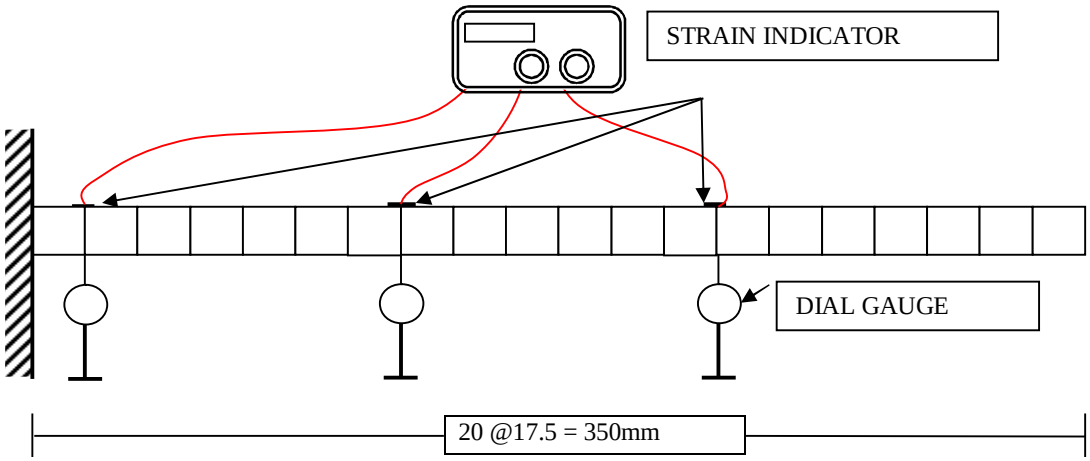

Fig 4.1.11: Schematic diagram of the experimental set up

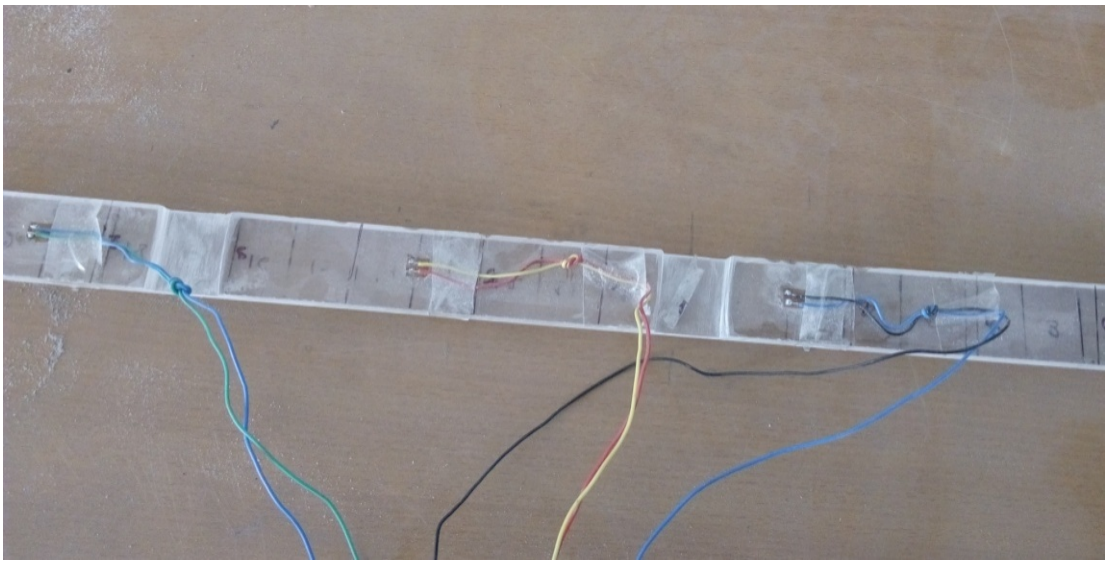

Fig 4.1.12: Strain gauges attached with the experimental acrylic beam

Different measured dimensions of the acrylic beam for UD, 1D1 and 2 D9-17 cases are reflected in Table 4.1.1.

Table 4.1.1: Measured dimensions of cantilever beam

Element Number	**Length (mm)**			**Width (mm)**			**Thickness (mm)**		
Damaged Condition	**UD**	**1D9**	**2D9-17**	**UD**	**1D9**	**2D9-17**	**UD**	**1D9**	**2D9-17**
Case I	350	350	350	25	25	25	8	7.6	7.6
Case II	350	350	350	25	25	25	8	7.2	7.2
Case III	350	350	350	25	25	25	8	6.4	6.4
Case IV	350	350	350	25	25	25	8	5.6	5.6
Case V	350	350	350	25	25	25	8	4.0	4.0

UD: Undamaged; 1D: Single element (9) damaged; 2D: Double element damage (9, 17)

.

4.1.2.2 Physical Properties of the specimen

The details of the different structural parameters based on the measurement of the undamaged and damaged beams are indicated in Table 4.1.2.

Table 4.1.2: Measured structural parameters of cantilever beam

Element Number	**Cross Sectional Area (mm^2)**			**Moment of Inertia (mm^4)**			**Mass Density (10^{-6} X Ns^2/mm^2)**		
Damaged Condition	**UD**	**1D9**	**2D9-17**	**UD**	**1D9**	**2D9-17**	**UD**	**1D9**	**2D9-17**
Case I	200	190	190	1066.667	914.533	914.533	1180	1180	1180
Case II	200	180	180	1066.667	777.600	777.600	1180	1180	1180
Case III	200	160	160	1066.667	546.133	546.133	1180	1180	1180
Case IV	200	140	140	1066.667	365.867	365.867	1180	1180	1180
Case V	200	100	100	1066.667	133.333	133.333	1180	1180	1180

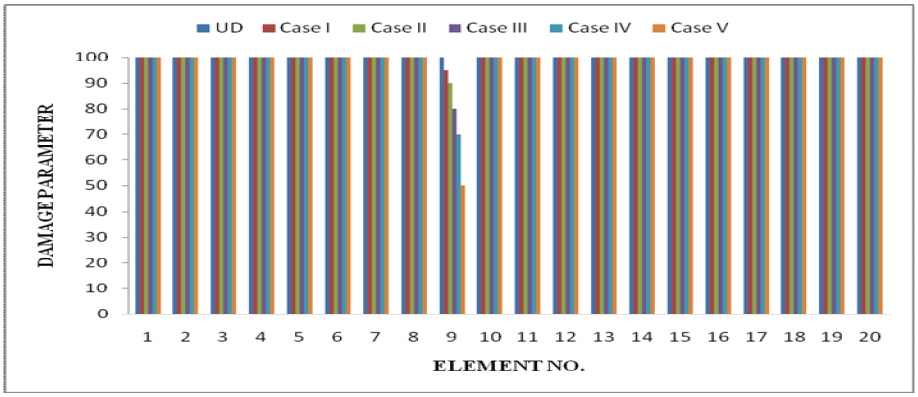

Fig 4.1.13: Graphical representation of various cases of single damage (1D9)

Fig 4.1.14: During testing of undamaged (UD) and single damage (1D9)

Measured dial gauge data as well as measured stain gauge data for different damage cases of undamaged (UD) and single damaged (1D9) are tabulated in Table 4.1.3 to Table 4.1.7.

Table 4.1.3 Deflection and strain data at specified nodes for undamaged case

Load(g)	**Dial gauge reading (mm)**			**Strain indicator reading (μ strain)**		
	DG1	**DG2**	**DG3**	**SG 1**	**SG2**	**SG3**
Initial	0	2.5	13.00	0.00	0.00	0.00
50	1.24	2.95	13.01	21.00	23.00	27.00
100	2.14	3.23	13.02	34.00	44.00	44.00
150	3.43	3.7	13.04	49.00	67.00	73.00
200	4.69	4.15	13.06	60.00	90.00	100.00

Load(g)	Dial gauge reading (mm)			Strain indicator reading (μ strain)		
	DG1	DG2	DG3	SG 1	SG2	SG3
250	5.8	4.54	13.07	75.00	112.00	125.00
300	7.21	5.00	13.10	95.00	135.00	156.00
350	8.55	5.55	13.12	115	158	186

DG=Dial Gauge; SG=Strain Gauge

Table 4.1.4: Deflection and stain data for single damage Case-I

Load(g)	Dial gauge reading(mm)			strain indicator reading (μ strain)		
	DG1	DG2	DG3	SG 1	SG2	SG3
Initial	0	0	23	0	0	0
50	1	0.33	23.025	14	22	27
100	2.36	0.85	23.045	28	47	52
150	4.65	1.32	23.075	42	69	78
200	5.03	1.85	23.11	56	93	110
250	6.24	2.28	23.13	70	116	135
300	7.49	2.76	23.16	82	137	163
350	8.8	3.24	23.19	96	159	191

Table 4.1.5: Deflection and stain data for single damage Case-II

Load(g)	Dial Gauge Reading (mm)			Strain Indicator (μ Strain)		
Initial	DG1	DG2	DG3	SG 1	SG2	SG3
0	0	0	12	0	0	0
50	1.06	0.34	12.01	12	21	21
100	2.46	0.89	12.04	25	43	54
150	3.73	1.36	12.075	37	64	81
200	4.69	1.67	12.09	51	86	100
250	5.83	2.14	12.12	66	108	125
300	7.36	2.67	12.15	80	132	159
350	8.78	3.19	12.18	94	156	190

Table 4.1.6: Deflection and stain data for single damage Case-III

Load(g)	Dial Gauge Reading (mm)			Strain Indicator Reading (μ Strain)		
	DG1	DG2	DG3	SG 1	SG2	SG3
Initial	0	0	12	0	0	0
50	1.46	0.46	12.03	19	20	31
100	2.63	0.86	12.05	24	42	53
150	3.88	1.3	12.08	32	65	77
200	5.27	1.79	12.11	45	88	105
250	6.14	2.31	12.14	56	111	137
300	7.28	2.75	12.17	63	131	159
350	9.09	3.23	12.2	77	154	185

Table 4.1.7: Deflection and stain data for single damage Case-IV

Load(g)	Dial Gauge Reading (mm)			Strain Indicator Reading (μ Strain)		
	DG1	DG2	DG3	SG 1	SG2	SG3
Initial	1	0	12	0	0	0
50	2.12	0.34	12.01	16	21	20
100	3.79	0.93	12.05	27	45	54
150	5.9	1.25	12.07	33	66	73
200	6.2	1.69	12.09	51	86	99
250	7.74	2.18	12.13	64	110	128
300	10.2	2.67	12.16	80	133	156
350	10.79	3.18	12.19	94	157	187

For double element damage case element no. 9 and 17 of the cantilever beam are damaged. Different damage cases are graphically represented in the Fig. 4.1.15. The test set up is shown in Fig. 4.1.16. Measured dial gauge reading and measured stain gauge reading for different damage cases (case I to case V) for 2D9-17 are presented in Table 4.1.8 to Table 4.1.12.

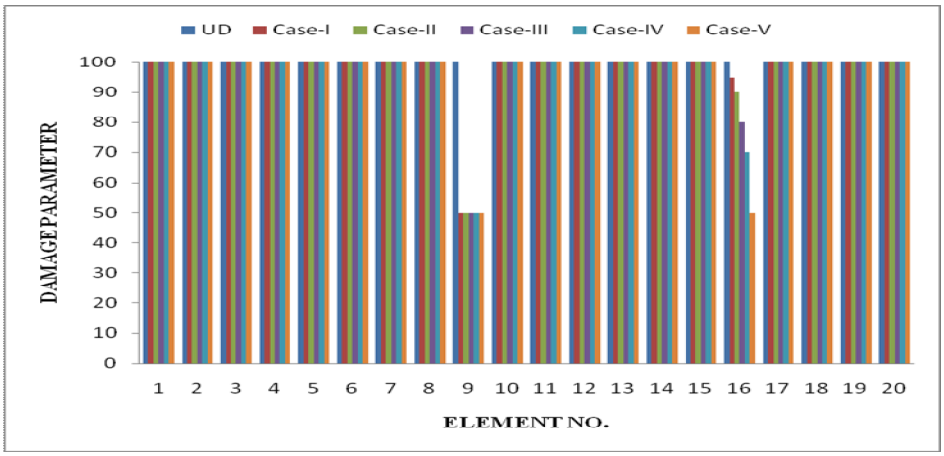

Fig 4.1.15: Graphical representation of various cases of double damage (2D9, 17)

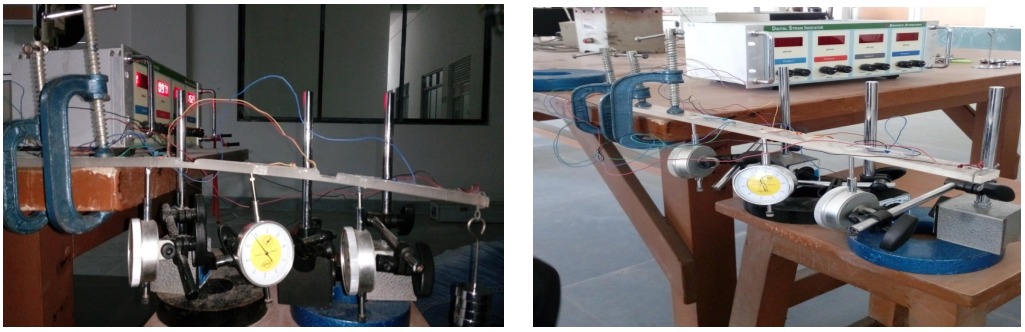

Fig 4.1.16: During testing of double damage (2D9, 17) of acrylic cantilever beam

Table 4.1.8: Deflection and stain data for double damage (2D9, 17) Case-I

Load(g)	Dial Gauge Reading (mm)			Strain Indicator Reading (μ Strain)		
	DG1	DG2	DG3	SG 1	SG2	SG3
Initial	1	8	12	0	0	0
50	2.29	8.41	12.02	17	23	24
100	3.51	8.79	12.04	25	43	46
150	4.88	9.22	12.07	36	66	73
200	6.4	9.71	12.095	56	88	102
250	7.77	10.14	12.12	79	110	126
300	9.36	10.66	12.15	97	133	156

Load(g)	Dial Gauge Reading (mm)			Strain Indicator Reading (μ Strain)		
	DG1	DG2	DG3	SG 1	SG2	SG3
350	10.67	11.08	12.18	117	154	181

Table 4.1.9: Deflection and stain data for double damage (2D9, 17) Case-II

Load(g)	Dial Gauge Reading (mm)			Strain Indicator Reading (μ Strain)		
	DG1	DG2	DG3	SG 1	SG2	SG3
Initial	1	8	7	0	0	0
50	2.21	8.35	7.015	15	21	22
100	3.61	8.84	7.04	26	41	49
150	4.79	9.18	7.06	36	62	68
200	6.47	9.74	7.095	53	86	102
250	7.9	10.21	7.12	74	108	127
300	8.87	10.74	7.16	85	132	156
350	10.03	11.23	7.185	96	155	184

Table 4.1.10: Deflection and Stain data for double damage (2D9, 17) Case-III

Load(g)	Dial Gauge Reading (mm)			Strain Indicator Reading (μ Strain)		
	DG1	DG2	DG3	SG 1	SG2	SG3
Initial	1	8	8	0	0	0
50	2.35	8.43	8.02	15	21	22
100	3.77	8.88	8.05	25	43	44
150	5.23	9.36	8.08	43	64	69
200	6.86	9.89	8.11	52	87	96
250	8.48	10.44	8.14	60	109	125
300	10.15	11	8.18	78	133	154
350	11.67	11.48	8.21	118	155	178

Table 4.1.11: Deflection and Stain data for double damage (2D9, 17) Case-IV

Load(g)	Dial Gauge Reading (mm)			Strain Indicator Reading (μ Strain)		
	DG1	DG2	DG3	SG 1	SG2	SG3
Initial	1	8	7	0	0	0
50	2.51	8.49	7.018	16	19	21
100	4.04	8.96	7.035	25	41	43
150	5.7	9.5	7.06	42	63	68
200	7.53	10.14	7.09	56	87	97
250	9.22	11.69	7.12	72	109	123
300	11.03	12.31	7.16	83	132	152
350	12.41	12.75	7.18	96	150	170

Table 4.1.12: Deflection and Stain data for double damage (2D9, 17) Case-V

Load(g)	Dial Gauge Reading (mm)			Strain Indicator Reading (μ Strain)		
	DG1	DG2	DG3	SG 2	SG3	SG4
Initial	1	8	8	0	0	0
50	2.92	8.63	8.015	13	19	16
100	4.17	9.39	8.035	27	40	37
150	7.81	10.32	8.07	41	63	65
200	9.89	11.03	8.09	54	81	84
250	12.18	11.83	8.12	68	101	106
300	14.8	12.75	8.16	82	123	131
350	17.18	13.58	8.19	96	144	156

4.1.3 Example II (Steel cantilever beam)

A cantilever beam of 500 mm span length is prepared from 50 mm wide and 15 mm thick rectangular steel bar. One edge of the beam is rigidly fixed. The statistical variations in length, width and thicknesses are measured. To have the variations as expected in the structures the specimens are intentionally not machined perfectly. Firstly the single element damage was introduced with 10% reduction of width of third element. Then the double element damage was introduced by 10% reduction of the width of third and fourth element. The details of the undamaged beam is shown in Fig. 4.1.17.

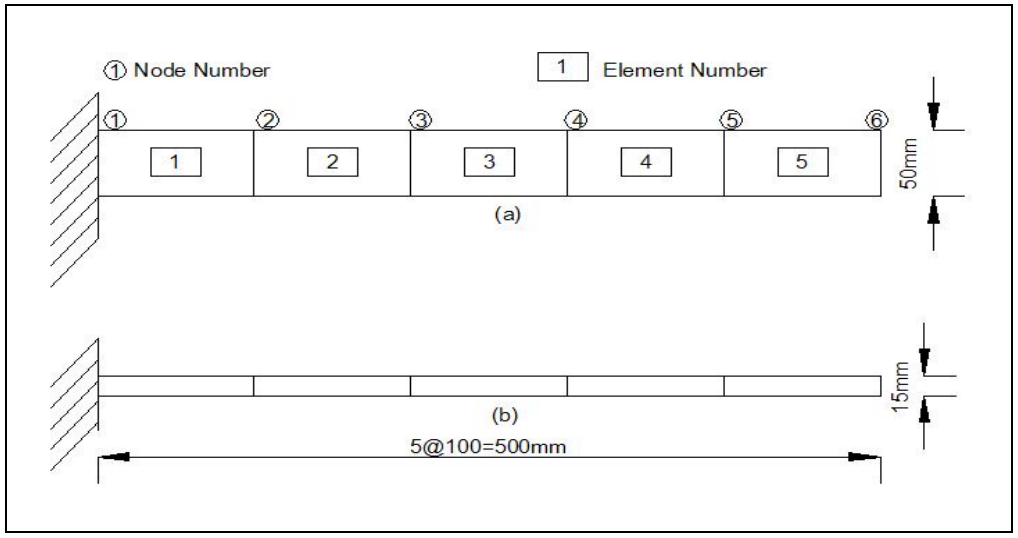

Fig 4.1.17: (a) Plan; and (b) Elevation of the undamaged steel cantilever beam

The details of the damaged test specimens for both single element (member 3) and double element (member 3 & 4) damage are shown in Fig 4.1.18 and Fig 4.1.19.

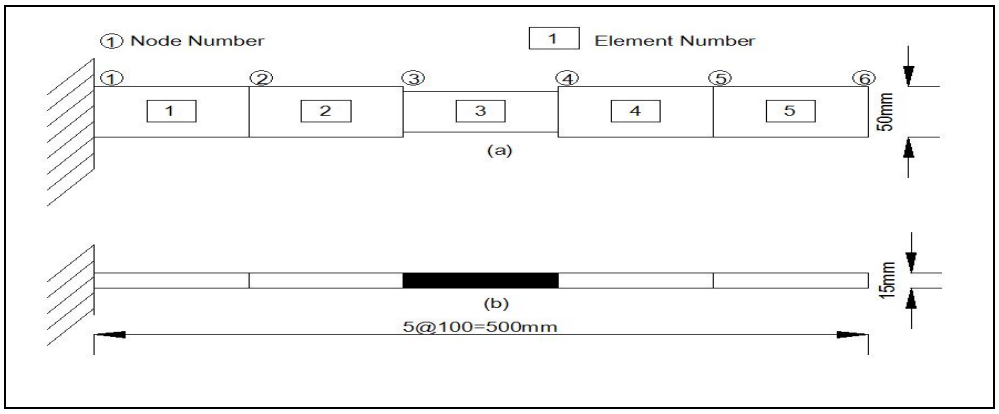

Fig 4.1.18: (a) Plan; and (b) Elevation of damaged (Single element) steel cantilever beam.

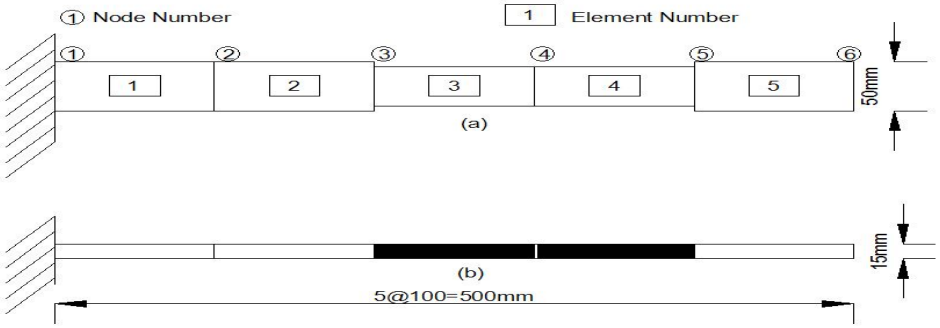

Fig 4.1.19: (a) Plan; and (b) Elevation of damaged (Multiple elements) steel cantilever beam

Different instruments like multimeter, strain indicator, dial gauges and also the test specimens are shown in Fig. 4.1.20 and Fig.4.1.21.

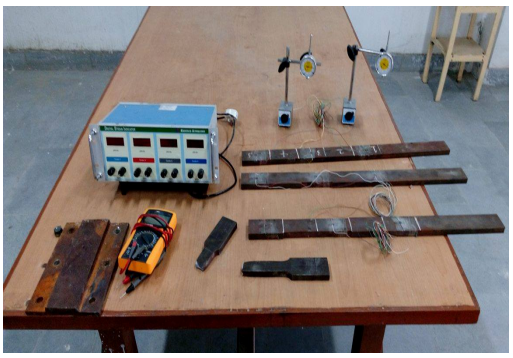

Fig4.1.20: Instruments used for the experiment

Fig 4.1.21: Strain gauges attached with beam

4.1.3.1 Physical Properties of the Specimen

The details of the measured geometric dimensions of the undamaged and damaged beams are shown in Table 4.1.13.

Table 4.1.13: Measured Dimensions of Cantilever Beams

Element Number	**Length (mm)**			**Width (mm)**			**Thickness (mm)**		
Damaged Condition	**UD**	**1D3**	**2D3,4**	**UD**	**1D3**	**2D3,4**	**UD**	**1D3**	**2D3,4**
1	500	500	500	50	50	50	15	15	15
2	500	500	500	50	50	50	15	15	15
3	500	500	500	50	45	45	15	15	15
4	500	500	500	50	50	45	15	15	15
5	500	500	500	50	50	50	15	15	15

The details of the structural parameters like area of cross section and area moment of inertia based on the measurement of the undamaged and damaged beams are indicated in Table 4.1.14.

Table 4.1.14: Measured Structural Parameters of Cantilever Beams

Element Number	**Cross Sectional Area (mm^2)**			**Moment of Inertia (10^4 X mm^4)**		
Damaged Condition	**UD**	**1D3**	**2D3,4**	**UD**	**1D3**	**2D3,4**
1	750	750	750	1.4062	1.4062	1.4062
2	750	750	750	1.4062	1.4062	1.4062
3	750	**675**	**675**	1.4062	**1.265**	**1.265**
4	750	750	**675**	1.4062	1.4062	**1.265**
5	750	750	750	1.4062	1.4062	1.4062

Experimental setup for undamaged and single damaged beam during testing are shown in Fig.4.1.22.

Fig 4.1.22: Schematic diagram of the Experimental Setup

The dial gauge reading and the strain indicator readings are represented in Table 4.1.15 for UD case. Similarly the dial gauge reading and the strain indicator readings for 1D3 case and 2 D 34 case are tabulated in Table 4.1.16 and in Table 4.1.17.

Table 4.1.15: Deflection and strain at specified nodes for undamaged case

Load(N)	**Dial gauge reading (mm)**		**Strain indicator reading (μ Strain)**		
	DG1	**DG2**	**SG1**	**SG2**	**SG3**
Initial	0	0	0	0	0
0.302	0.04	0.02	0	0	0
3.929	0.52	0.20	5	4	0
6.425	0.85	0.34	7	6	1
10.051	1.34	0.52	11	10	1
11.490	1.54	0.61	12	11	2
12.929	1.74	0.69	13	12	2
15.872	2.14	0.85	14	15	2
18.687	2.53	1.00	17	18	3
21.474	2.96	1.15	21	20	3
22.871	3.11	1.24	22	22	3
24.371	3.32	1.33	22	23	4
25.506	3.49	1.39	23	24	4
26.083	3.56	1.42	24	25	4

Load(N)	Dial gauge reading (mm)		Strain indicator reading (μ Strain)		
	DG1	DG2	SG1	SG2	SG3
27.131	3.72	1.48	25	26	4
27.836	3.82	1.53	26	26	4

Table 4.1.16: Deflection and strain at specified nodes for single damaged case (1D3)

Load(N)	Dial Gauge Reading (mm)		Strain Indicator Reading (μ Strain)		
	DG1	DG2	SG1	SG2	SG3
0	0	0	0	0	0
0.302	0.04	.01	0	0	0
3.929	0.54	0.21	6	4	1
6.425	0.90	0.35	9	7	1
10.051	1.42	0.56	16	11	1
11.490	1.65	0.64	18	13	1
12.929	1.86	0.78	20	15	1
15.872	2.31	0.91	25	18	2
18.687	2.74	1.10	29	21	2
21.474	3.24	1.29	34	24	2
22.871	3.48	1.40	36	25	2
24.371	3.74	1.50	38	27	2
25.506	3.94	1.59	40	28	2
26.083	4.04	1.64	41	29	2
27.131	4.22	1.71	43	30	2
27.836	4.34	1.77	44	31	2

Table 4.1.17: Deflection and strain at specified nodes for double damage case (2D3, 4)

Load(N)	Dial Gauge Reading (mm)		Strain Indicator Reading (μ Strain)		
	DG1	DG2	SG1	SG2	SG3
0	0	0	0	0	0
0.302	0.04	0.01	1	0	0
3.929	0.55	0.20	6	4	0
6.425	0.92	0.34	11	7	1
10.051	1.45	0.51	16	10	1
11.490	1.70	0.59	18	12	2
12.929	1.90	0.67	21	14	2
15.872	2.33	0.84	27	17	2
18.687	2.76	1.20	32	20	3
21.474	3.26	1.30	36	23	3
22.871	3.51	1.41	39	25	4
24.371	3.76	1.52	41	26	4
25.506	3.97	1.61	43	28	4
26.083	4.06	1.65	44	28	5
27.131	4.24	1.74	46	29	5
27.836	4.37	1.80	47	30	5

4.2 Dynamic testing

Experimental modal test with excitation is carried out on laboratory model of the test structure. The responses are measured simultaneously along with the excitation force in time-domain and the real time data are acquired in a computer based data acquisition system in case of Experimental modal analysis(EMA). Operational modal testing (OMA) is also performed without measuring the time signal of forcing function.The measured data in time-domain are immediately transferred to frequency domain by the in-built software of real time Fast Fourier Transformation (FFT). The frequency response function (FRF) is then evaluated through the post processing technique. The modal parameters are extracted at the selected degrees of freedoms by curve fitting method on the evaluated frequency response functions. This chapter

presents the details of experimental set up, measurement technique adopted and the post analysis of the acquired dynamic response data for the extraction of modal parameters.

4.2.1 Experimental setup for the dynamic test:

a) **Signal analyzer box (Dynamic data acquisition system)**

The A4404 - SAB is a pocket sized 4-channel vibration analyzer. The A4404 – SAB is to be connected to any computer by USB and generally used for data analyzing, collecting and the recording of vibration signals. The instrument is enhanced by modules for dynamic balancing, measurement of run up and coast down and acoustic measurement mode. The instrument is equipped with an expert system developed by Adash**,** which can also automatically detects structural faults. The instrument is powered directly by USB connection. So no external power is needed. A4404 Signal Analyzer Box is shown below in Fig. 4.2.1.

Fig. 4.2.1: Signal analyzer box.

b) Acceleration transducer (CEMB)

The TA18S transducer picks up seismically the absolute vibrations of the structure by being fitted directly to the supports of the vibrating part of the structure. It supplies an output signal directly proportional to the vibration of the point to which it is fastened. Such recorded signals are subsequently processed by one of the measuring channel of a CEMB serial “T” or “N” processing unit. Acceleration transducers details are shown in Fig. 4.2.2 and Fig. 4.2.3.

Fig. 4.2.2: Accelerometer in different view.

Fig. 4.2.3: All eight accelerometers.

c) ICP impact hammer (Model 086C03)

The ICP impulse force test hammer adapts FFT analyzer for structural behaviour testing.Impulse testing of the dynamic behavior of mechanical structures involves striking the test object with the force-instrumented hammer. It is shown in Fig.4.2.4.

Fig 4.2.4: Impact hammer model 086C03

d) Unitronic liycy data cable

Unitronic Liycy cable as shown in Fig. 4.2.5 is a screened data cable for low frequency applications. The cable is designed for fixed installation and for conditional flexible use. It is used in dry and damp interiors but not appropriate for outside usage.

Fig 4.2.5: Unitronic Liycy Data Cable

e) Unidirectional shaking table

For the development in the field of earthquake engineering, experimental study is required. To study the effects of earthquake, laboratory facilities are needed. The development has reached to a stage where earthquake simulation is achieved in laboratory using shaking table. The shake table consist of three parts with motor, rpm control panel and table base. The schematic diagram of the shake table used for this experiment is shown Fig. 4.2.6 and Fig. 4.2.7. Position of holes to fix the test specimen and also the slots for roller are shown in Fig. 4.2.8.

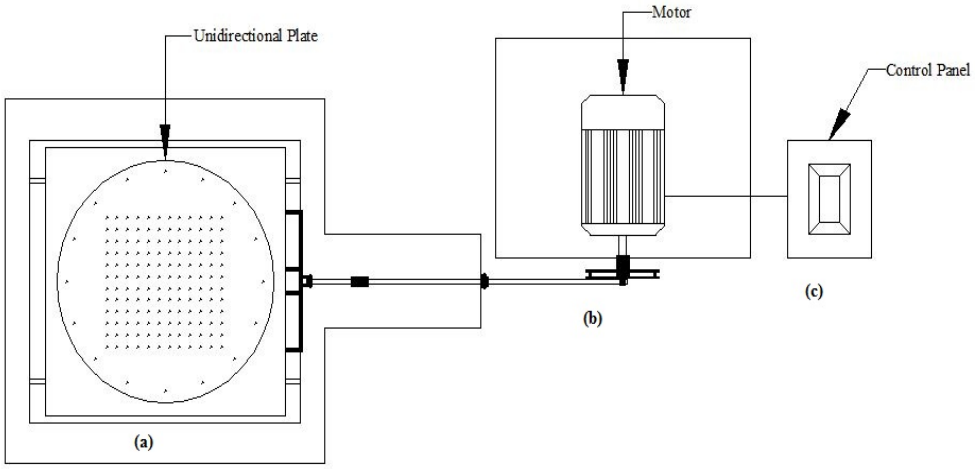

Fig 4.2.6: Schematic plan of the full set up (a) Shake table, (b) Motor, (c) Control panel

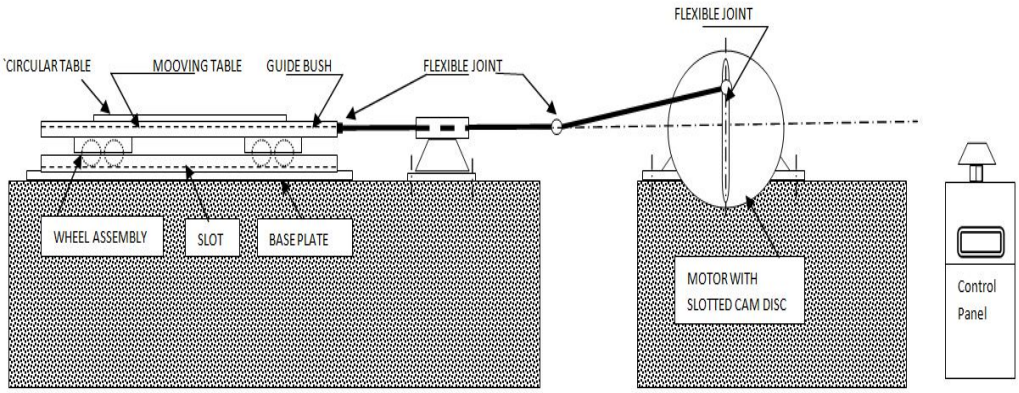

Fig 4.2.7: Schematic Elevation of unidirectional shaking table

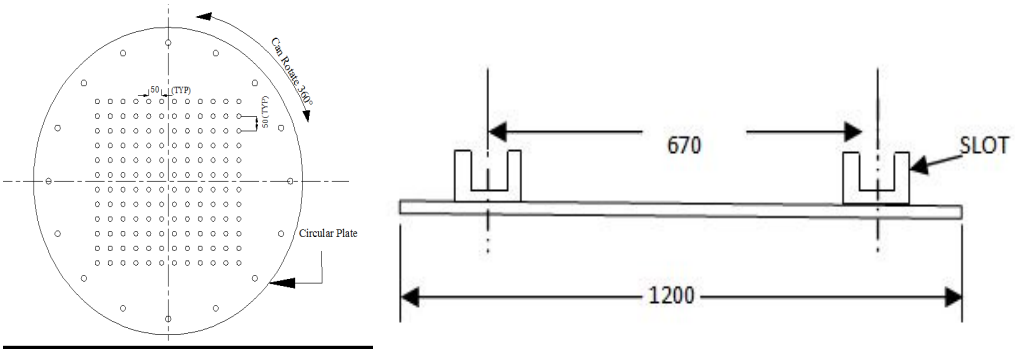

Fig 4.2.8: Holes arrangements and slots dimensions are in mm

The shaking table is constructed in the laboratory and Fig. 4.2.9 reflects the casting of base slab and also the template for the positioning of anchor bolts.

Fig 4.2.9: Reinforcement details and bolt for top plate fixing during concrete casting.

The shaking table is operated by a 15HP motor with maximum of 1500 rpm and 300mm amplitude is shown Fig. 4.2.10. Rpm of the motor is controlled by a control panel shown in Fig. 4.2.11.

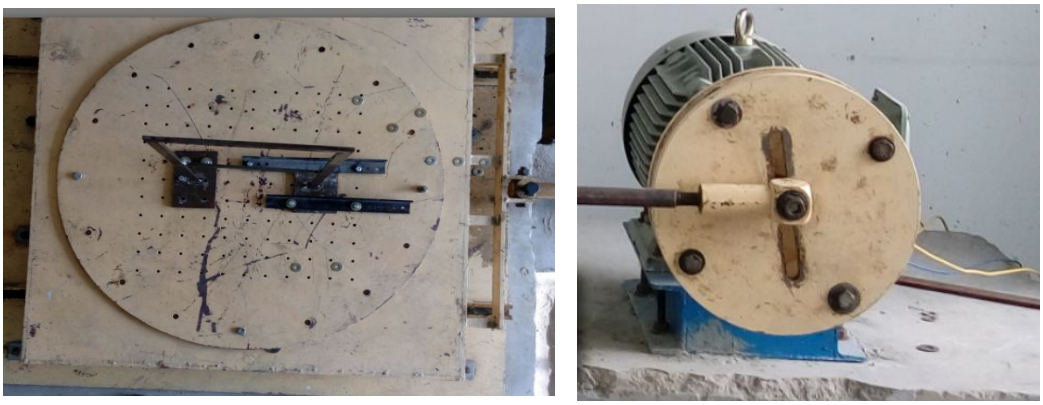

Fig 4.2.10: Plan of shaking table and motor with amplitude controller for the unidirectional shaking

Fig 4.2.11: Control panel for the shake table for rpm control

4.2.2 Experimental modal analysis:

For this experiment, a cantilever beam of steel of dimension 500mm × 50mm × 15mm is selected. One accelerometer is kept 30mm apart from fixed end and the corresponding measurement is noted. The excitation is produced by impact hammer at a distance of 40mm apart from the fixed end. In this experiment a single accelerometer is used to measure the response and hence it is called single response technique. After measuring the readings as Fig 4.2.12, natural frequency against phase change of FRF are extracted.

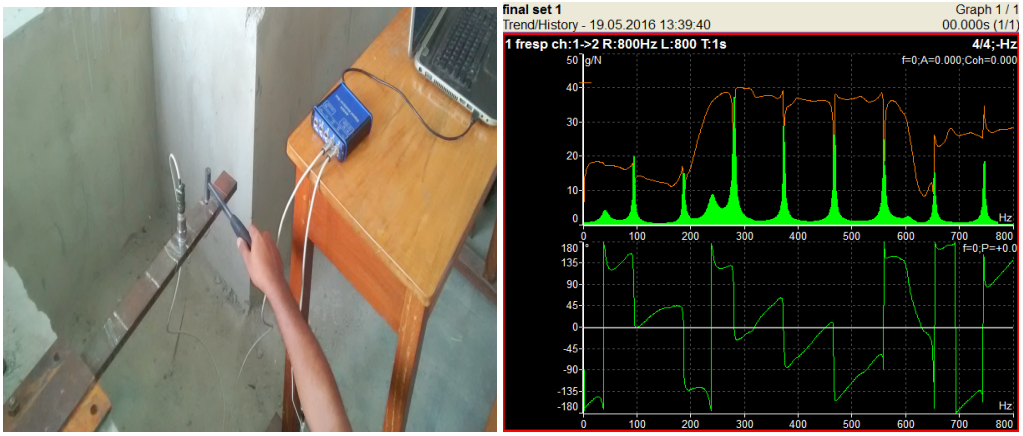

Fig. 4.2.12: a) During testing and b) coherence and phase change for the cantilever beam

Although there is a lots of peak as shown in the Fig. 4.2.12, but the first three 180° phase change happened in 38Hz, 238Hz and 559Hz. So these are the natural frequency of the object tested and tabulated in Table 4.2.1.

Table 4.2.1: Extracted Natural Frequency (Hz)

Modes	Natural Frequency(Hz)
1	38
2	238
3	559

4.2.3 Operational modal testing:

a) Undamaged scenario (UD)

Operational modal testing is performed on the same steel cantilever beam as described in the experimental setup for undamaged steel cantilever beam is shown in Fig. 4.2.13

Fig4.2.13: Operational modal testing of undamaged (UD) cantilever beam

The recorded time signals for all four accelerometers are shown in Fig.4.2.14 and subsequent extraction of natural frequencies using frequency domain decomposition (FDD) is shown in Fig. 4.2.15.

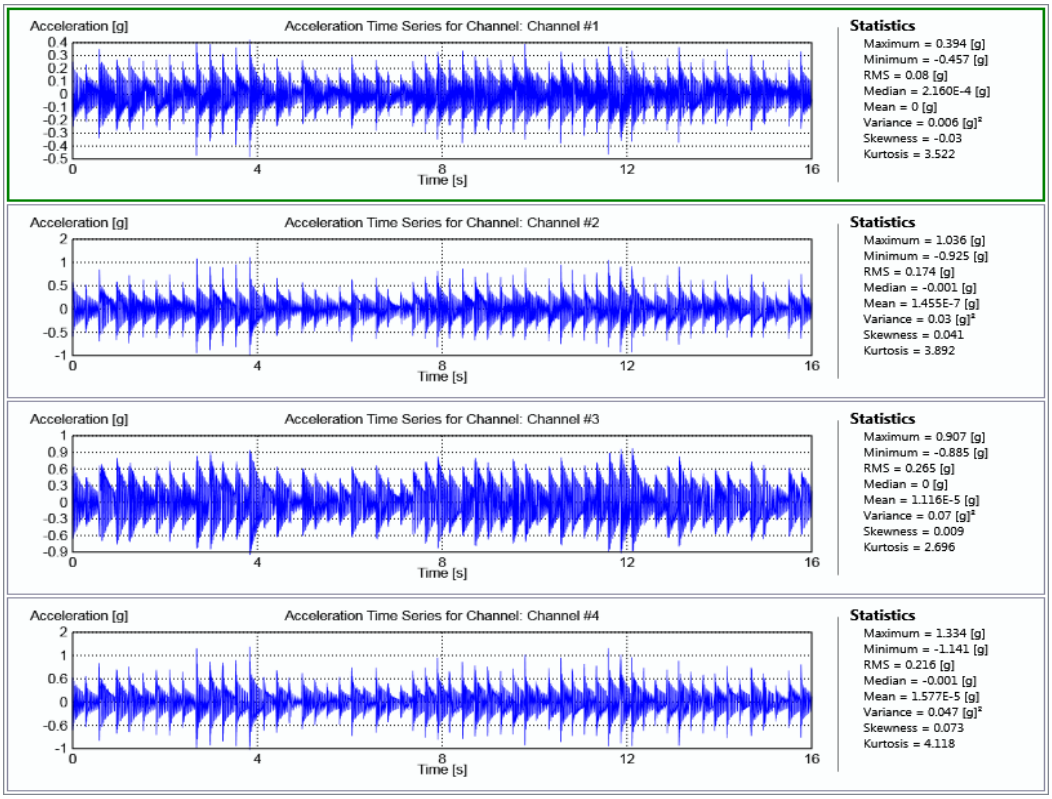

Fig. 4.2.14: Measured signals recorded in the data acquisition system by all four channels

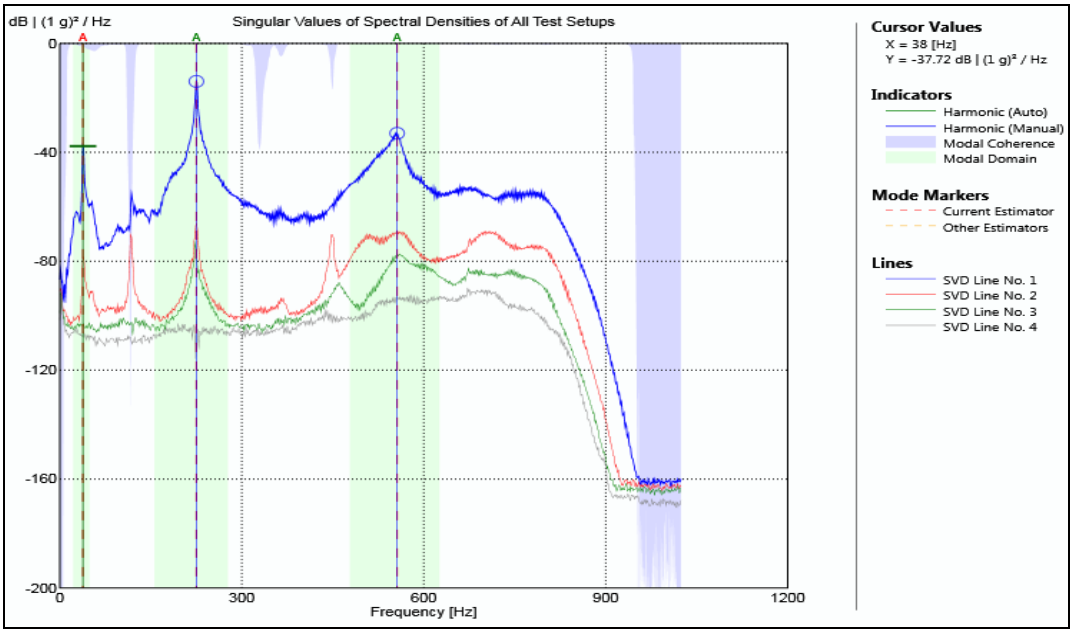

Fig. 4.2.15: Estimation from frequency domain decomposition (FDD)

b) Single damage scenario (1D3)

The experimental setup for single element damaged steel cantilever beam is shown in Fig. 4.2.16. The recorded time signals for four channels are shwon in Fig. 4.2.17. The estimation of the natural frequencies is reflected in Fig. 4.2.18.

Fig. 4.2.16: Experimental set up for the single damage (1D3) cantilever beam

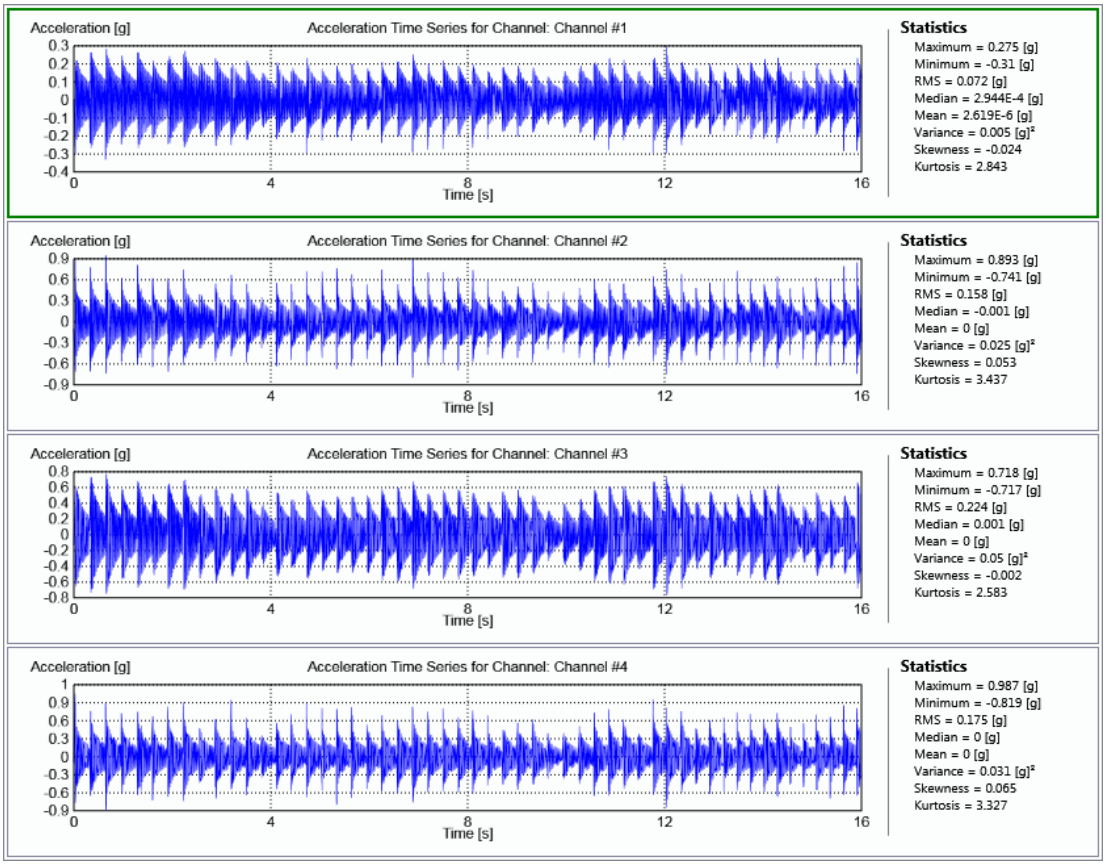

Fig. 4.2.17: Recorded acceleration time signals by all four sensors.

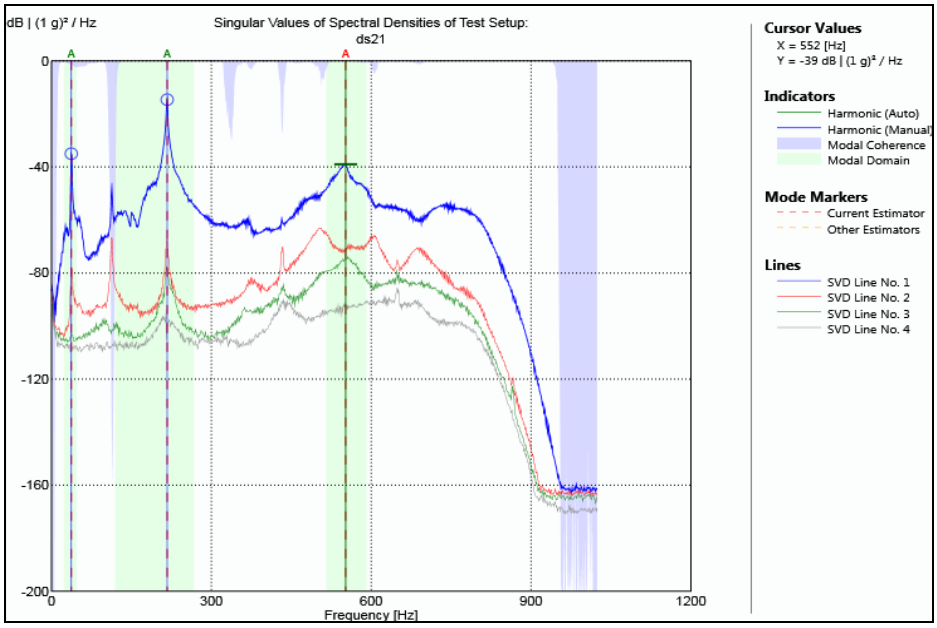

Fig. 4.2.18: Estimation from frequency domain decomposition (FDD)

Extraction of the natural frequencies and mode shapes done after post processing of the time signals as recorded in ARTeMIS software and the extracted mode shapes are shown below in Fig. 4.2.19 and Fig. 4.2.20.

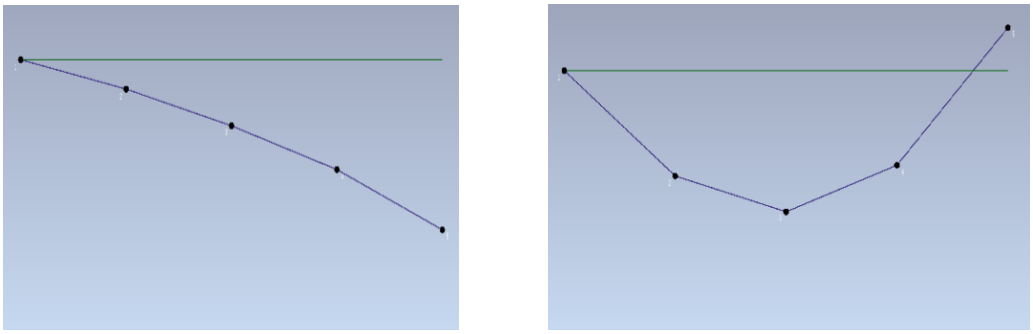

Fig. 4.2.19: Extracted first and second operational mode shapes.

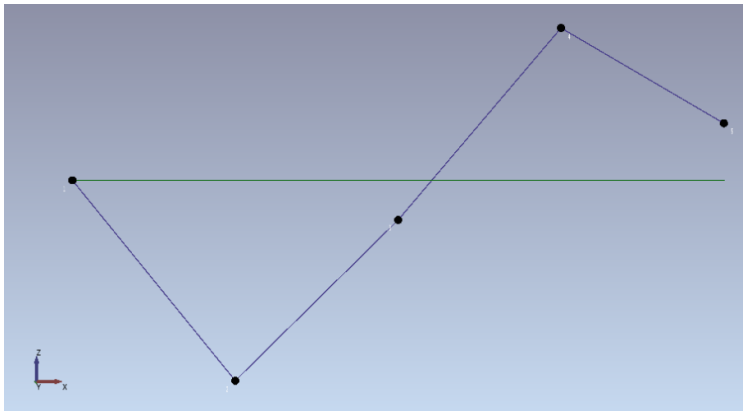

Fig. 4.2.20: Extracted third operational mode shapes.

c) Double damage scenario (2D34)

The experimental setup for damaged cantilever beam of sample 2 is shown in Fig. 4.2.21. In this specimen (10%) damage is in the 3rd and 4th element.

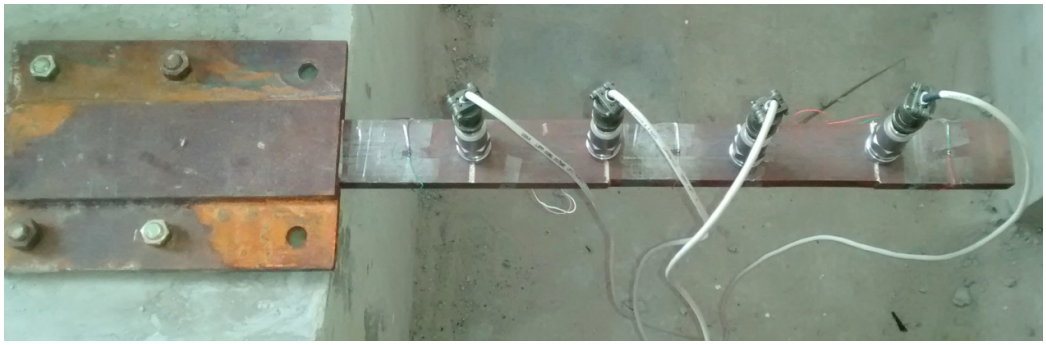

Fig. 4.2.21: During experiment for the steel cantilever beam (double element damage)

The change in acceleration against time obtained for all four accelerometers is shown below in Fig.4.2.22.

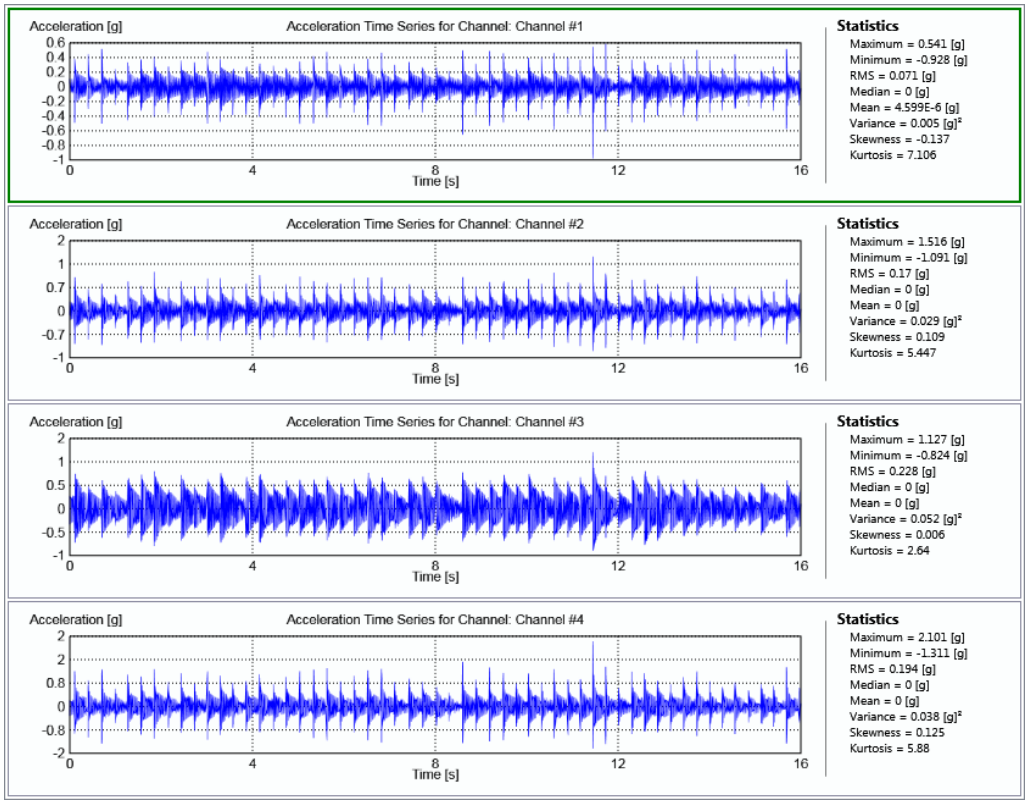

Fig. 4.2.22: Recorded acceleration time signals by all four sensors for double element damage case

The estimation from frequency domain decomposition (FDD) method is given in Fig. 4.2.23.

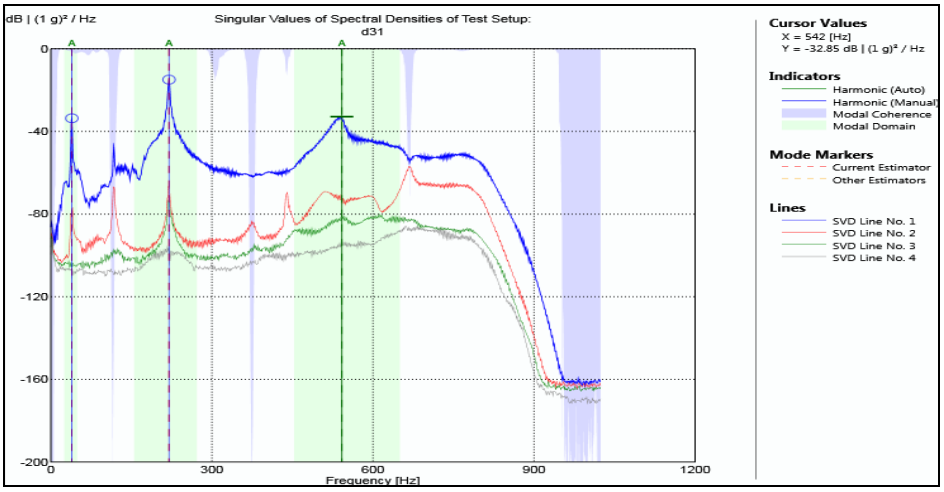

Fig. 4.2.23: Estimation from frequency domain decomposition (FDD) for double element damage

The extracted mode shape for first three natural frequency are shown below in Fig.4.2.24 and Fig.4.2.25. Extracted first three natural frequencies are shown in Table 4.2.2.

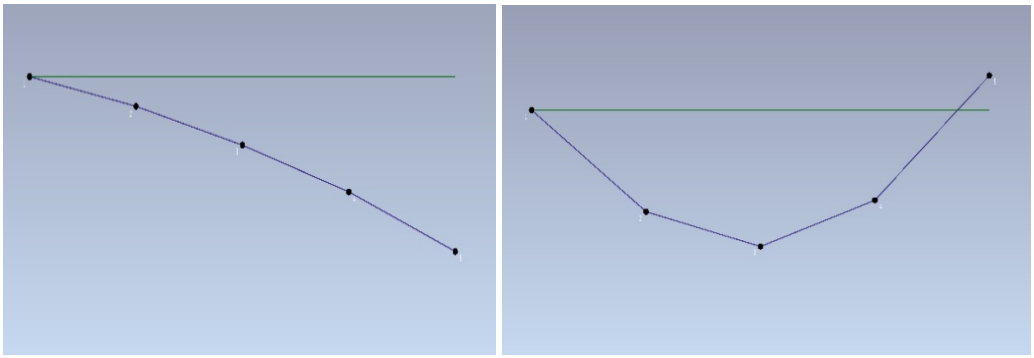

Fig. 4. 2.24: Extracted first and second operational mode shapes for double element damage.

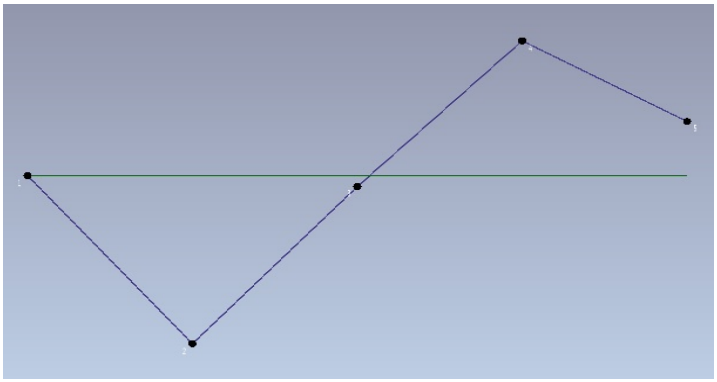

Fig. 4.2.25: Extracted third operational mode shapes for double element damage.

Table 4.2.2: Extracted first three natural frequencies of the cantilever for different damage states

Modes	**Natural Frequency(Hz)**		
	Undamaged(UD)	**Single element damage(1D3)**	**Double element damage(2D34)**
1	38	37	39
2	235	217	220
3	556	552	542

4.2.4 Example VI (Steel portal frame)

For this experiment a single bay two storey portal frame of steel of dimension 600mm × 300mm, having total height of 600mm is prepared as shown in Figure 4.2.26(a). Frame is properly fixed on the base plate of the unidirectional shaking table. In this experiment eight numbers accelerometers are placed to measure the response. The statistical variations in length, width and thicknesses are measured. Details of the frame with node numbers and member numbers are shown below. All the accelerometers are mounted on the frame as shown in the Fig 4.2.26 (b, c).The frame is excited mechanically to get the vibration data that to be analyzed for the modal data. Excitation is done in shake table. The base plate is vibrated at different rpm of the motor for forced vibration and vibration signals are recorded through all eight number of accelerometers.

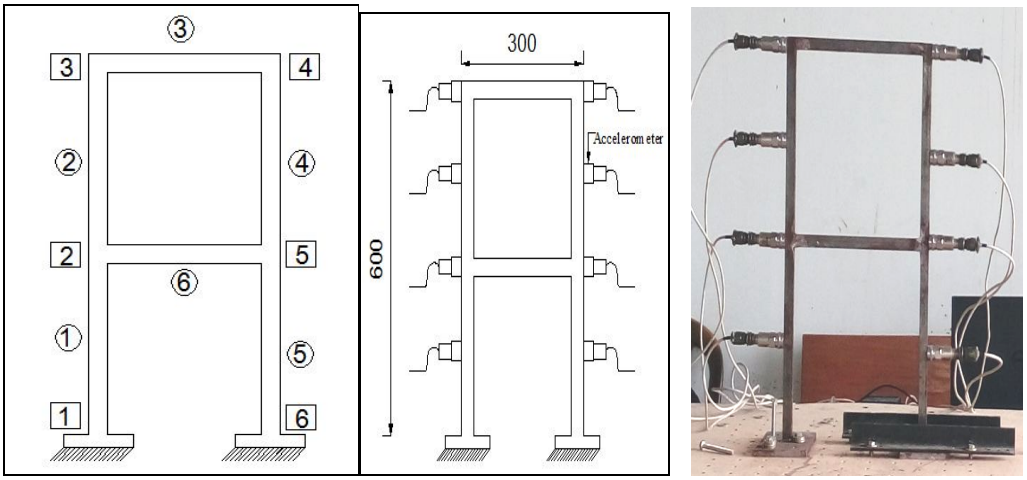

Fig 4.2.26: a) schematic portal frame b) schematic and c) actual position of accelerometers

The schematic diagram for the test set up is shown in Fig.4.2.27 and also full experimental set-up during testing is shown in Fig.4.2.28.

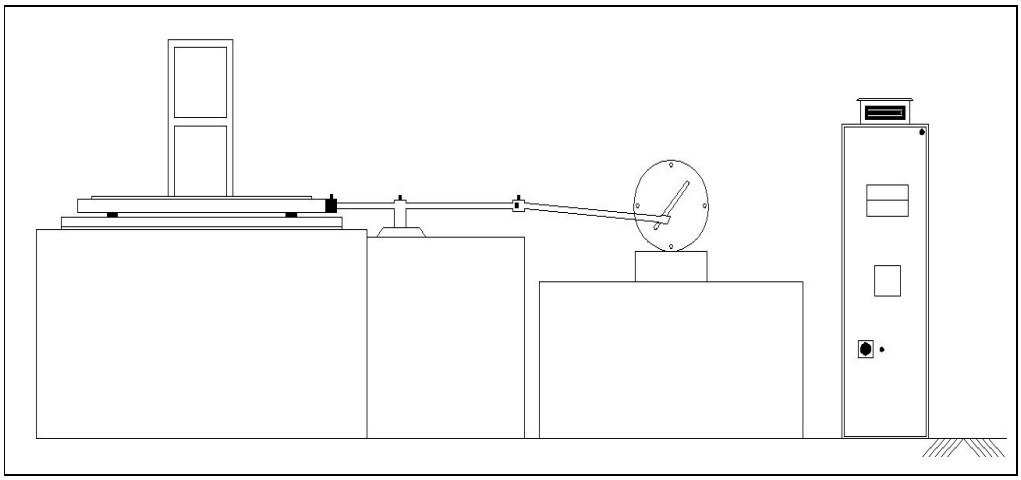

Fig 4.2.27: Schematic diagram of the uni directional shake table system

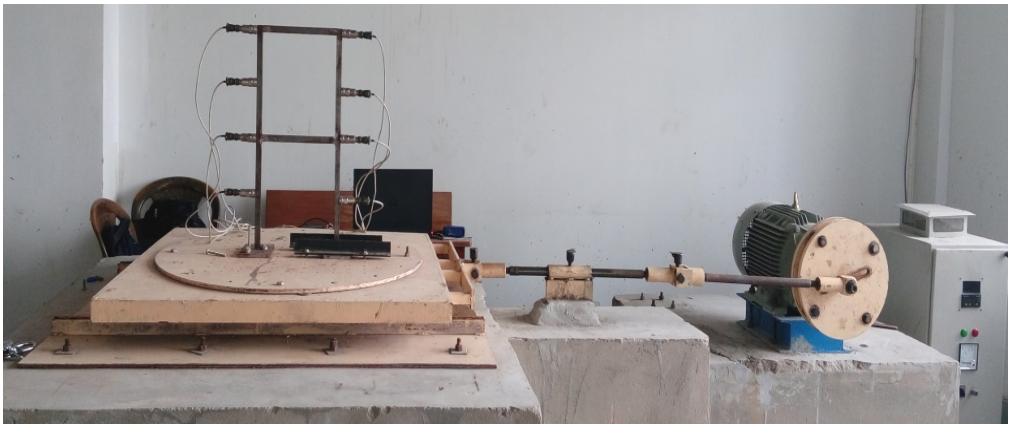

Fig 4.2.28: Full setup for the experiment (Uni directional shake table system along with control panel and motor and experimental portal frame and accelerometers with other accessories)

The measurement of time signals for all eight accelerometer are repeated for several times changing different motor RPM. The test is also performed for all three different damage cases. However, such typical time signal data for all accelerometers are shown in Fig.4.2.29 for undamaged case considering motor RPM as 15.

The geometric properties of the undamaged portal frame is shown in Table 4.2.3 and also structural properties are described in Table 4.2.4. Undamaged and different damage scenario of the portal frame is represented in Table 4.2.5.

Table 4.2.3: Measured geometric data of the steel portal frame

Member No.	Length (mm)	Width (mm)	Thickness (mm)
1	300	19.16	6.05
2	300	19.16	6.05
3	6.05	300	19.16
4	300	19.16	6.05
5	300	19.16	6.05
6	6.05	300	19.16

Table 4.2.4: Different undamaged structural properties of the steel portal frame

MEMBER TYPE	Column	Beam
ELEMENT NO.	1,2,4,5	3,6
C/S AREA	0.0001159 sqm	0.0001159 sqm
MOMENT OF INERTIA	3.546×10^{-9} (m^4)	3.546×10^{-9} (m^4)

Damage identification is performed for different damage cases as shown below

UD : Undamaged state – No damage in any element.
CASE I (1D3) : Single element damaged state at element nos. 3.
CASE II (2D13) : Double element damaged state at element nos. 1 and 3.
CASE III (3D134): Multiple damaged state at element nos. 1, 3 and 4.

Table 4.2.5: Details of damages (%) reduction in c/s for undamaged and damaged cases

DAMAGE CASES	ELEMENT NO					
	1	2	3	4	5	6
UD	-	-	-	-	-	-
CASE – I	-	-	**10**	-	-	-
CASE – II	**10**	-	**10**	-	-	-
CASE – III	**10**	-	**10**	**10**	-	-

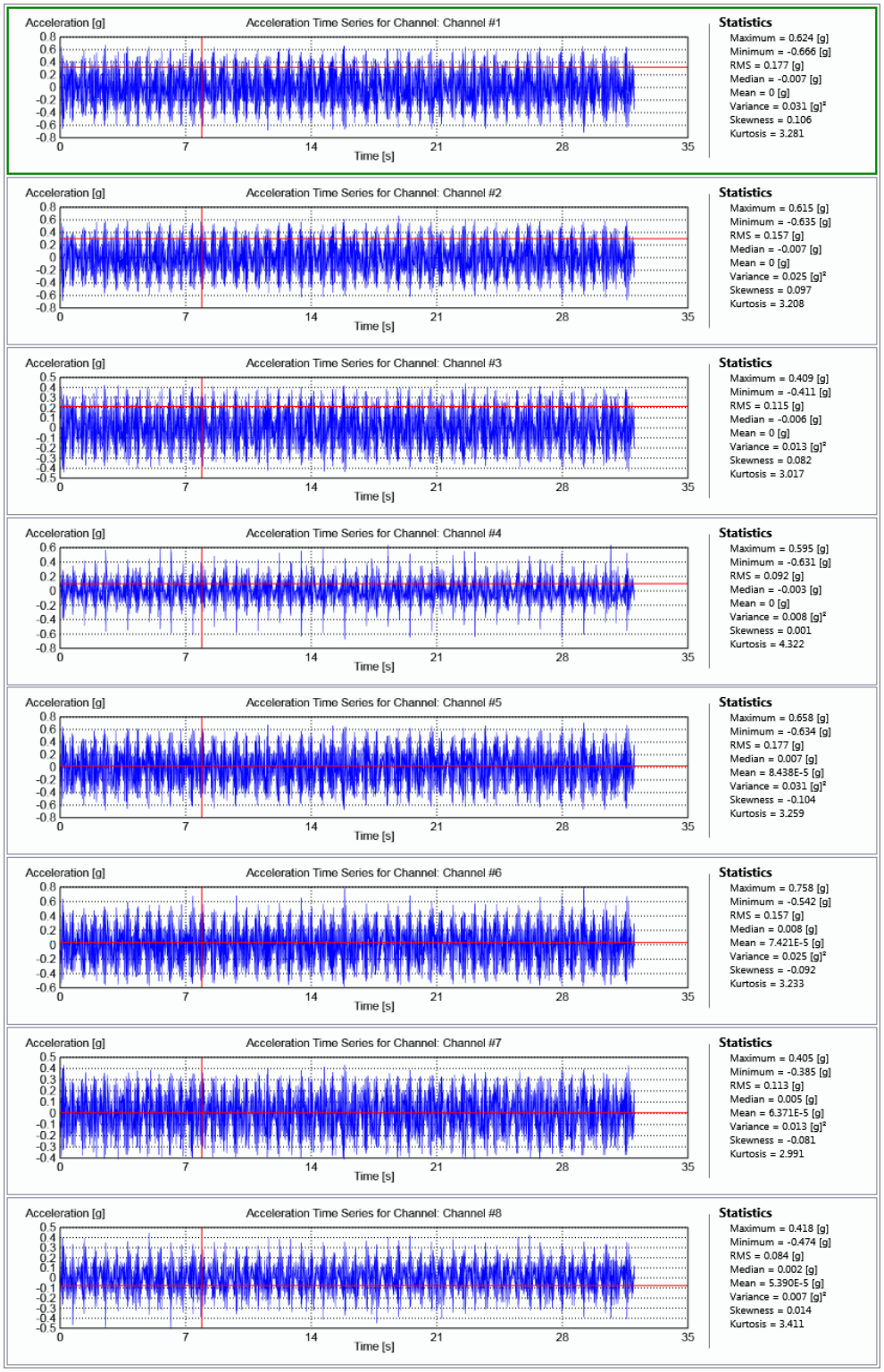

Fig 4.2.29: Typical time signal for the undamaged case at a motor rpm 15

The extracted natural frequencies for first three modes and for UD and other damage cases (1D3, 2D 13 and 3D134) are presented in Table 4.2.6.

Table 4.2.6: Extracted first three natural frequencies of the portal frame for different damage states

Modes	**Natural Frequency(Hz)**			
	Undamaged(UD)	**Single element damage(1D3)**	**Double element damage(2D13)**	**Triple element damage(3D134)**
1	56	55	55	54
2	189	184	182	174
3	392	390	383	354

Chapter – 5

Results & Discussions

5.0 General

The validation of the proposed models for the detection of damage in structural systems is carried out with few numerical and experimental examples. The effect of the noise in measured static and modal data on the identified structural properties is also studied. The applicability of the proposed methods for various multiple damage scenarios with various degree of damage is explored. The effect of the number of measurements of modal data on the identified properties is also studied. Subsequently, various damage scenarios of different structures have been solved to demonstrate the applicability of the proposed different models. The following examples are studied to validate the proposed damage identification models based on equation error approach.

Table 5.0.1: Details of example considered

Sl No.	Example No	Structural Type	Material	Used for	
				Numerical	Experimental
1	Ex-1	Cantilever Beam	Acrylic	√	√
2	Ex-2	Cantilever Beam	Steel		√
3	Ex-3	Fixed - Fixed Beam	Steel	√	
4	Ex-4	13 Member Pratt Truss	Steel	√	
5	Ex-5	RCC Gable Frame	RCC	√	
6	Ex-6	Portal Frame	Steel		√

Table 5.0.2: Details of different numerical models validated with different examples

Model Name	Forward Approach	SLD	SSD	DFS	DFC	DMS	Static Experimentation	Dynamic Experimentation
Examples								
Ex-1	√						√	
Ex-2		√	√	√			√	√
Ex-3					√			
Ex-4		√	√	√				
Ex-5						√		
Ex-6						√		√

5.1 Example - I (Acrylic cantilever beam)

A Cantilever beam of uniform cross-section (350mm wide x 8 mm thick) of acrylic material discretized by 20 no of beam elements as shown in Fig. 5.1.1 is considered.

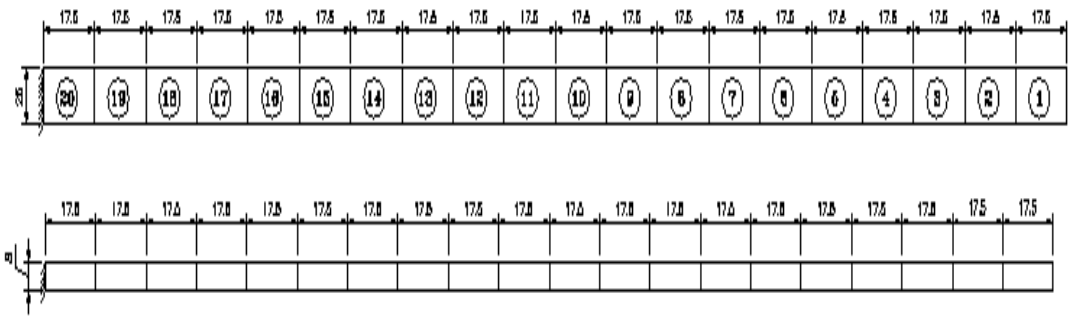

Fig. 5.1.1: A 350 mm cantilever beam made of Acrylic material

The geometric properties of the beam are given in Table 5.1.1. The node no and element no of the beam are shown below in Fig 5.1.2

Table 5.1.1: Geometric and material properties of the cantilever beam (Ex-1)

Length (mm)	Height (mm)	Width (mm)	Mass density (Kg/m3)	Modulus of Elasticity (E)(GPa)
350	8	25	1180	3.3

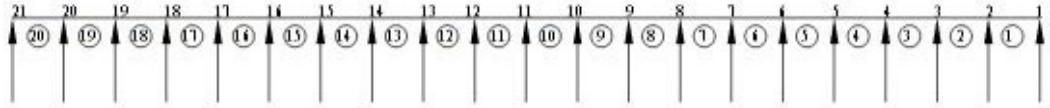

Fig. 5.1.2: Schematic diagram showing the nodes and elements of the beam

The d.o.f. of cantilever beam are shown in the Fig 5.1.2 and Fig 5.1.3.

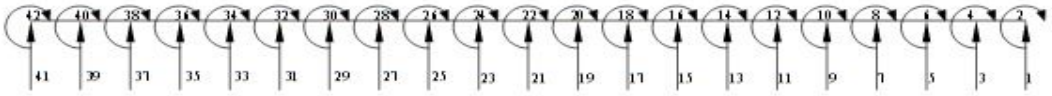

Fig. 5.1.3: Schematic diagram showing the degrees of freedom of the beam

5.1.1 **Damage Scenario**:

Single element damage:

The reduction of thickness for element No. 9 is gradually increased from 5% to 50% for single damaged (1D 9) case. Undamaged and various single element damaged cases are shown in Table 5.1.2.

Table 5.1.2:Details of damages (% Reduction of thickness) for single Element Damage at element no. 9

Damage Case	Reduction of thickness (%)
Undamaged	0%
Damage Case I	5%
Damage Case II	10%
Damage Case III	20%
Damage Case IV	30%
Damage Case V	50%

Multiple element damage:

In case of double element damage, the reduction of thickness for element no 17 is gradually increased from 5% to 50% keeping 50% thickness reduction for element no 9. The various double element damage (2 D 9, 17) scenario is shown in Table 5.1.3

Table 5.1.3: Details of damages (% Reduction of thickness) for double Element damage

Damage Case	Reduction of thickness (%) at element 9	Reduction of thickness (%) at element 17
Case I	50%	5%
Case II	50%	10%
Case III	50%	20%
Case IV	50%	30%
Case V	50%	50%

Static analysis is performed for all the damage cases and the change in the deflection for UD and different 1D9 cases are shown in Table no 5.1.4.

Table 5.1.4: Deflection at various nodes for UD and 1 D 9 case

Node	**UD**	**1D9 (5%)**	**1D9 (10%)**	**1D9 (20%)**	**1D9 (30%)**	**1D9 (50%)**
1	1.25763	1.25752	1.25813	1.26266	1.27456	1.35937
2	1.17379	1.17351	1.17387	1.17749	1.18761	1.26173
3	1.08999	1.08954	1.08964	1.09236	1.10071	1.16412
4	1.00631	1.00569	1.00553	1.00735	1.01394	1.06665
5	0.92293	0.92214	0.92172	0.92263	0.92745	0.96946
6	0.84006	0.8391	0.83842	0.83843	0.84147	0.87279
7	0.75797	0.75684	0.75591	0.75501	0.75629	0.7769
8	0.67703	0.67573	0.67453	0.67273	0.67224	0.68215
9	0.59762	0.59615	0.5947	0.59199	0.58974	0.58895
10	0.52024	0.51875	0.51726	0.51428	0.5113	0.50534
11	0.44541	0.44413	0.44284	0.44027	0.43771	0.43257
12	0.37373	0.37265	0.37156	0.3694	0.36723	0.3629
13	0.30586	0.30497	0.30408	0.3023	0.30052	0.29697
14	0.24252	0.24181	0.2411	0.23969	0.23828	0.23545
15	0.18449	0.18396	0.18342	0.18234	0.18127	0.17912
16	0.13264	0.13225	0.13187	0.13109	0.13032	0.12878
17	0.08787	0.08761	0.08736	0.08684	0.08633	0.08531
18	0.05115	0.051	0.05085	0.05055	0.05026	0.04966
19	0.02352	0.02345	0.02338	0.02325	0.02311	0.02284
20	0.00608	0.00606	0.00605	0.00601	0.00598	0.00591

It is observed that the deflections at various nodes are increasing with the increase of percentage of damage.

The comparison of theoretical and experimental deflections at node no 8 of the cantilever beam for UD and different cases of single element damage (1D9) are shown in Fig 5.1.4 and Fig 5.1.5 below.

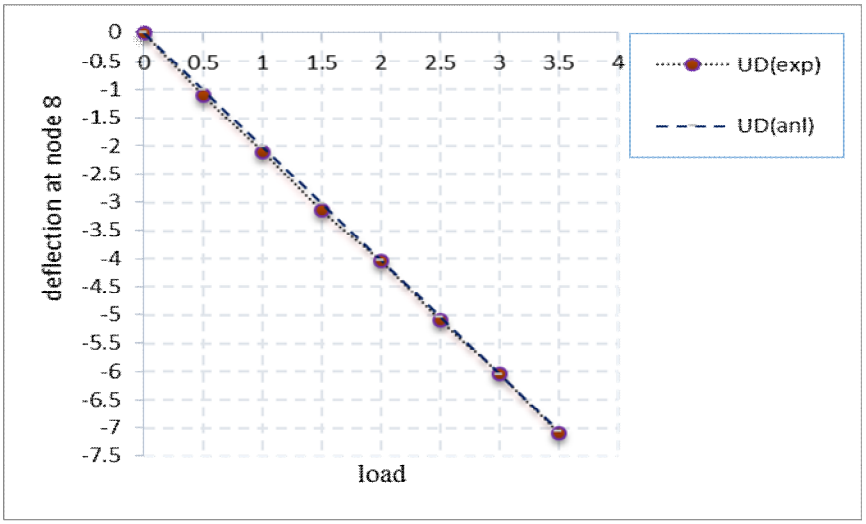

Fig 5.1.4: Comparison of analytical and experimental deflection for UD case

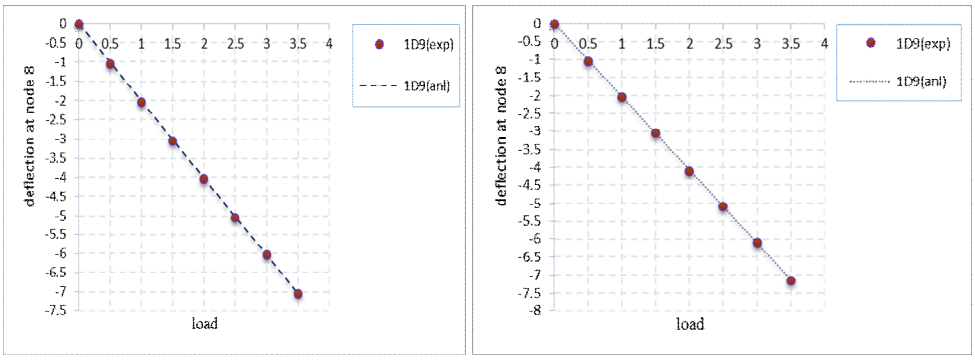

Fig 5.1.5: Comparison of analytical and experimental deflection for 1D9 case (case I and case V)

Similarly the change of deflection at all nodes for the different double element damage cases are shown in table 5.1.5.

Table 5.1.5: Deflection at various nodes for UD and 2 D 9-17 case

Node	UD	2-D9 (50%), D17 (5%)	2-D9 (50%) ,D17(10%)	2-D9(50%) D17 (20%)	2-D9(50%) D17 (30%)	2-D9 (50%) D17(50%)D
1	1.25763	1.38189	1.4097	1.48873	1.61998	2.3157
2	1.17379	1.28288	1.30901	1.38324	1.50655	2.16012
3	1.08999	1.18392	1.20836	1.2778	1.39314	2.00457
4	1.00631	1.08508	1.10783	1.17248	1.27987	1.84915
5	0.92293	0.98653	1.0076	1.06745	1.16689	1.69402
6	0.84006	0.88849	0.90787	0.96294	1.05442	1.5394

Node	UD	2-D9 (50%), D17 (5%)	2-D9 (50%) ,D17(10%)	2-D9(50%) D17 (20%)	2-D9(50%) D17 (30%)	2-D9 (50%) D17(50%)D
7	0.75797	0.79124	0.80893	0.85921	0.94273	1.38556
8	0.67703	0.69513	0.71113	0.75662	0.83219	1.23287
9	0.59762	0.60056	0.61488	0.65557	0.72319	1.08172
10	0.52024	0.51559	0.52822	0.56412	0.62379	0.94017
11	0.44541	0.44146	0.4524	0.48351	0.53522	0.80945
12	0.37373	0.37043	0.37969	0.406	0.44976	0.68184
13	0.30586	0.30313	0.3107	0.33223	0.36802	0.55796
14	0.24252	0.24025	0.24613	0.26287	0.29071	0.4385
15	0.18449	0.18255	0.18675	0.19869	0.21858	0.32422
16	0.13264	0.13085	0.13336	0.14051	0.15244	0.21593
17	0.08787	0.08602	0.08684	0.0892	0.09318	0.11452

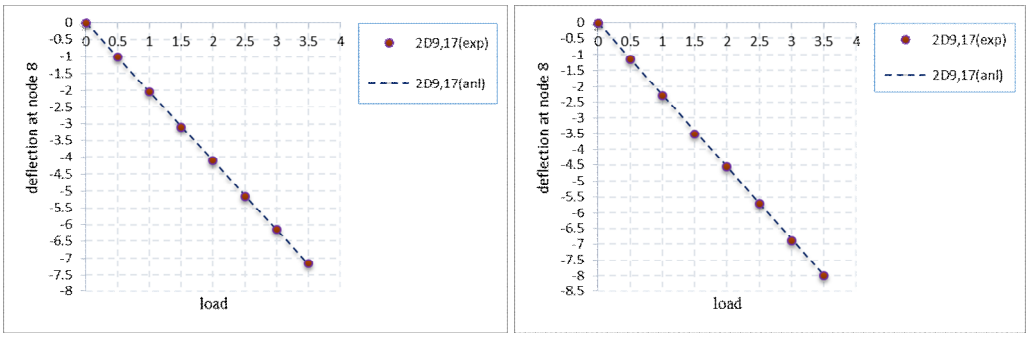

Fig 5.1.6: Comparison of analytical and experimental deflection for 2D9, 17 case (case I and case V)

It is observed that the deflection at all the degrees of freedom are increasing with the increase of damage percentage in case of 1D9. Similar observations are also found for double element damage (2D9-17) cases. The increment in deflection for double element damage is much higher than the single element damage case.

The comparison of numerically obtained eigen values and natural frequencies for different damage cases both for 1D9 and 2D9-17 are shown in Fig 5.1.6 and Fig 5.1.7. The change in numerically obtained first and second mode shapes at few selected d.o.f are presented in Table 5.1.8 and Table 5.1.9 for undamaged and different single and double element damage cases.

Table 5.1.6: Change of Eigen value and frequency for different damage (%) for 1D9 case (Numerical)

DAMAGE (%)	1D9					
	1st Mode		2nd Mode		3rd Mode	
	Eigen value	Frequency (Hz)	Eigen value	Frequency (Hz)	Eigen value	Frequency (Hz)
0(UD)	101.03362	1.5998517	3945.6149	9.9977923	30776.904	27.922817
5	100.99828	1.5995718	3897.6216	9.9368012	30651.346	27.865802
10	100.90972	1.5988704	3837.7275	9.860157	30497.428	27.795749
20	100.50106	1.5956296	3671.3153	9.644009	30082.135	27.605848
30	99.582519	1.5883212	3419.2838	9.3070992	29480.207	27.328263
50	93.805241	1.5415596	2533.8587	8.011945	27553.252	26.420023

Table 5.1.7: Change of Eigen value and frequency for different damage (%) for 2D9-17 case (Numerical)

DAMAGE (%)	2D9 17					
	1st Mode		2nd Mode		3rd Mode	
	Eigen value	Frequency (Hz)	Eigen value	Frequency (Hz)	Eigen value	Frequency (Hz)
0(UD)	101.03362	1.5998517	3945.6149	9.9977923	30776.904	27.922817
5	99.102991	1.5844923	3895.1558	9.9336574	30661.925	27.87061
10	96.785427	1.5658557	3831.4133	9.8520422	30507.75	27.800452
20	90.675137	1.5156219	3651.3954	9.61781	30049.943	27.591073
30	81.970291	1.4410366	3373.5281	9.2446172	29329.146	27.258156
50	54.139603	1.1711278	2367.0554	7.7437439	26811.65	26.062048

Table 5.1.8: Change of first mode shape at selected d.o.f. for UD and different damage cases (Numerical)

First mode shape measured at 5th 9th 13th and 17th degree of freedom		
UD	1D9	2D 9,17
-0.219106251	-0.217709429	-0.218977775
-0.184301802	-0.182903611	-0.184165005
-0.150093899	-0.148689987	-0.149923377
-0.117127073	-0.115707992	-0.116869926

Table 5.1.9: Change of second mode shape at selected d.o.f. for UD and different damage cases (Numerical)

Second mode shape measured at 5th 9th 13th and 17th degree of freedom		
UD	**1D9**	**2D 9, 17**
-0.037849593	-0.037586209	0.037648765
-0.004753057	-0.004429654	0.004491099
0.023411428	0.023955898	-0.023897259
0.043173199	0.044229936	-0.044174051

It is clearly found that the change of the first natural frequency is not so significant whereas, the change of the second and third natural frequency are substantial with the incorporation of damages. The change in first and second mode shapes are significant as measured in selected d.o.f.

5.2 Example- II (Steel cantilever beam)

A steel cantilever beam of uniform cross-section (50mm wide x 15 mm thick) of steel is discretized by 20 no of beam elements as shown in Fig.5.2.1 is considered. The schematic diagram of the steel cantilever beam is shown in the Fig.4.1.17 .The data considered for this example are, modulus of elasticity (E) =$2.1x10^{11}N/m^2$, mass per unit volume is =7850kG/cum. So, mass per length in Kg /m is (7850 X Cross sectional area). The schematic plan and elevation of the undamaged as well as 2D56 and 4D5678 are shown in Fig. 4.1.17, Fig. 4.1.18 and Fig. 4.1.19. The details of the measured dimensions of the undamaged and damaged beams are shown in Table 5.2.1. Structural parameters of the beam are shown in Table 5.2.2.

Table5.2.1: Measured dimensions of steel cantilever beam

Element Number	**Length (mm)**			**Width (mm)**			**Thickness (mm)**		
Damaged Condition	**UD**	**2D56**	**4D5678**	**UD**	**2D56**	**4D5678**	**UD**	**2D56**	**4D5678**
1	500	500	500	50	50	50	15	15	15
2	500	500	500	50	50	50	15	15	15
3	500	500	500	50	50	50	15	15	15

Element Number	Length (mm)			Width (mm)			Thickness (mm)		
Damaged Condition	**UD**	**2D56**	**4D5678**	**UD**	**2D56**	**4D5678**	**UD**	**2D56**	**4D5678**
4	500	500	500	50	50	50	15	15	15
5	500	500	500	50	45	45	15	15	15
6	500	500	500	50	45	45	15	15	15
7	500	500	500	50	50	45	15	15	15
8	500	500	500	50	45	45	15	15	15
9	500	500	500	50	50	50	15	15	15
10	500	500	500	50	50	50	15	15	15

UD: Undamaged; 2D: Double element (5, 6) damaged; 4D: Multiple element damaged (5, 6, 7, 8)

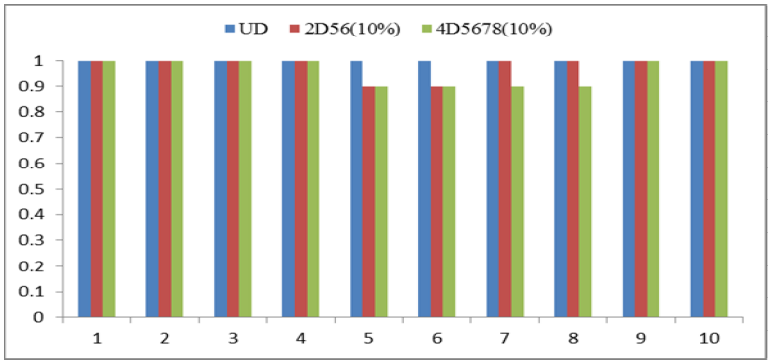

Fig 5.2.1: Graphical representation of various scenarios of UD and multiple damage

The details of the measured structural parameters based on the measurement of the undamaged and damaged beams are indicated in Table 5.2.2.

Table 5.2.2: Damaged structural parameters of steel cantilever beam

Element Number	Cross Sectional Area (mm^2)			Moment of Inertia (10^4 X mm^4)		
Damaged Condition	**UD**	**2D56**	**4D5678**	**UD**	**2D56**	**4D5678**
1	750	750	750	1.406	1.406	1.406
2	750	750	750	1.406	1.406	1.406
3	750	**750**	**675**	1.406	1.406	1.406
4	750	750	**675**	1.406	1.406	1.406

Element Number	Cross Sectional Area (mm^2)			Moment of Inertia (10^4 X mm^4)		
Damaged Condition	UD	2D56	4D5678	UD	2D56	4D5678
5	750	**675**	**675**	1.406	**1.265**	**1.265**
6	750	**675**	**675**	1.406	**1.265**	**1.265**
7	750	750	**675**	1.406	1.406	**1.265**
8	750	**750**	**675**	1.406	1.406	**1.265**
9	750	750	**750**	1.406	1.406	1.406
10	750	750	750	1.406	1.406	1.406

The experimental and analytical variation of the deflection for undamaged and different damage cases are plotted for Fig 5.2.2 to Fig 5.2.4.

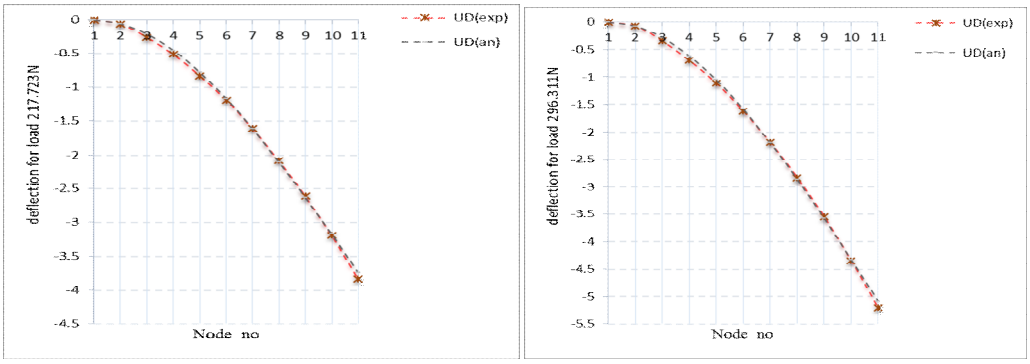

Fig 5.2.2: Comparison of analytical and experimental deflection for UD case

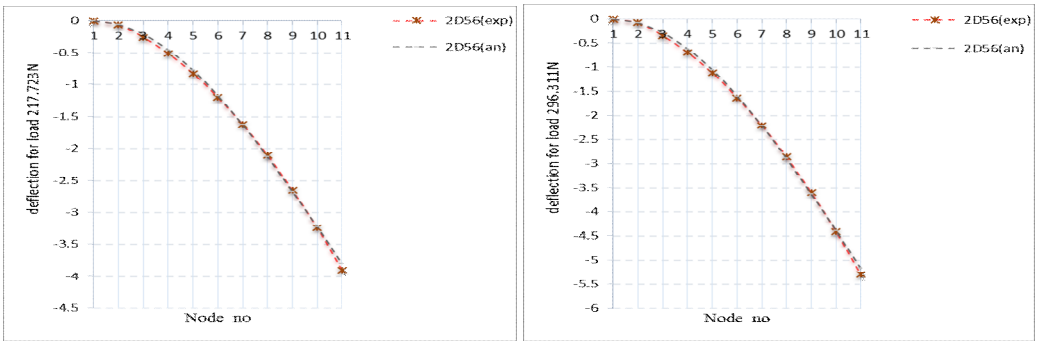

Fig 5.2.3: Comparison of analytical and experimental deflection for 2D56 case

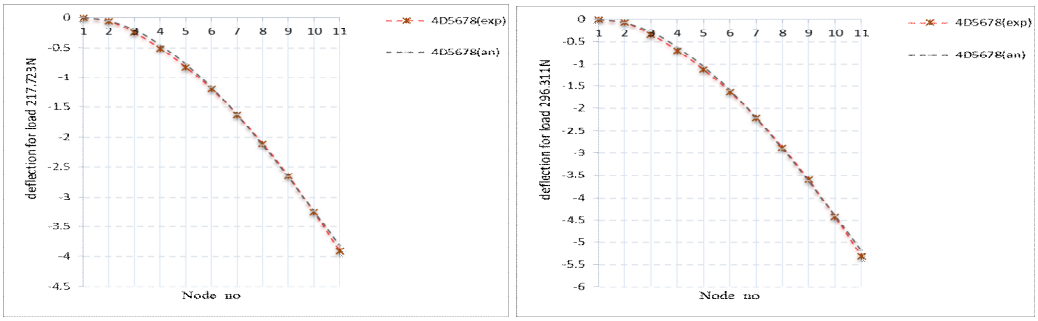

Fig 5.2.4: Comparison of analytical and experimental deflection for 4D5678 case

It is noted that the deflection for both analytical results are quite close. It is also seen that both analytical and experimental deflection increases due to increase of load applied and also due to the increase of damage extent.

The analytical eigenvalues and natural frequencies for UD and different damage cases are expressed from Table 5.2.3. Also a comparison between analytical and experimental natural frequencies are expressed in Table 5.2.4.

Table 5.2.3: Change of Eigen value and frequency for different damage (%) cases

Damage Case	1st Mode		2nd Mode		3rd Mode	
	Eigen Value	Frequency(Hz)	Eigen Value	Frequency(Hz)	Eigen Value	Frequency(Hz)
UD	87174.9	47.000	3599231	302.000	29391209	863.000
2D56	83504.8	46.000	3273263	288.000	27779203	839.000
4D5678	83504.8	46.000	3205425	285.000	26664872	822.000

Table 5.2.4: Comparison of Eigen value for analytical and experimental for different damage

Damage Case	1st Mode		2nd Mode		3rd Mode	
	Eigen Value (anl.)	Eigen Value(exp)	Eigen Value (anl.)	Eigen Value(exp.)	Eigen Value (anl.)	Eigen Value(exp.)
UD	87174.9	56985.300	3599231	1997841.000	29391209	12199596.000
2D56	83504.8	60024.000	3273263	1910035.000	27779203	11592963.000
4D5678	83504.8	54025.600	3205425	1858298.000	26664872	12024694.000

Table 5.2.5: Comparison of natural frequencies value for different damage

First three natural frequencies(Hz)					
UD		**2D56**		4 **UD5678**	
Numerical	**Experimental**	**Numerical**	**Experimental**	**Numerical**	**Experimental**
40	38	39	37	38	36
240	235	221	217	230	220
570	556	560	552	554	542

The change in the experimentally obtained mode shapes in few selected d.o.f for first mode shape is presented in Table 5.2.6 and the same for second mode shape is shown in Table 5.2.7.

Table 5.2.6: Change of mode shapes at selected d.o.f. for different damage (%) cases (Experimental)

First mode shape measured at 5^{th} 9^{th} 13^{th} and 17^{th} degree of freedom		
UD	**2D56**	**4D5678**
0.023077261	0.022535236	0.022284421
0.083102102	0.081215822	0.080328423
0.166798869	0.164231274	0.162495734
0.262597955	0.260067527	0.257945799

Table 5.2.7: Change of mode shapes at selected d.o.f. for different damage (%) cases (Experimental)

Second mode shape measured at 5^{th} 9^{th} 13^{th} and 17^{th} degree of freedom		
UD	**2D56**	**4D5678**
0.030823823	0.03098971	0.030385163
0.070444782	0.071971311	0.071005306
0.061810155	0.06390334	0.064494751
-0.005216696	-0.00385707	-0.002188827

The variation of the both analytical and experimental curvature for UD and different damage cases are plotted in Fig 5.2.5 and Fig 5.2.6.

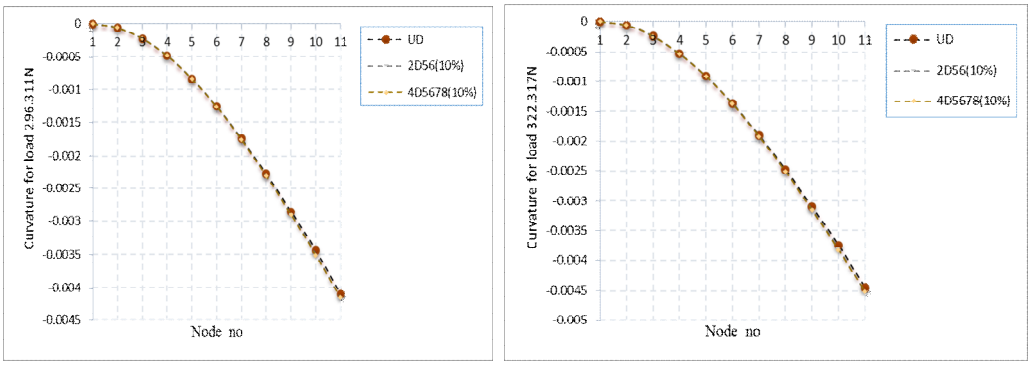

Fig 5.2.5: Variation of analytical curvature for different damage conditions

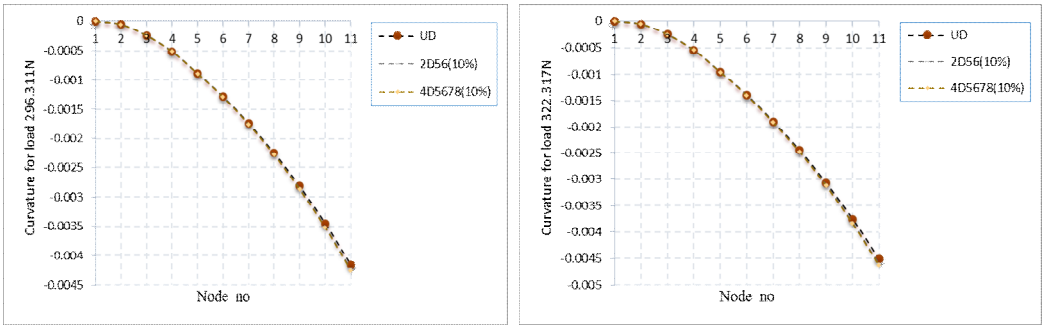

Fig 5.2.6: Variation of experimental curvature for different damage conditions

It is also seen that both analytical curvature and experimental curvature increases from fixed end to the free end. However, the variation is not significant for the different damage cases.

Measured static deflection and strain data at selected d.o.f. are mixed with the random noises and used for UD and different damage states to check the accuracy of the model **SLD** and **SSD**. The predicted error and estimated value for axial rigidity and bending rigidity of each element with various noise level are shown form Fig.5.2.7 to Fig.5.2.12 for UD and different damage conditions.

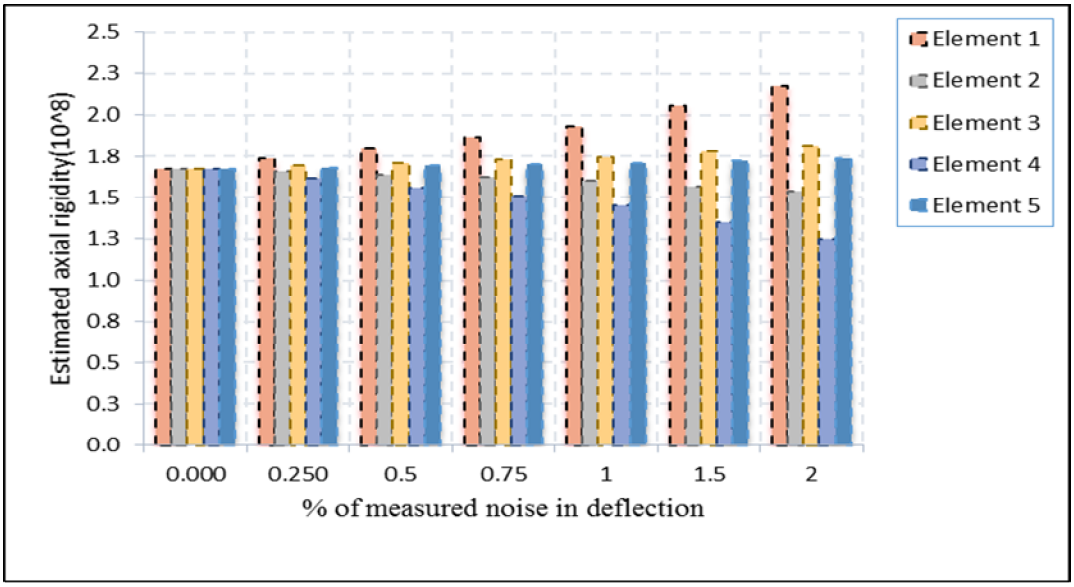

Fig 5.2.7: Predicted value of axial rigidity for UD case with different noise level

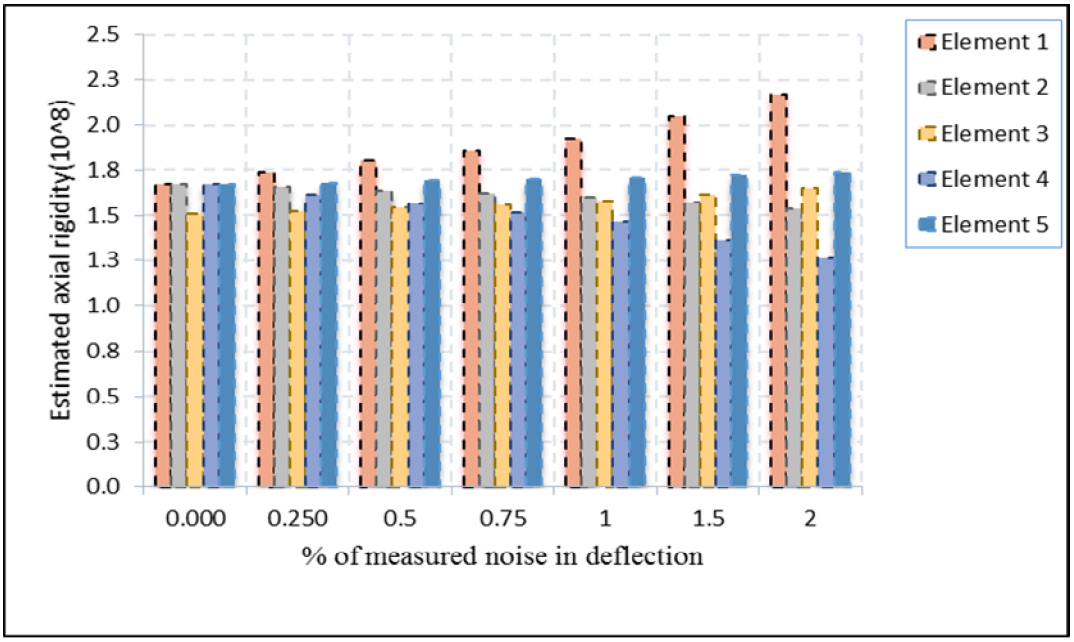

Fig 5.2.8: Predicted value of axial rigidity for 1D3 case with different noise level

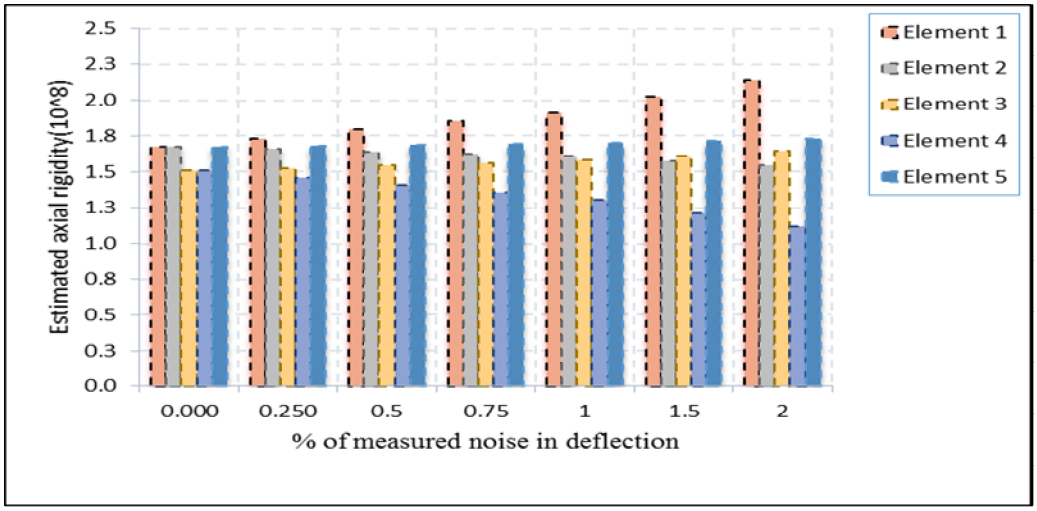

Fig 5.2.9: Predicted value of axial rigidity for 2D34 case with noise level

It is noted that axial rigidity and bending rigidity of both undamaged and damaged elements are predicted element wise with higher accuracy for the various damage states of the beam, provided accurate measured deflection data are available.

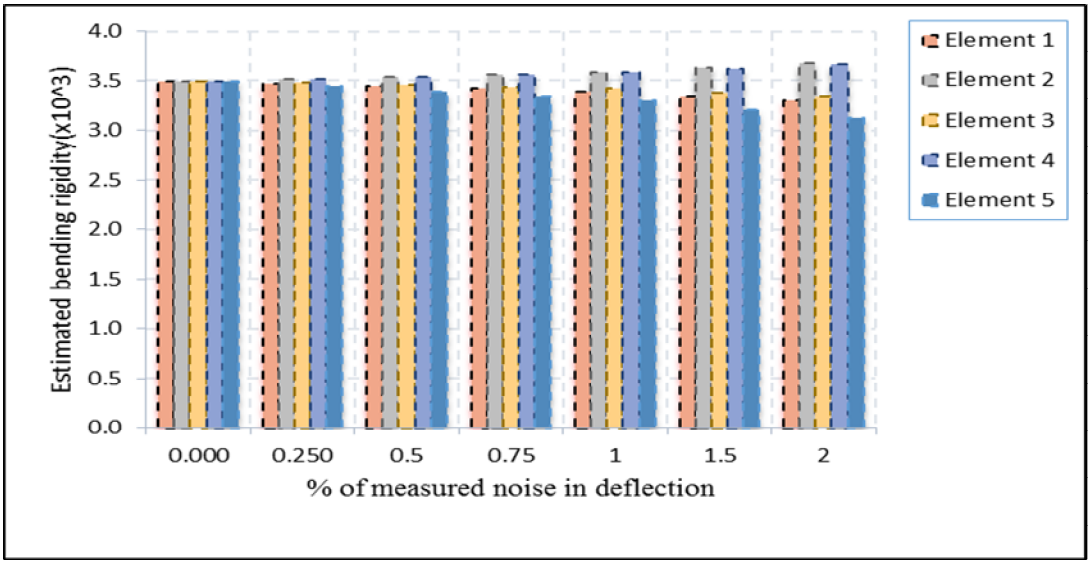

Fig 5.2.10: Predicted value of bending rigidity for UD case with noise level

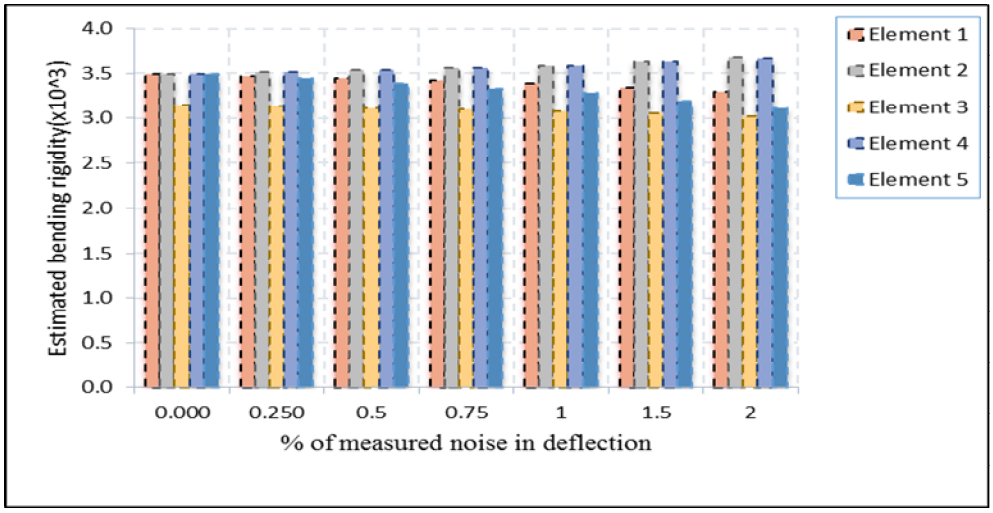

Fig 5.2.11: Predicted value of bending rigidity for 1D3 case with noise level

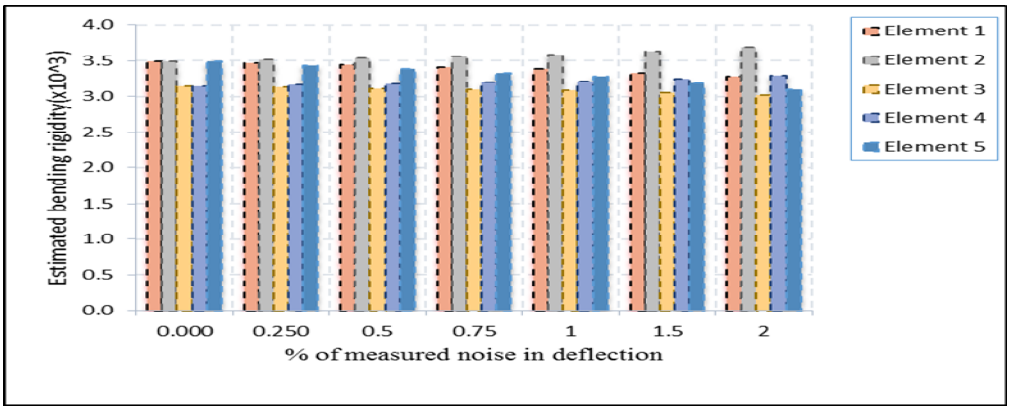

Fig 5.2.12: Predicted value of bending rigidity for 2D34 case with noise level

It is observed that axial rigidity and bending rigidity of both undamaged and damaged elements are predicted with sufficient accuracy for the various damage states of the beam using available measured strain data.

Measured modal data are mixed with the random noises and used for this model for undamaged and different damage state to check the accuracy of numerical model **DFS**. The predicted error and estimated value for axial rigidity and bending rigidity of each element with various noise level are shown form Fig.5.2.13 to Fig. 5.2.24 for UD and different damage level. It is found that the structural parameters like axial rigidity, bending rigidity of both undamaged and damaged elements are predicted with greater

accuracy for the various damage states of the beam provided accurate measured modal data are available. The prediction of structural parameters is effected by the presence of noise. However, the presence of noise in the measurement of modal data is inevitable. Thus the effect of the presence of noise in the measured data on the accuracy of the predicted structural properties is important to be studied. Similarly, the applicability of the proposed method in case of large structure with multiple damages is also important to be studied. It is seen that accuracy in the estimated axial rigidity and bending rigidity decreases for increased noise level. Also it is observed that the accuracy in prediction parameter for different element are varying due to the presence of random type noise. The random type noise also influence the error percentage to become a random one as the estimation of the parameter are associated with the iterative process and for different noise level the noisy modal parameters like frequencies and noisy mode shapes at selected d.o.f. are randomly varying.

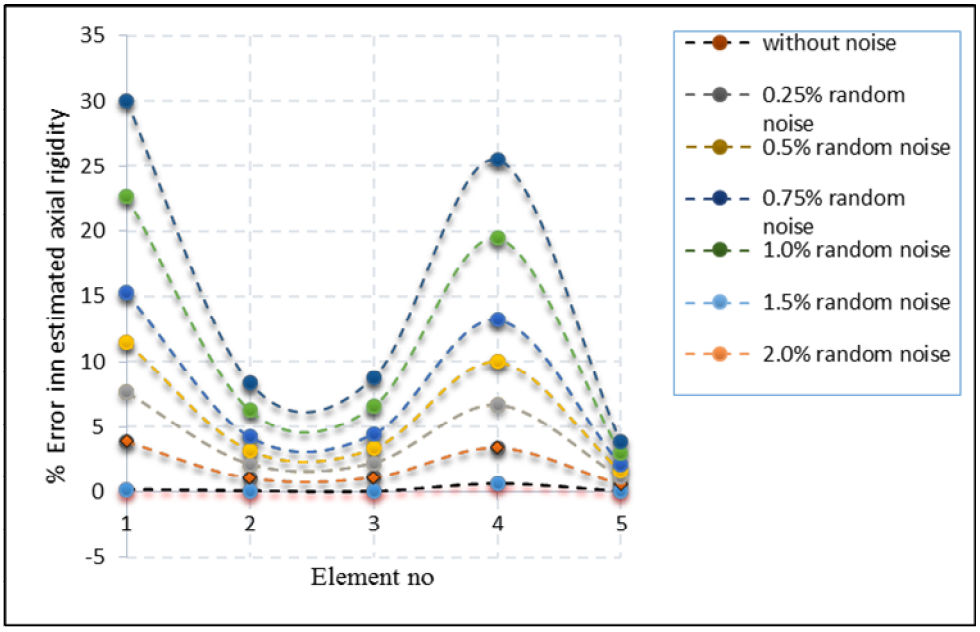

Fig 5.2.13: Error (%) for predicted axial rigidity with element for different noise in UD case

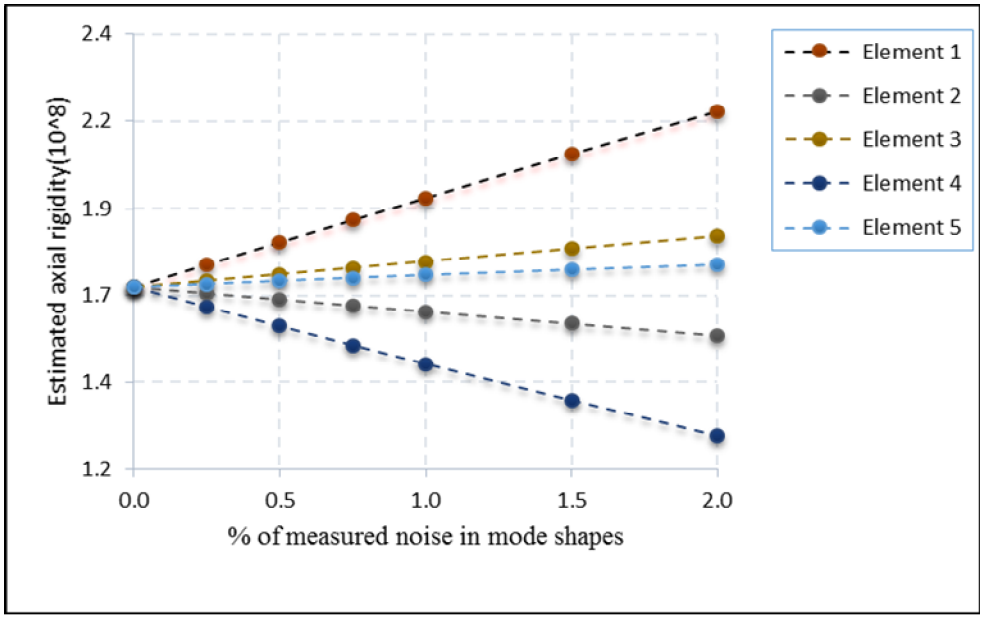

Fig 5.2.14: Predicted axial rigidity with measured noise for different element in UD case

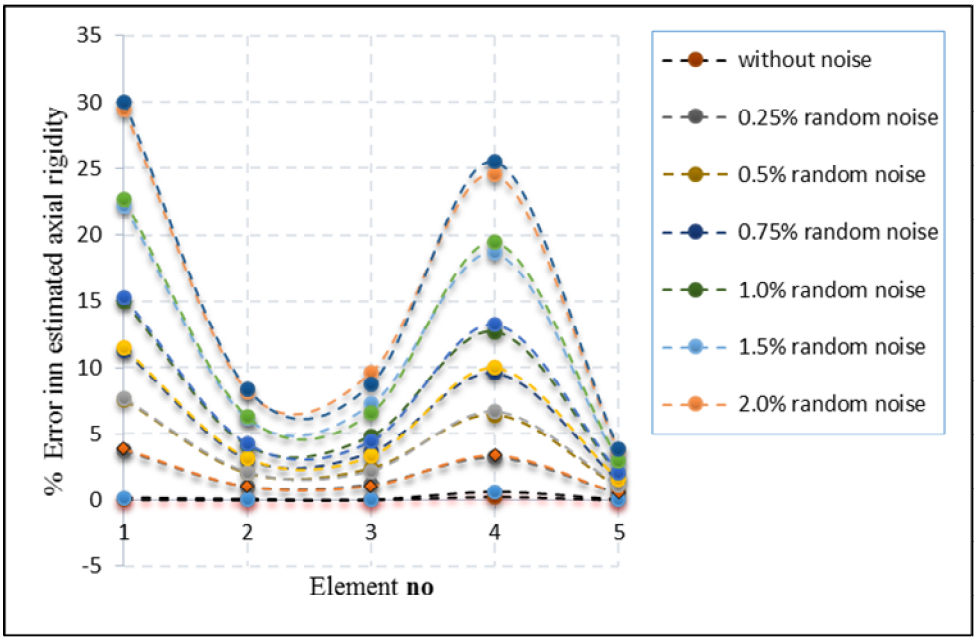

Fig 5.2.15: Error (%) for predicted axial rigidity with element for different noise in 1D3 case

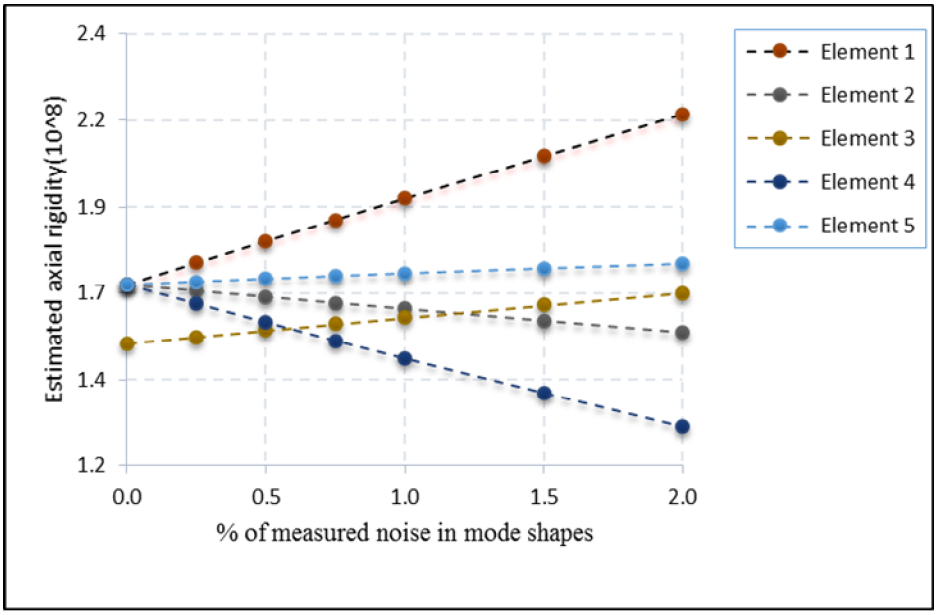

Fig 5.2.16: Predicted axial rigidity with measured noise for different element in 1D3 case

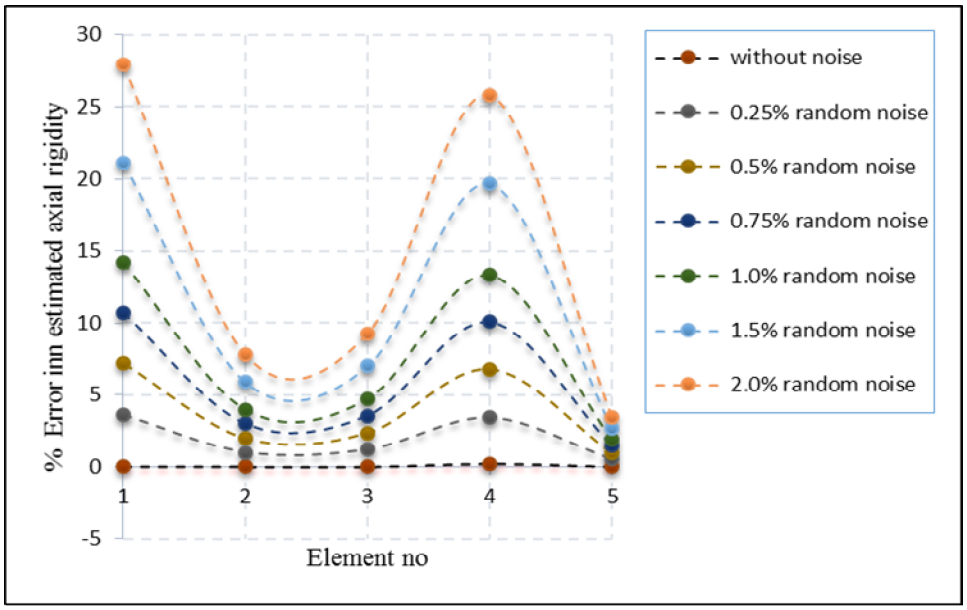

Fig 5.2.17: Error (%) for predicted axial rigidity with element for different noise in 2D34 case

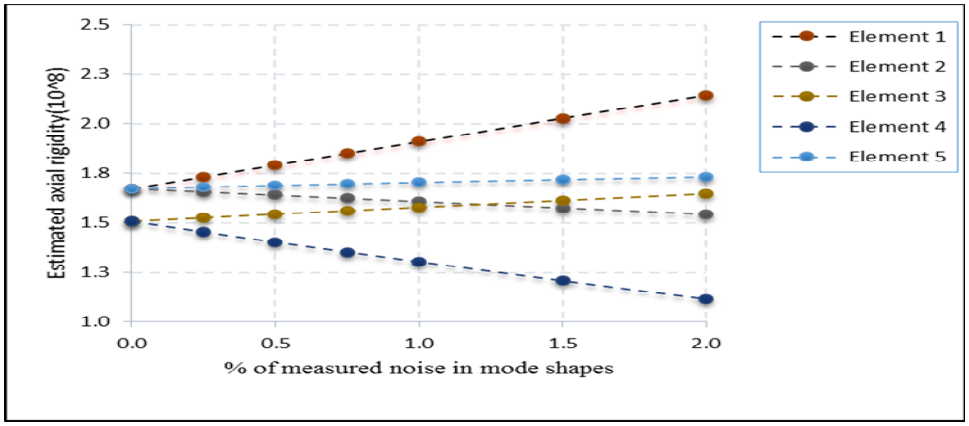

Fig 5.2.18: Estimated axial rigidity with measured noise for different element in 2D34 case

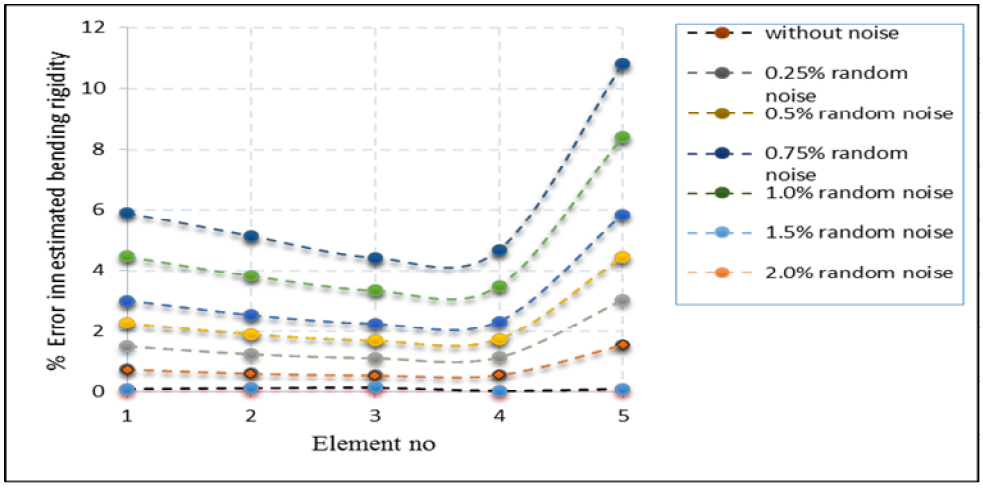

Fig 5.2.19: Error (%) in estimated bending rigidity with for different element for UD case

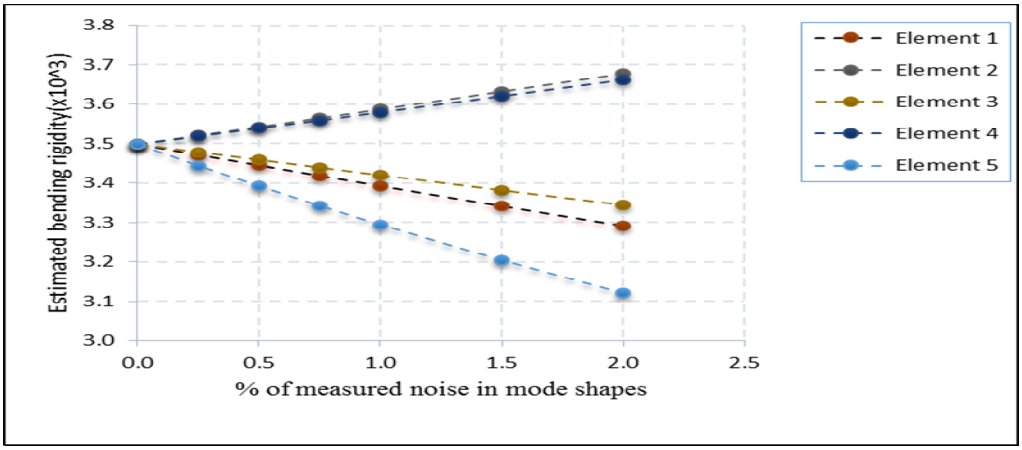

Fig 5.2.20: Plot of bending rigidity with measured noise in mode shapes for different UD case

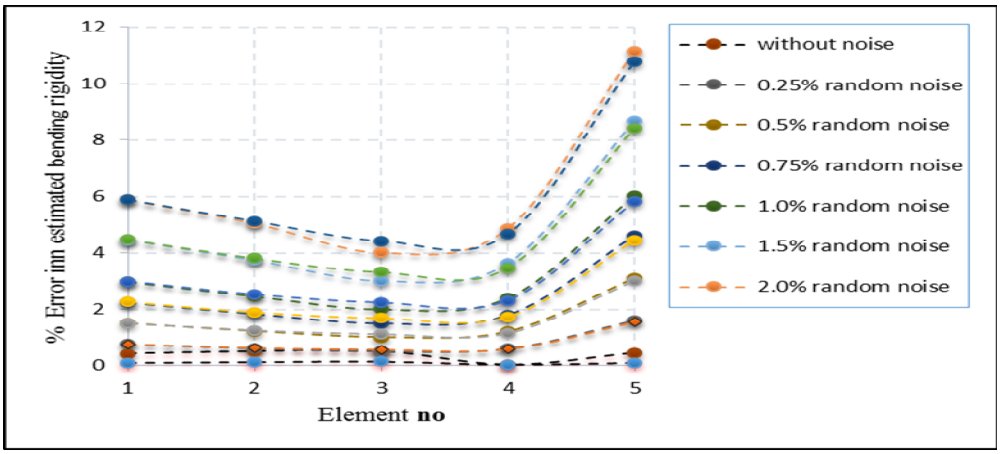

Fig 5.2.21: Error (%) in estimated bending rigidity with for different element for 1D1 case

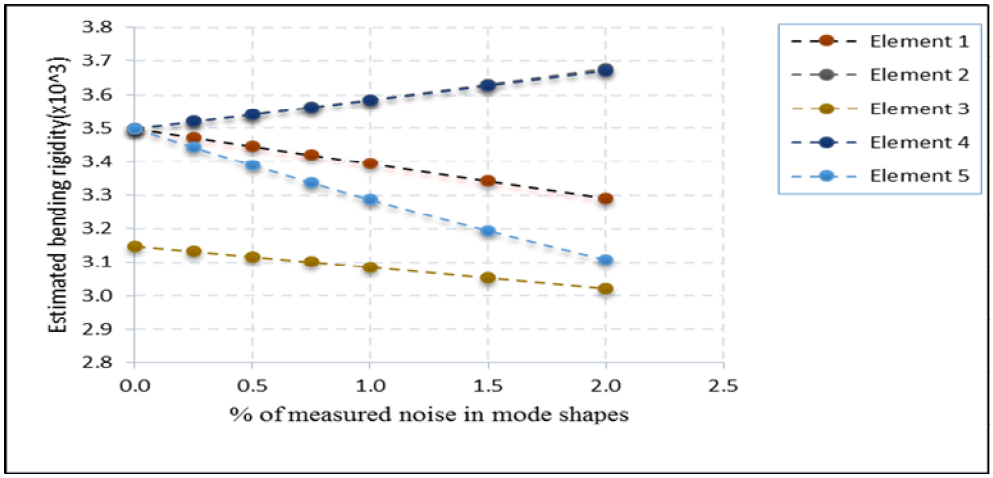

Fig 5.2.22: Plot of bending rigidity with measured noise in mode shapes for different 1D3 case

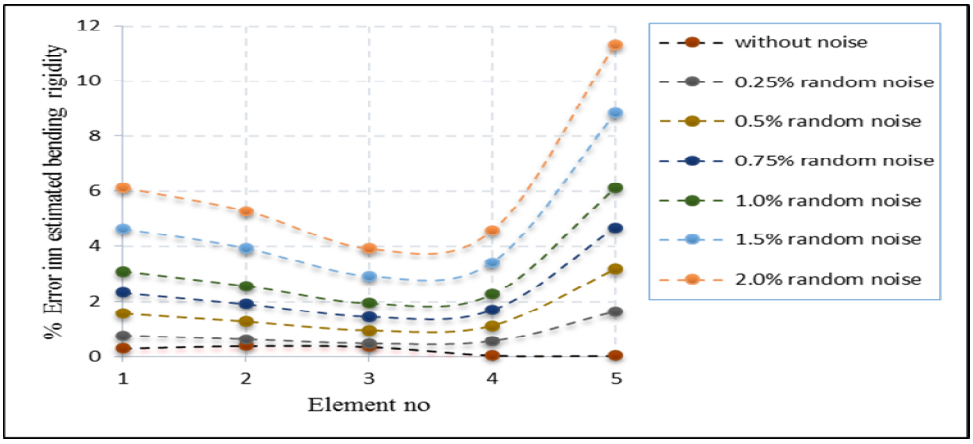

Fig 5.2.23: Error (%) in estimated bending rigidity with for different element for 2D34 case

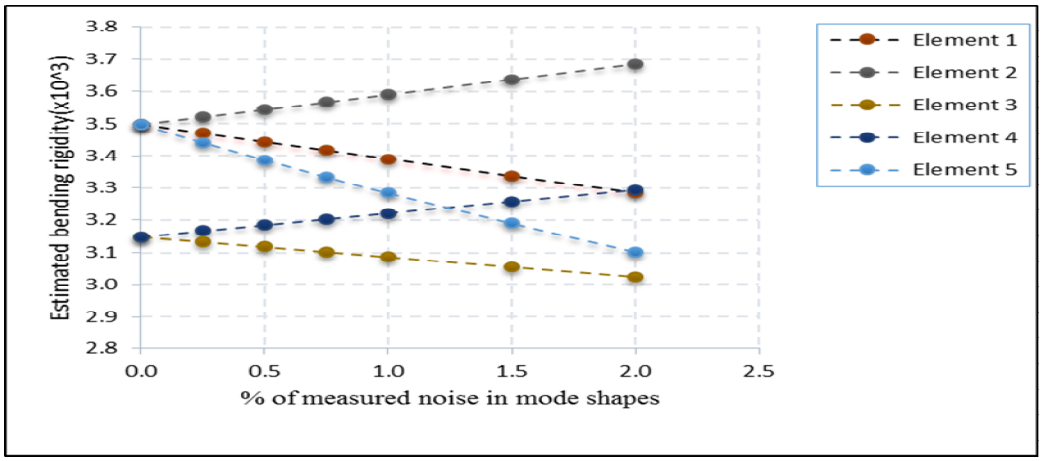

Fig 5.2.24: Plot of bending rigidity with measured noise in mode shapes for different 2D34 case

It is found that the estimated error is lower in case of bending rigidity in comparison with the axial rigidity. The measurement of dynamic responses in the direction of bending may have contributed the greater accuracy of the bending rigidity prediction. It seems that error in prediction of axial rigidity may be reduced by putting accelerometers in horizontal direction.

The error in the predicted parameters for each element with the no of measured modes are studied in Fig 5.2.25 to 5.2.30 for UD and different damage cases.

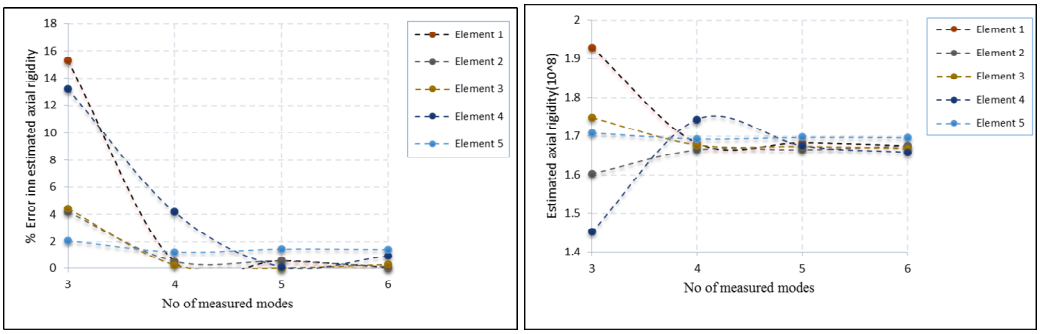

Fig 5.2.25: Error and predicted axial rigidity with measured mode for different element for UD case

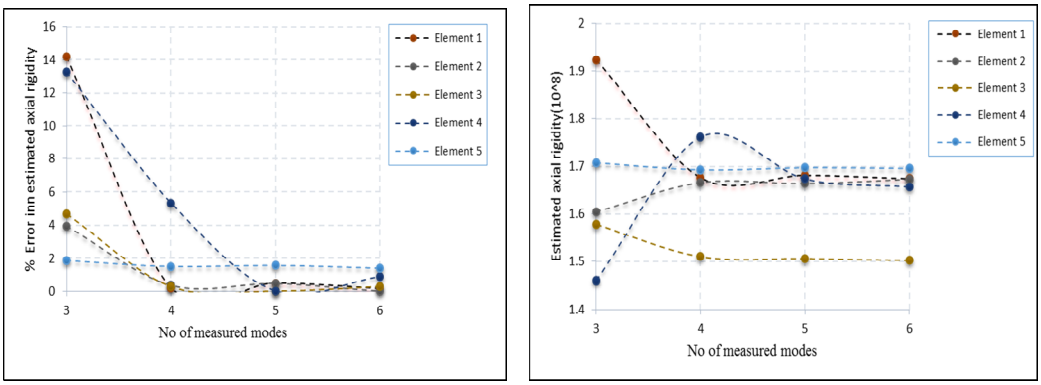

Fig 5.2.26: Error and predicted axial rigidity with measured mode for different element for 1D3 case

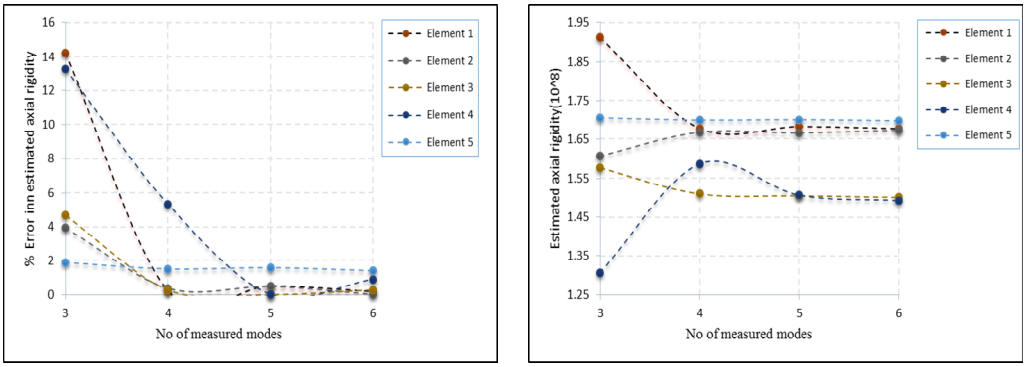

Fig 5.2.27: Error and predicted axial rigidity with measured mode for different element for 2D34 case

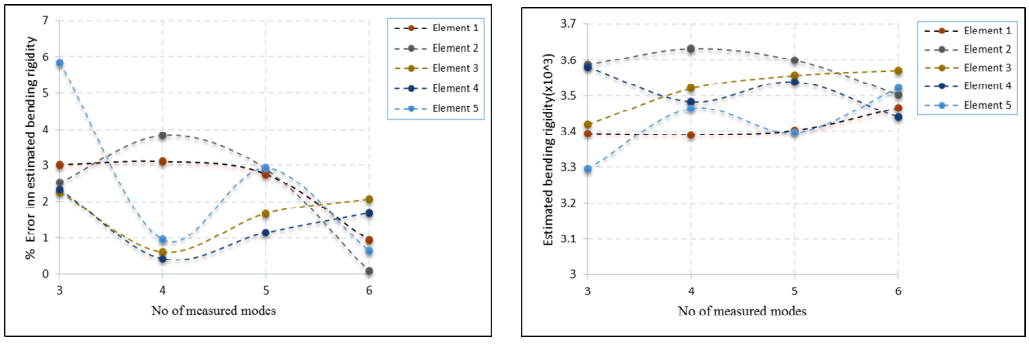

Fig 5.2.28: Error and predicted bending rigidity with measured mode for different element for UD case

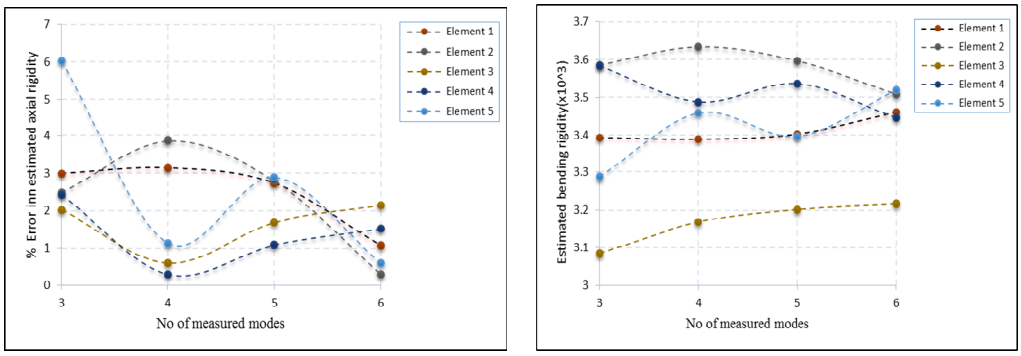

Fig 5.2.29: Error and predicted bending rigidity with measured mode for different element for 1D3 case

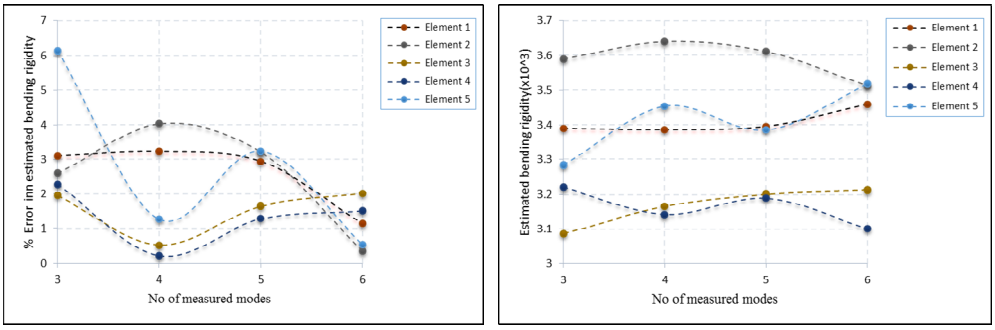

Fig 5.2.30: Error and predicted bending rigidity with measured mode for different element for 2D34

It is clearly observed from Fig 5.2.25 to 5.2.30 that the accuracy of prediction of the structural parameters depend on the number of measurement of modal data. The model is able to accurately p**r**edict the structural parameters provided noise-free data of large number of measured modes are available as observed in Example II. But in practice, the availability of large number of modal data is difficult. The presence of noise, which is generally random in nature mixed with the measured data, is also inevitable in practice. It is also observed earlier that noisy data decreases the accuracy of the identified parameter by the proposed method. Hence this method may not be suitable for all type of large structures to identify the structural parameters precisely by the proposed deterministic approach using the limited measured data mixed with random measurement noise.

5.3 Example-III: (Steel fixed-fixed beam)

A uniform beam with the ends fixed against translation and rotation is considered for this example. For analysis, the beam has been divided into four equal elements in the finite element framework. The dimensions (meter) and the degrees of freedoms are shown in Fig. 5.3.1.The different geometric and mechanical properties of the undamaged beam is shown in Table 5.3.1.

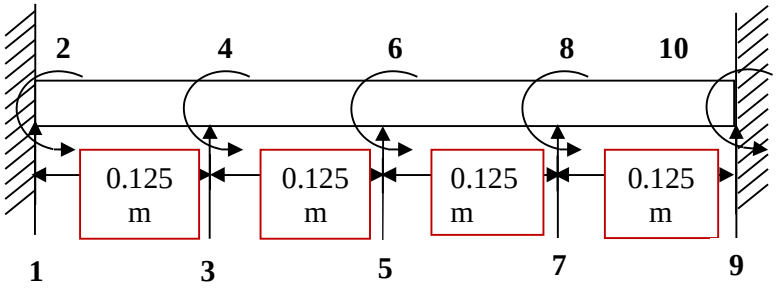

Fig 5.3.1: Different degrees of freedom of the fixed- fixed beam

Table 5.3.1: Different undamaged properties of the beam:

Member No	Length (m)	Width(m)	Depth(m)	Mass Density(Kg/m3)	Modulus of Elasticity (E)kN/sqm
1	0.125	0.05	0.015	7850	2.1×10^{11}
2	0.125	0.05	0.015	7850	2.1×10^{11}
3	0.125	0.05	0.015	7850	2.1×10^{11}
4	0.125	0.05	0.015	7850	2.1×10^{11}

Analysis performed for different undamaged and different damage cases as shown below:

UD : Undamaged state – No damage in any element.

CASE I (1D1) : Single element damaged state element no. 1.

CASE II (2D13) : Multiple damaged state element nos. 1 and 3.

Two types of multiple damages in terms of reduced values of their original axial rigidity (AE), bending rigidity (EI) of different extent at various locations are

considered. The details of damage extent for these damage cases are shown in Fig 5.3.2 and Fig 5.3.3.

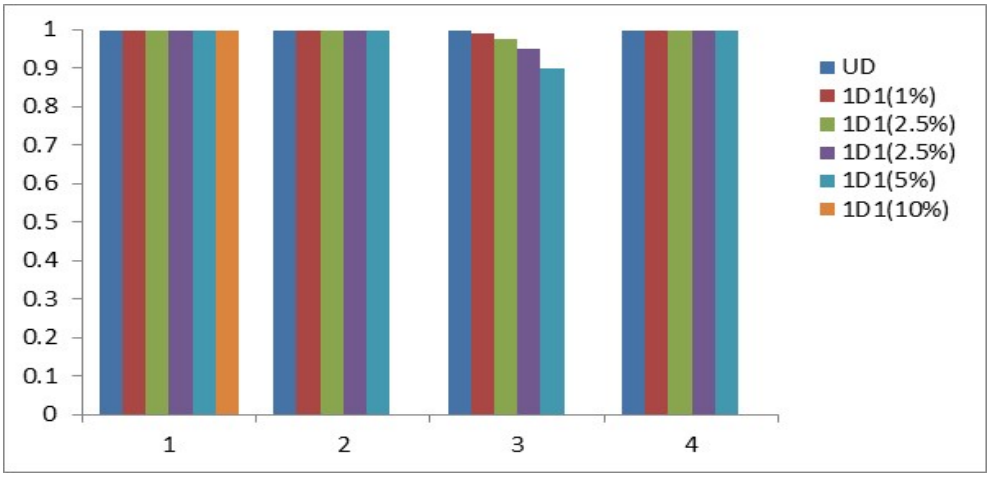

Fig 5.3.2: Graphical representation of various scenarios of UD and single element damage

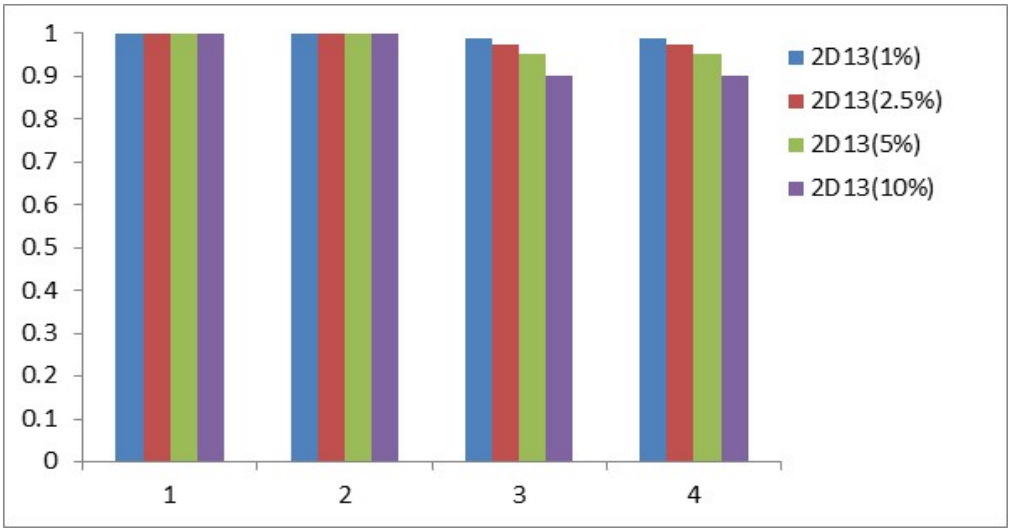

Fig 5.3.3: Graphical representation of various scenarios of UD and double element damage

The variation of analytical vertical deflection at different nodes for UD, different single element and double element damages are plotted in Fig 5.3.4.

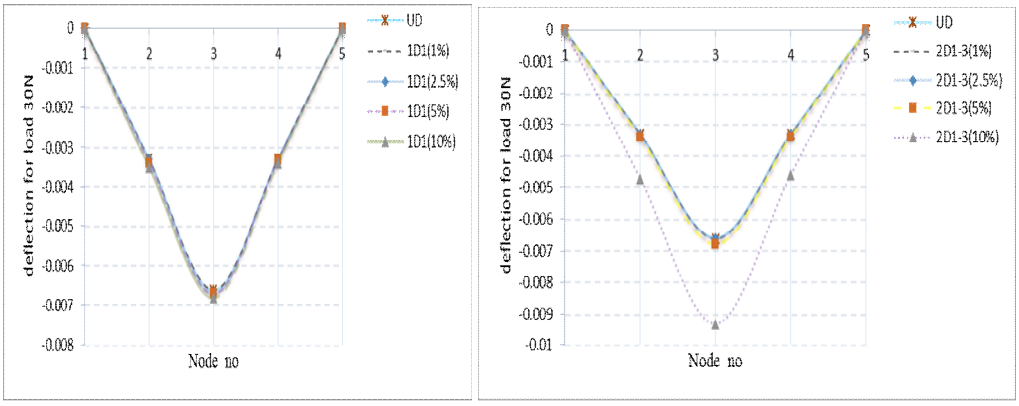

Fig 5.3.4: Variation of analytical deflection for different damage conditions (1D1 and 2D13)

It is observed that deflection values increases significantly for the increase of damage. The change in the eigen values and the natural frequencies are studied in Table 5.3.2 and Table 5.3.3 for UD, different single element and double element damages. The normalized first and second mode shapes are plotted in Fig 5.3.5 and Fig 5.3.6.

Table 5.3.2: Change of Eigen values and frequency for different damage (%) for 1D1 case

DAMAGE (%)	1D1					
	1st Mode		2nd Mode		3rd Mode	
	Eigen value	Frequency (Hz)	Eigen value	Frequency (Hz)	Eigen value	Frequency (Hz)
0(UD)	4029472.49	319.5	29269388.46	861.1	123890445.1	1771.6
1%	4016870.551	319	29208237.18	860.2	123555001.8	1769.2
2.5%	3999260.994	318.3	29120020.45	858.9	123052689.5	1765.6
5%	3969163.182	317.1	28964271.53	856.6	122189994.5	1759.4
10%	3909308.61	314.7	28640575.58	851.8	120349612.1	1746.1

Table 5.3.3: Change of Eigen value and frequency for different damage (%) for 2D1, 3 case

DAMAGE (%)	2D13					
	1st Mode		2nd Mode		3rd Mode	
	Eigen value	Frequency (Hz)	Eigen value	Frequency (Hz)	Eigen value	Frequency (Hz)
0(UD)	4029472.49	319.5	29269388.46	861.1	123890445.1	1771.6
1%	4009318.861	318.7	29120020.45	858.9	123261862	1767.1
2.5%	4009318.861	318.7	29120020.45	858.9	123261862	1767.1

DAMAGE (%)	2D13					
	1st Mode		2nd Mode		3rd Mode	
	Eigen value	Frequency (Hz)	Eigen value	Frequency (Hz)	Eigen value	Frequency (Hz)
5%	3926719.22	315.4	28526369.45	850.1	120722093.8	1748.8
10%	3822835.821	311.2	27753170.52	838.5	117417707.5	1724.7

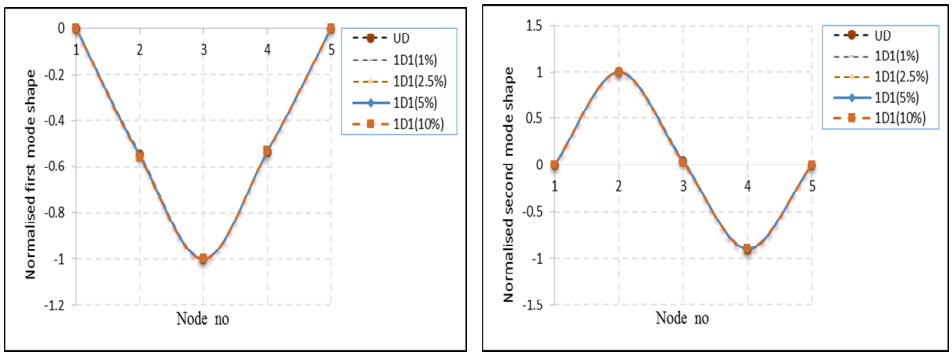

Fig 5.3:5: Variation of analytical first and second mode shapes for different damage (1D1)

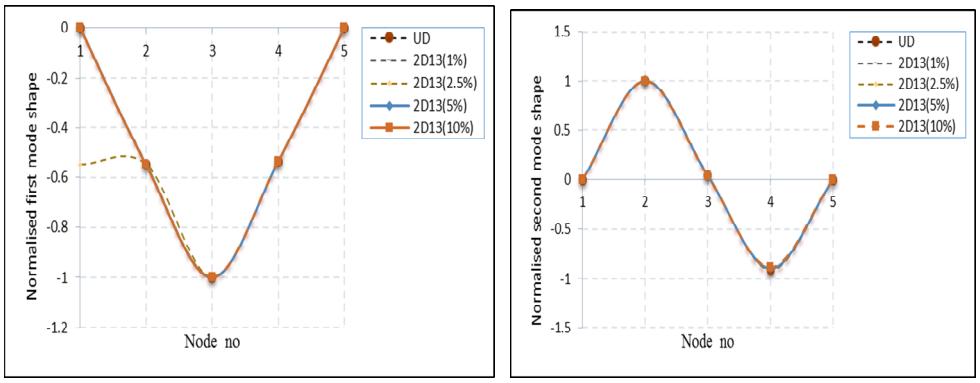

Fig 5.3.6: Variation of analytical first and second mode shapes for different damage (2D13)

It is observed that Eigen values and the first three natural frequencies are reduced for all different damage cases. However, there is very small variation in the normalized mode shapes for different damage conditions.

The predicted error and estimated value for bending rigidity of each element with various noise level are shown form Fig.5.3.7 to Fig.5.3.9 for undamaged and different damage level using numerical model **DFC**. It is noted that the accuracy in prediction parameter for different element are different.

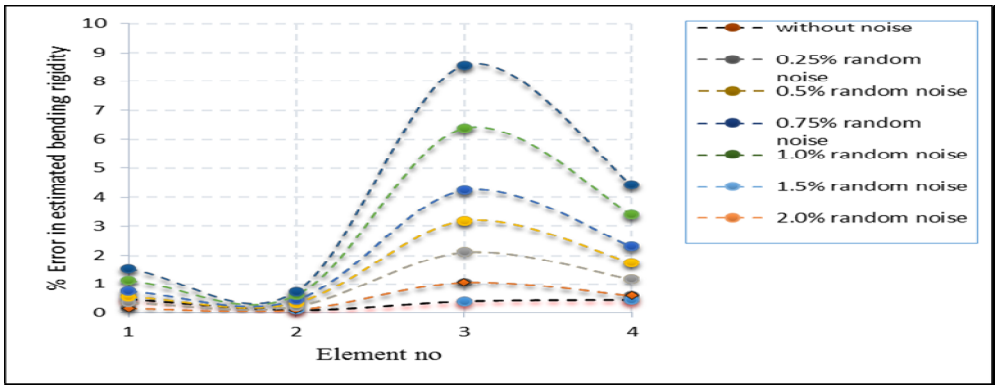

Fig 5.3.7: Error (%) in estimated bending rigidity with for different element for UD case for

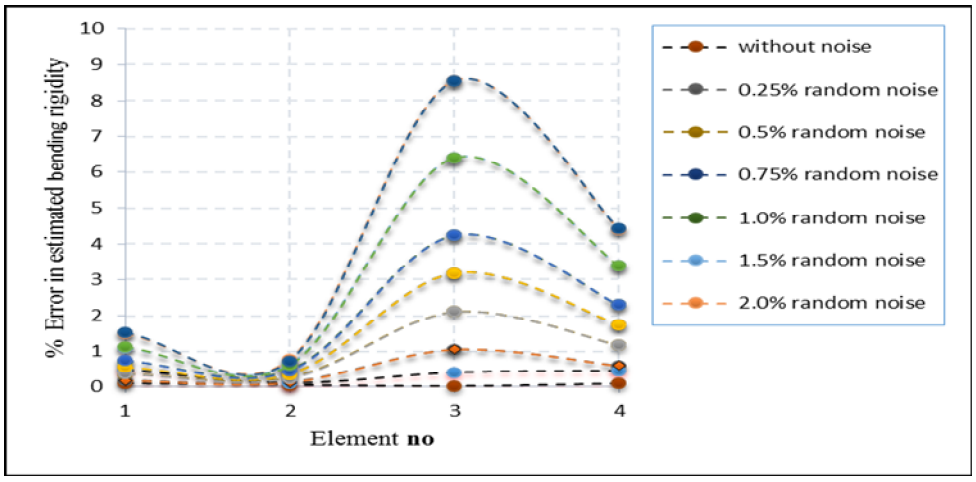

Fig 5.3.8: Error (%) in estimated bending rigidity with for different element for 1D1 case

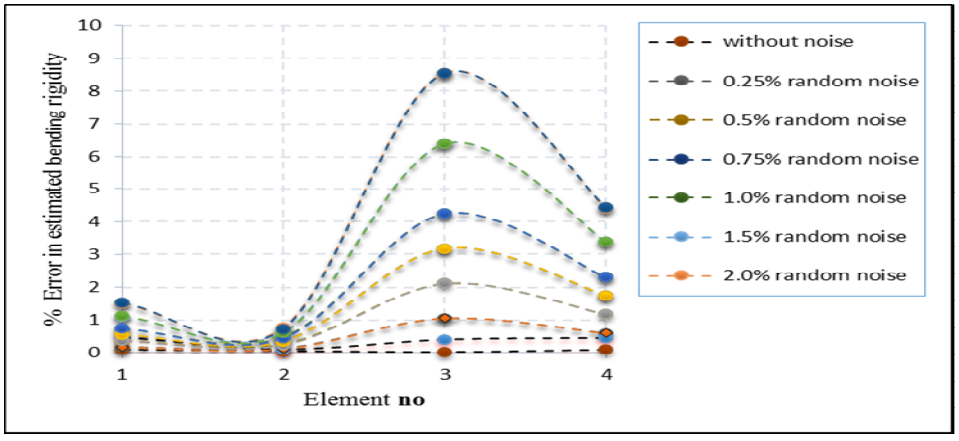

Fig 5.3.9: Error (%) in estimated bending rigidity with for different element for 2D13 case

The estimated value for bending rigidity of each element with various noise level are shown form Fig.5.3.10 to Fig.5.3.12 for UD and other different damage cases.

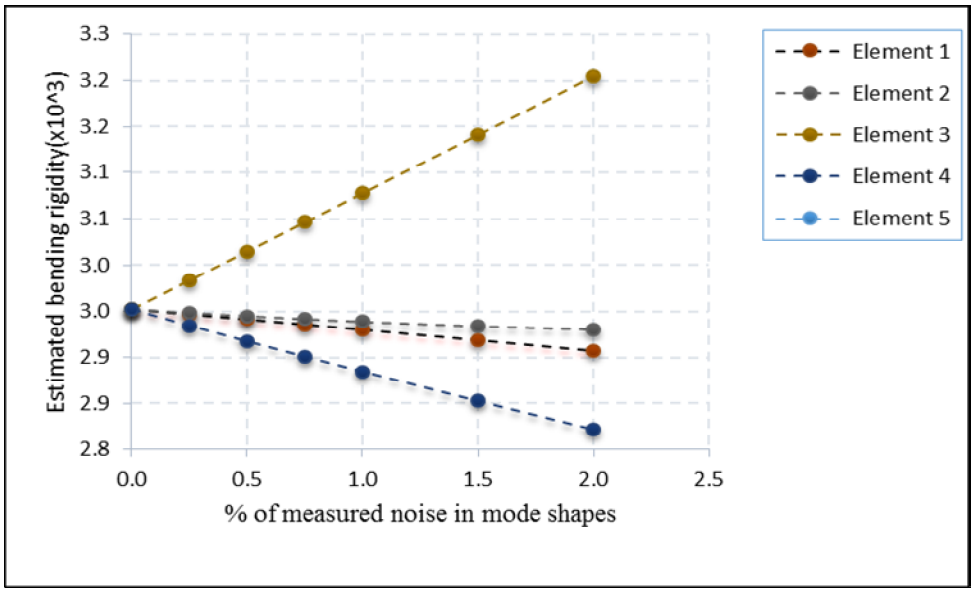

Fig 5.3.10: Estimated bending rigidity with measured noise for UD case

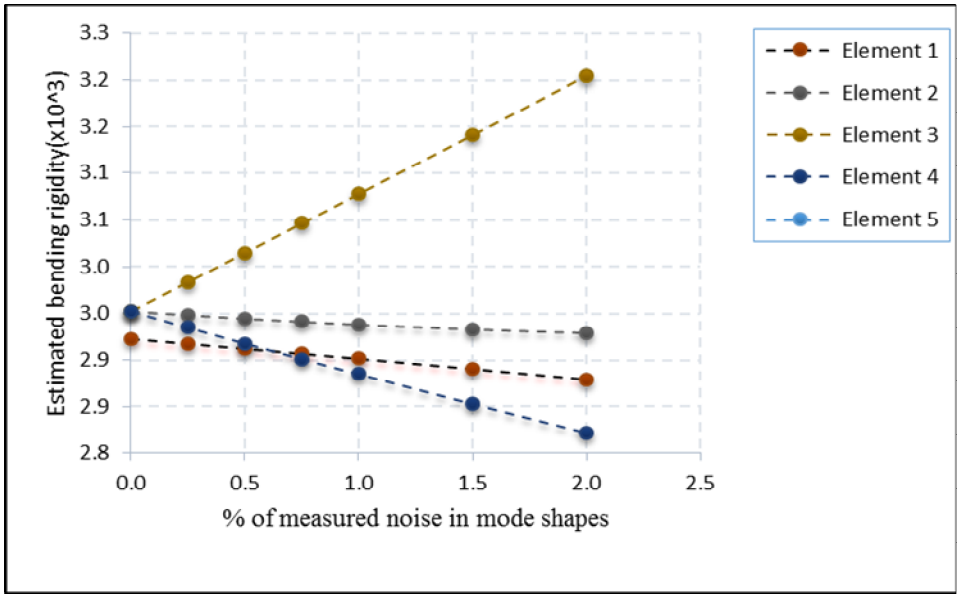

Fig 5.3.11: Estimated bending rigidity with measured noise for 1D1 case

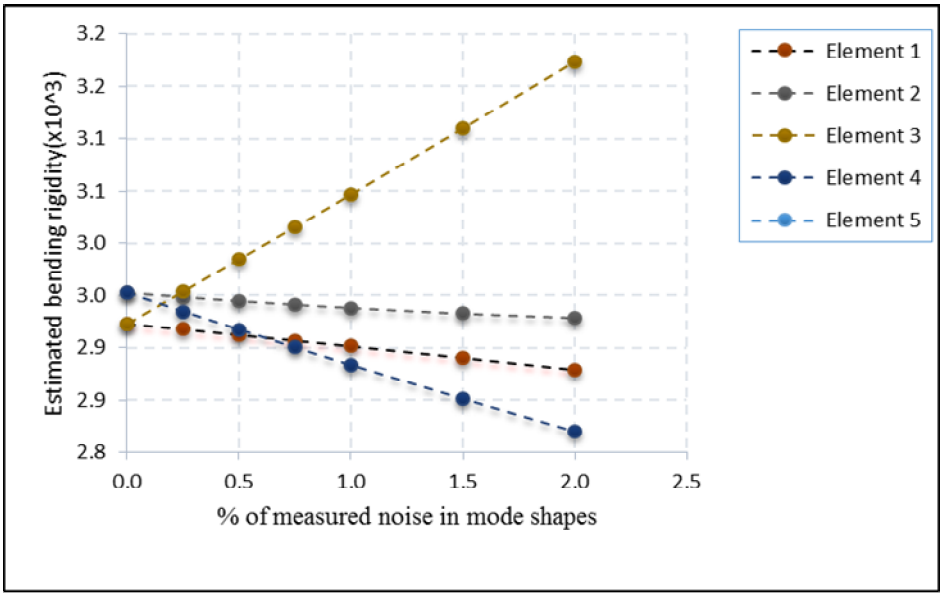

Fig 5.3.12: Estimated bending rigidity with measured noise for 2D13 case

It is noticed that accuracy in the estimated bending rigidity decreases for increased random measurement noise level in the mode shapes.

The estimated error for bending rigidity of each element with no of measured mode shapes are shown form Fig.5.3.13 and Fig.5.3.14 for 1D1 and 2D13 cases.

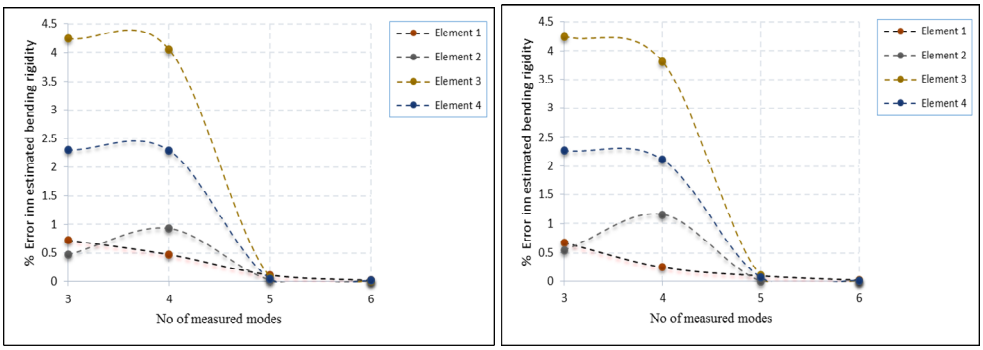

Fig 5.3.13: Error (%) in estimated bending rigidity for different mode shapes (1D1 and 2D13 case)

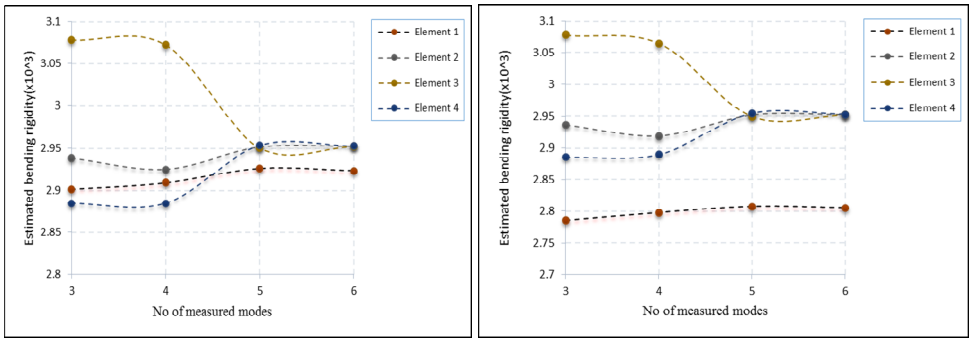

Fig 5.3.14: Estimated bending rigidity for different element with mode shapes (1D1 and 2D13 case)

The errors in the estimation of axial rigidity, bending rigidity using the proposed deterministic parameter identification model seems to be smaller. The error is within 4.5% even in the presence of high percentage of random noise like 2.0%, which may be more reliable. It is noted that the accuracy of the estimation increases in general with the use of increased number of measurement. The effect of measurement noise on the estimated structural parameters by this identification model is also studied. It is observed that the accuracy of the estimation decreases with the increase of the noise level. It is also noted that the accuracy of estimation further decreases with the decrease in the number of measurement. The errors in the estimations of structural parameters using modal data measured at the first three modes for different noise level are lesser and may be acceptable.

5.4 Example-IV (13 member steel Pratt Truss)

The schematic diagram of a thirteen (13) element symmetrical Pratt Truss as shown in Fig. 5. 4.1 is numerically demonstrated. The top chord and bottom chord is taken as ISMC 150. The other major and minor bracing members and also the vertical strut members are considered as ISA 90x90x8.

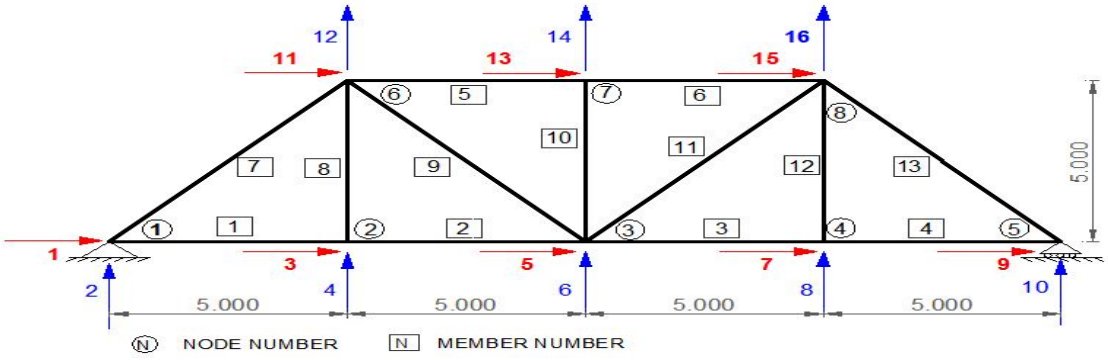

Fig 5.4.1: 13 member steel Pratt Truss

The modulus of elasticity and the density of the material of the truss are taken as $2.0x10^{11}$ KN/sqm and $7.85x10^{3}$ kg/cum respectively. The undamaged structural properties are described in Table 5.4.1.

Table 5.4.1 : Undamaged structural properties of the structure

MEMBER TYPE	Top Chord	Bottom Chord	Diagonals	Verticals
ELEMENT NO.	1,2,3,4	5,6	7,9,11,13	8,10,12
AREA (SQM)	$4.500x10^{-3}$	$1.1250x10^{-2}$	$5.625x10^{-3}$	$7.200x10^{-3}$
I_{XX} (M^4)	1.215×10^{-5}	3.600×10^{-5}	1.400×10^{-5}	3.240×10^{-5}

Four cases of multiple damage state along with the undamaged state are considered for identification of the structural parameters using analytically simulated modal data. The degree of damage from 10% is introduced in elements 2, 4,5,6,7 8, 9, 10, 12 &13.

Case I: Undamaged state (UD) – No damage in any element.

Case II: Damaged state (2D35) – Damages at element no 3 and 5.

Case III: Damaged state (4D 2, 6, 9, 12) – Damages at element no 2, 6, 9 and 12.

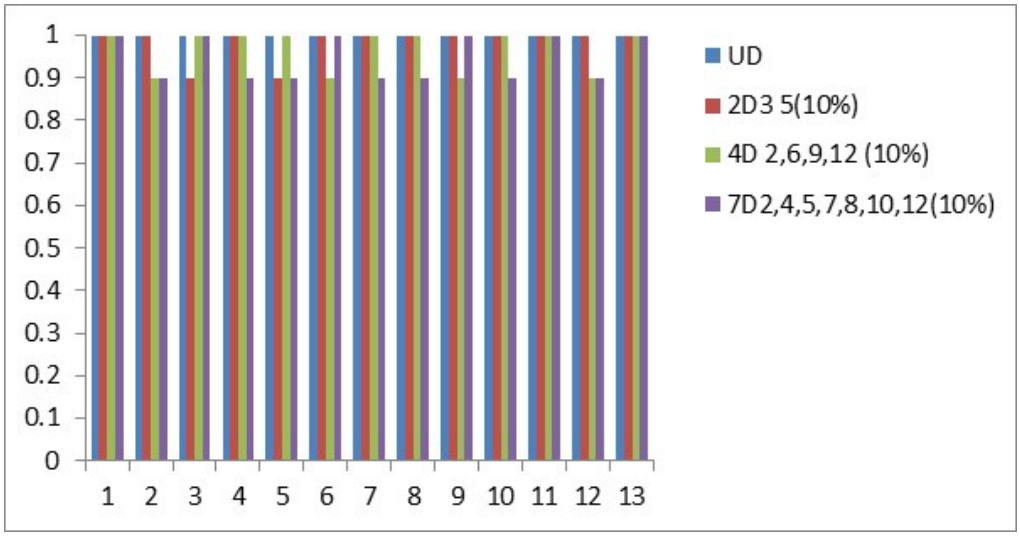

Fig 5.4.2: Graphical representation of various scenarios of UD and multiple element damage

Pratt Truss is used to demonstrate the applicability of the proposed **SLD, SSD** and **DFS** model. The numerically obtained maximum deflection is plotted in Fig. 5.4.3 for UD and different damage conditions.

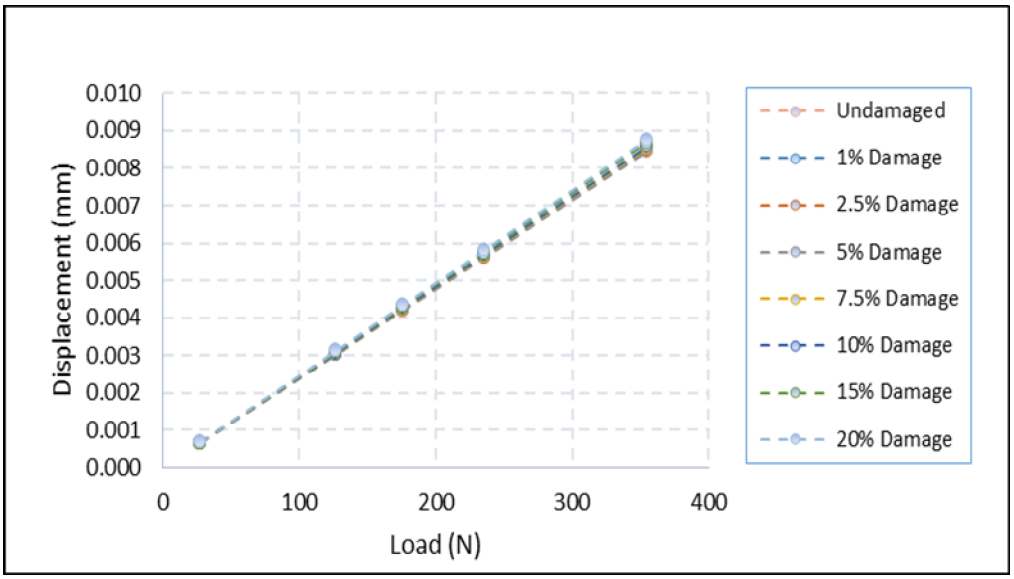

Fig 5.4.3: Plot of static displacement(mm) vs load(N)

The errors of estimation of the axial rigidity using **SLD and SSD** for different damage cases are studied and shown in Fig. 5.4.4 – Fig.5.4.6.

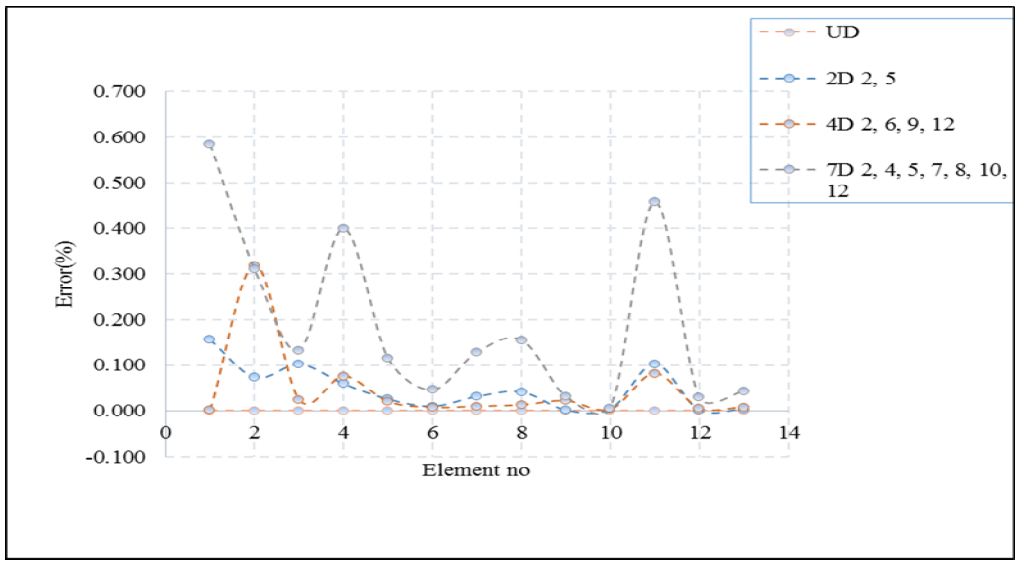

Fig 5.4.4:Error (%) in estimated axial rigidity with for different element without noise

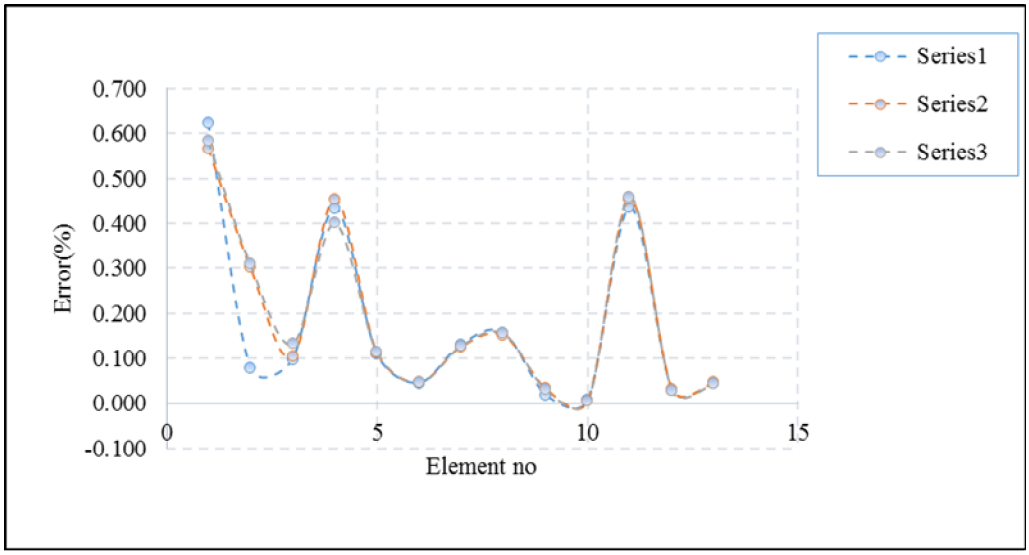

Fig 5.4.5: Error (%) in estimated axial rigidity with for different element for 2D35 case

It is observed that using **SLD and SSD** models structuctural parametrs are identified with sufficient accuracy if the random mesurement noise is absent. But this model predict structural parameters with some error using limited measured data even for small presence of intrinsic random noise.

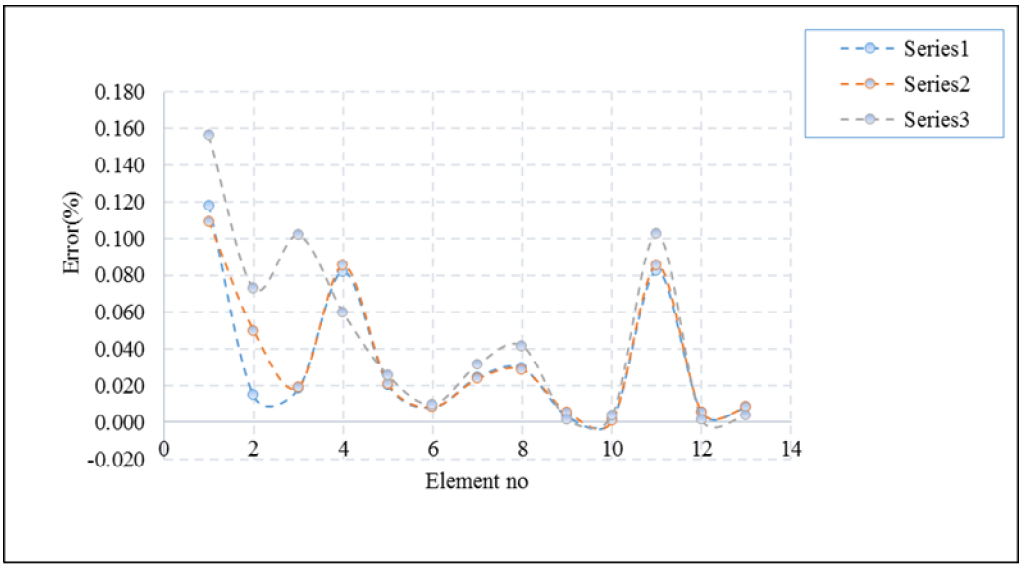

Fig 5.4.6: Error (%) in estimated axial rigidity with for different element for 4D2,6,9,12 case

The errors of estimation of the structural parameters for different number of measurements are studied and shown in Fig. 5.4.7 – Fig.5.4.11.

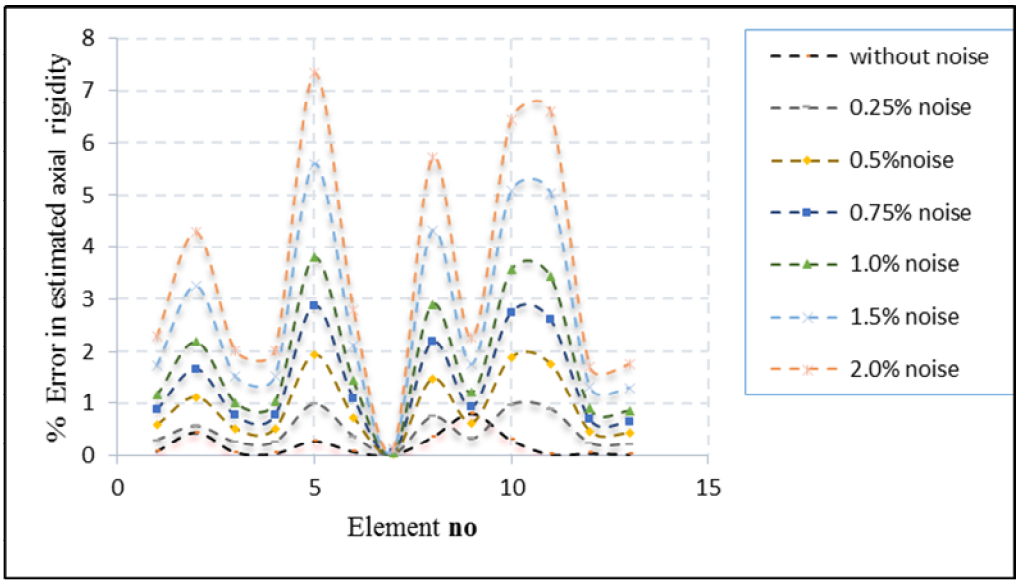

Fig 5.4.7: Error (%) in estimated axial rigidity with for different element for UD case

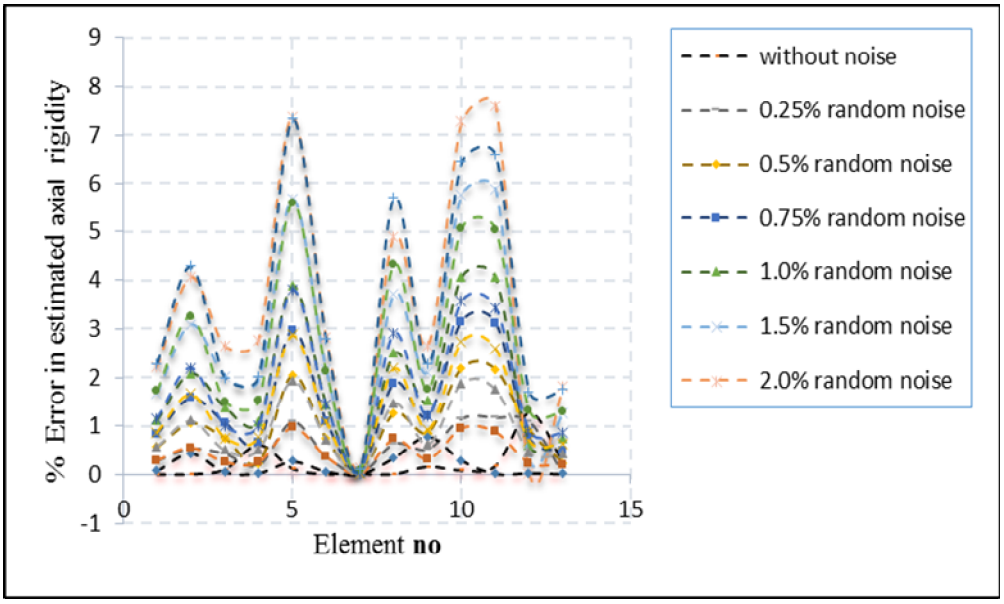

Fig 5.4.8: Error (%) in estimated axial rigidity with for different element for 2D34(10%) case

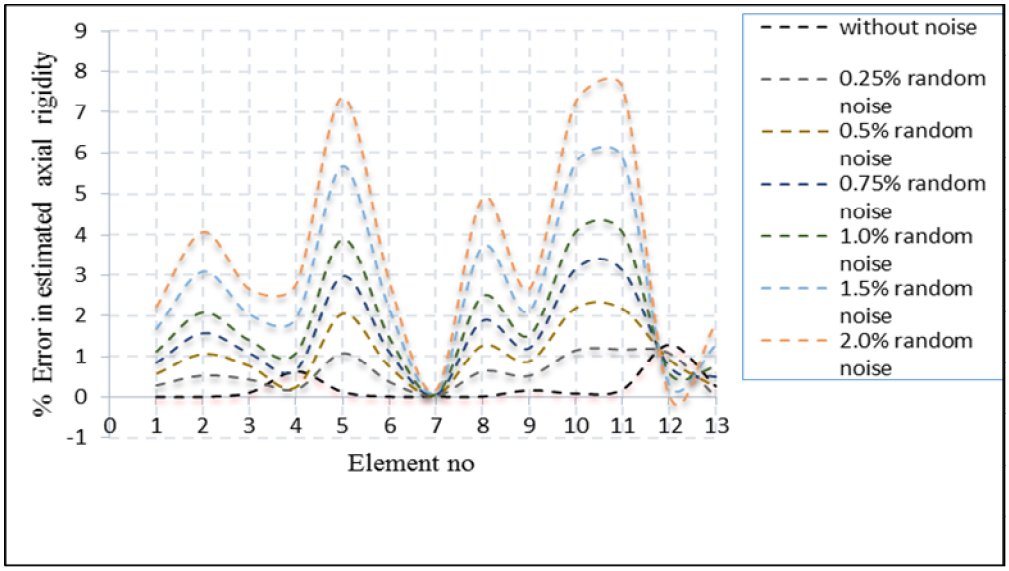

Fig 5.4.9: Error (%) in estimated axial rigidity with for different element for 4D2,6,9,12(10%) case

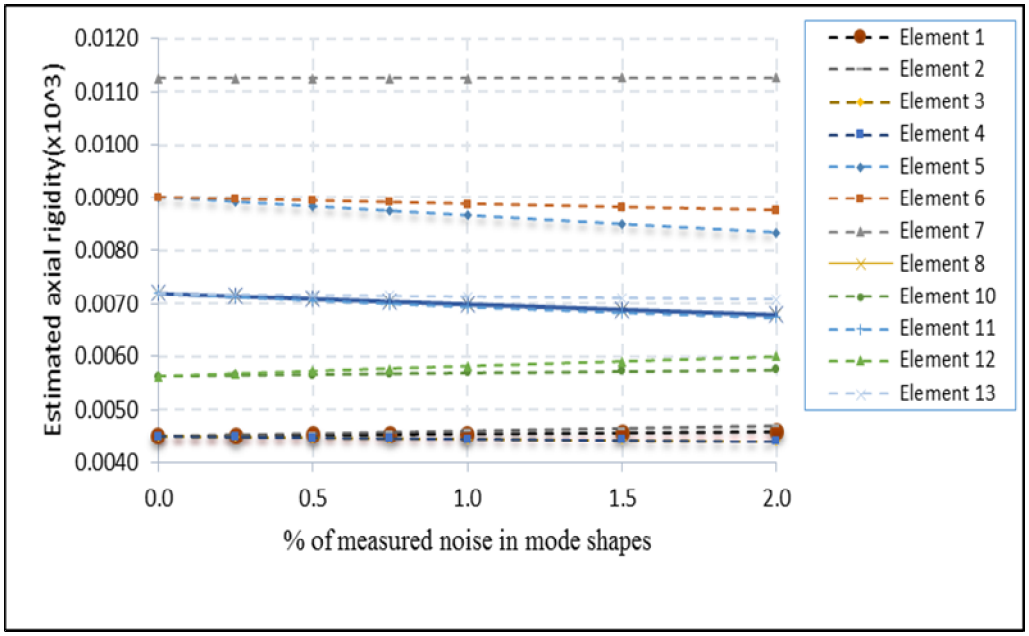

Fig 5.4.10: Estimated axial rigidity with measured noise in mode shapes for UD case

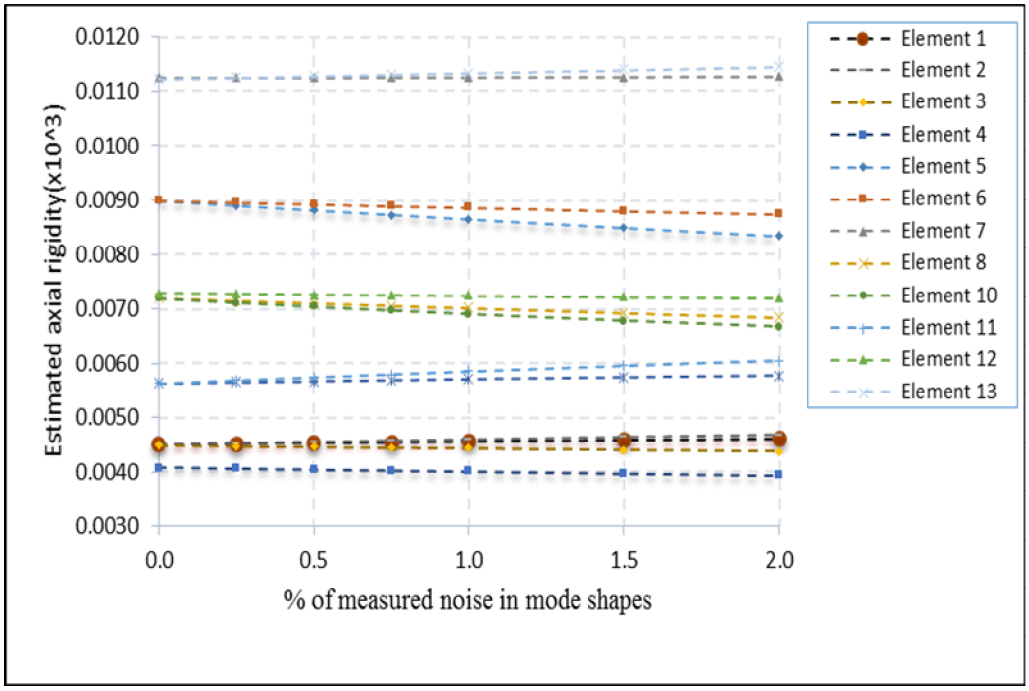

Fig 5.4.11: Estimated axial rigidity with measured noise in mode shapes for 1D4 (10%) case

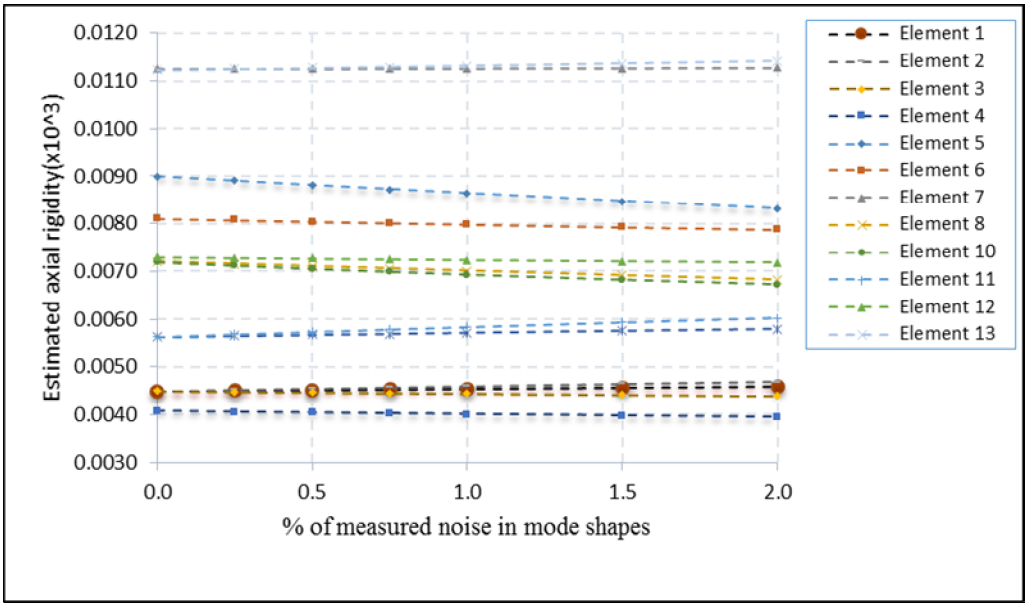

Fig 5.4.12: Estimated axial rigidity with measured noise in mode shapes for 2D 46 (10%) case

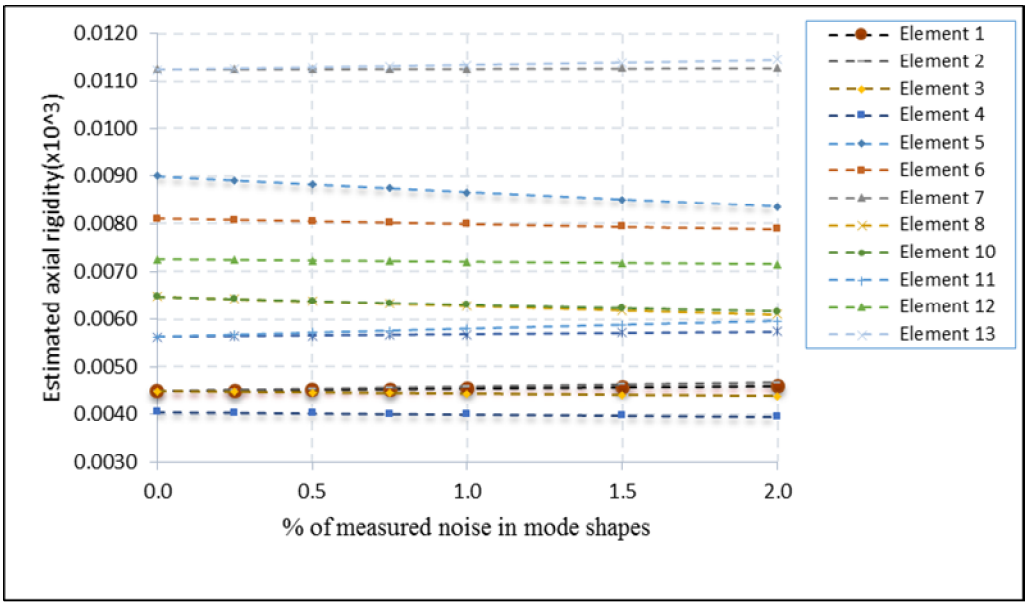

Fig 5.4.13: Estimated axial rigidity with measured noise in mode shapes for 3D 468 (10%) case

It is observed that the accuracy of the estimation of structural parameters decreases significantly with the increase of noise level. In most of the elements the error in the estimated structural parameters are maximum of 8% for the noise level of maximum of 2.0% in measured mode shapes.

5.5 Example V (RCC gable frame)

A gable frame is considered for the validation of the proposed numerical model **DMS.** The dimensions (in meter) are shown in Fig: 5.5.1 and the degrees of freedoms are shown in Fig: 5.5.2.

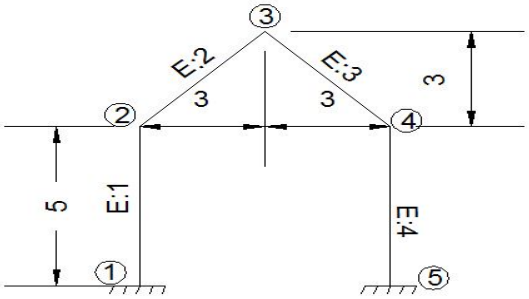

Fig. 5.5.1. Frame with node and member

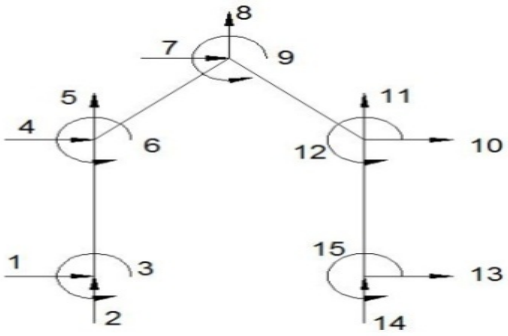

Fig.5.5.2. Degrees of Freedom of the frame

Geometric and structural properties of the gable frame is shown in Table 5.5.1 and also different damage scenario is described in Table 5.5.2.

Table 5.5.1: Different undamaged properties of the frame

Member No	Length (m)	Breadth(m)	Depth(m)	Mass Density(Kg/m3)	Modulus of Elasticity (E)kN/sqm
1	5	0.25	0.25	2500	2.236×10^{10}
2	4.2426	0.25	0.25	2500	2.236×10^{10}
3	4.2426	0.25	0.25	2500	2.236×10^{10}
4	5	0.25	0.25	2500	2.236×10^{10}

Analysis performed for different damage cases as shown below

UD : Undamaged state – No damage in any element.

CASE I: (1D3) : Single element damaged state at element nos. 3.

CASE II: (2D34) : Double element damaged state at element nos. 3 and 4.

Table 5.5.2: Different damage percentage of the gable frame

DAMAGE CASES	ELEMENT NO			
	1	**2**	**3**	**4**
UD	-	-	-	-
CASE – I	-	-	**10**	-
CASE – II	-	-	**10**	**10**

The proposed **DMS** model is employed initially at its undamaged state using limited modal data of the first three modes measured at selected three translation degrees of freedom. The measured limited data is coupled with unbiased normally distributed random noise up to 2 percent. The effect of the extent of damage on the accuracy of the proposed energy based method is studied. The errors of estimated axial rigidity, bending rigidity of the undamaged and different damaged state are shown in Fig 5.5.3 to Fig 5.5.8.

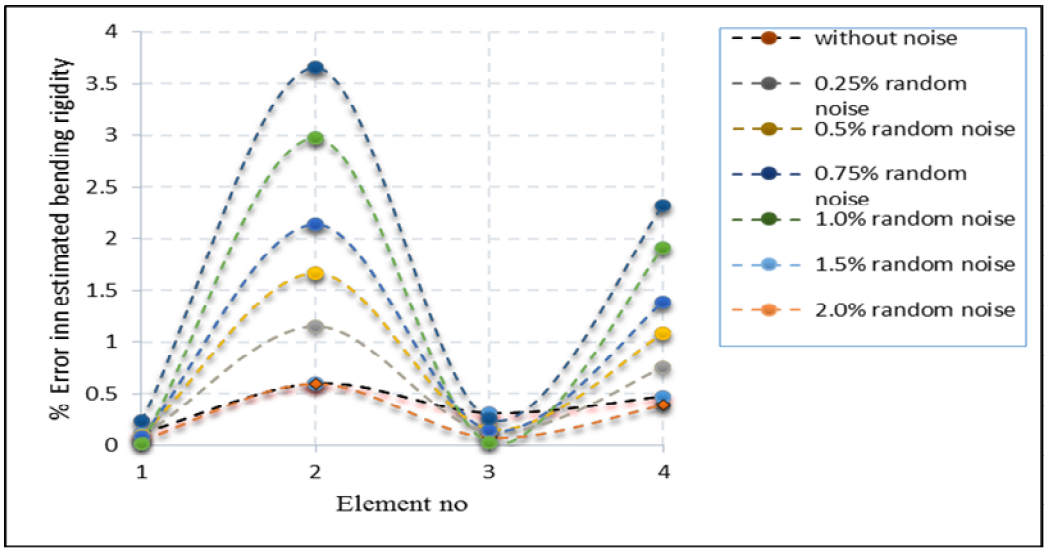

Fig 5.5.3: Error (%) in estimated bending rigidity with measured noise in mode shapes for UD case

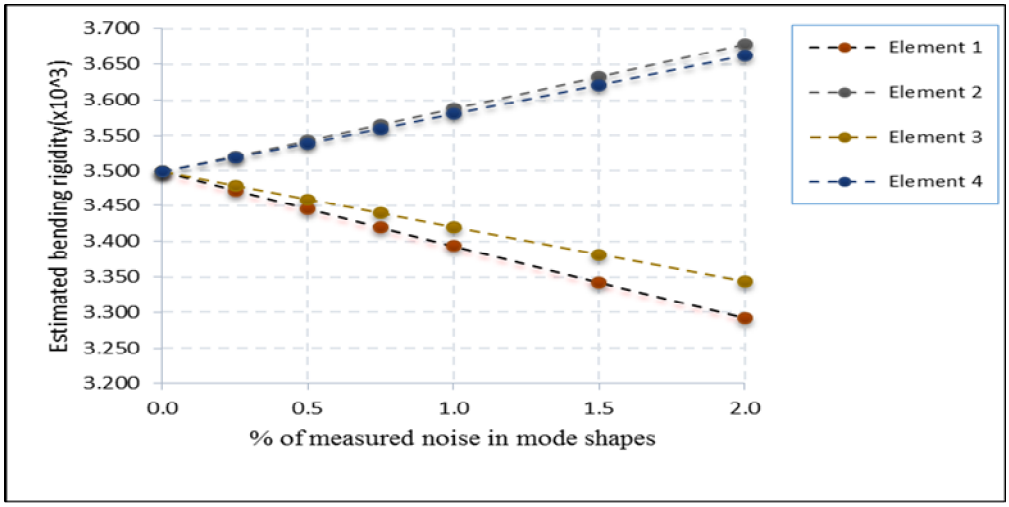

Fig 5.5.4: Estimated bending rigidity with measured noise in mode shapes for UD case

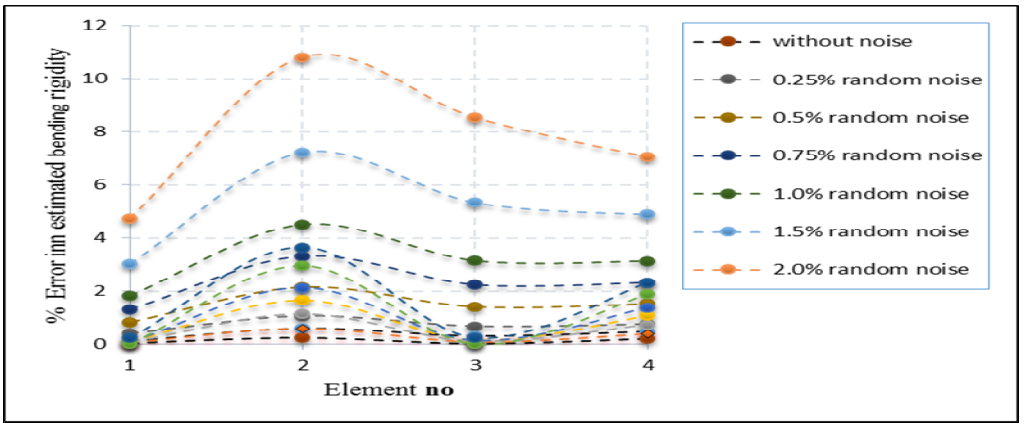

Fig 5.5.5: Error (%) in estimated bending rigidity with for different element for 1D3(10%) case

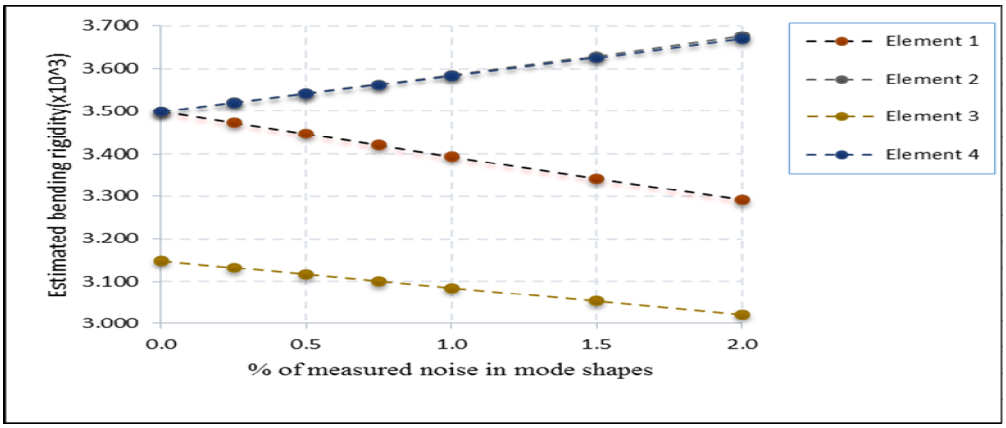

Fig 5.5.6: Estimated bending rigidity with measured noise in mode shapes for 1D3 (10%) case

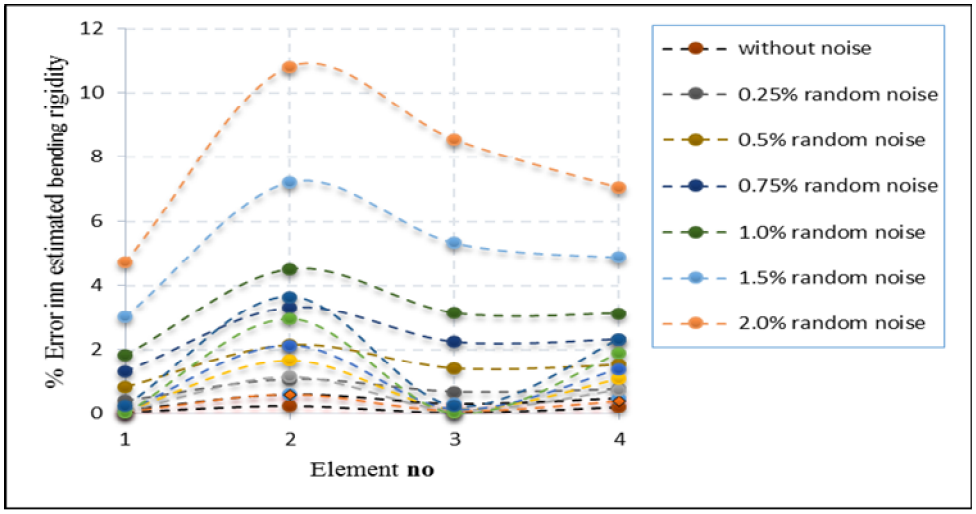

Fig 5.5.7: Error (%) in estimated bending rigidity with for different element for 2D34(10%) case

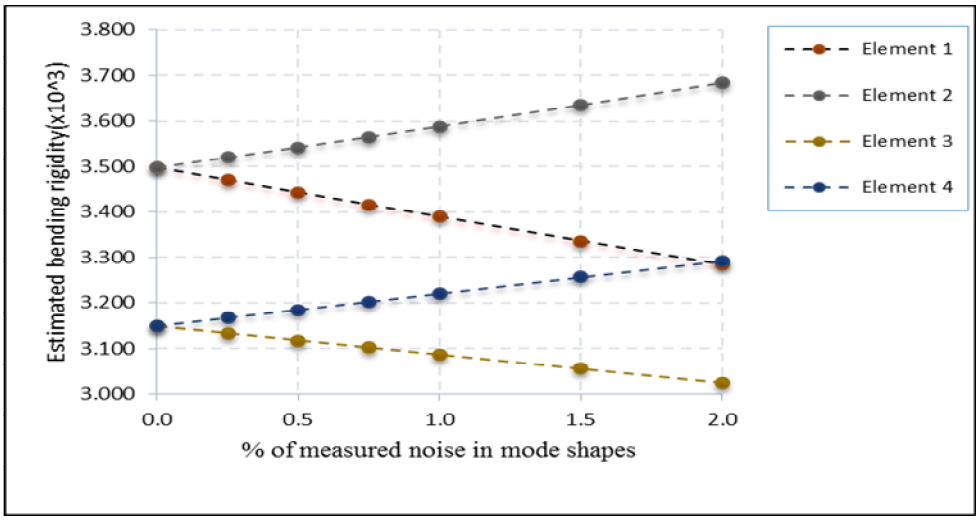

Fig 5.5.8: Estimated bending rigidity with measured noise in mode shapes for 2D34(10%) case

It is encouraging to note that the errors in the estimation of the above structural parameters at different states of damages by the proposed model are less than 3.5% of the base value).

The errors in the estimated bending rigidity by the proposed **DMS** model with various level of random noise in the limited modal data measured at the selected degrees of freedom are shown in Fig 5.5.9 to Fig 5.5.11.

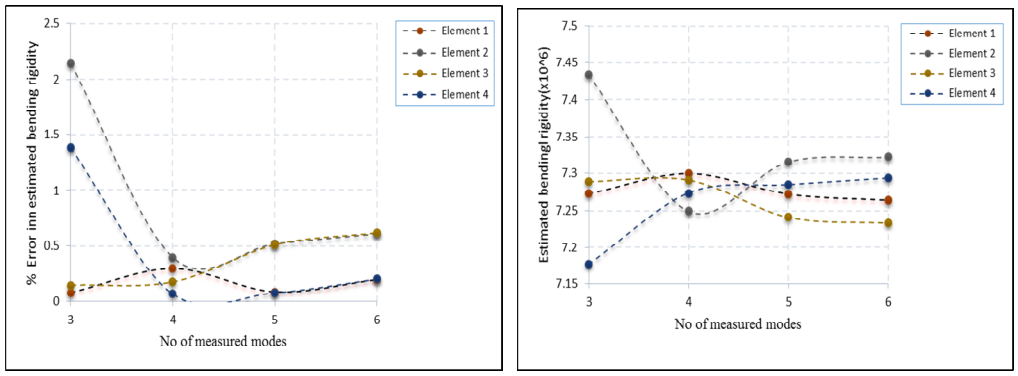

Fig 5.5.9: Error (%) and estimated bending rigidity with measured mode for UD case

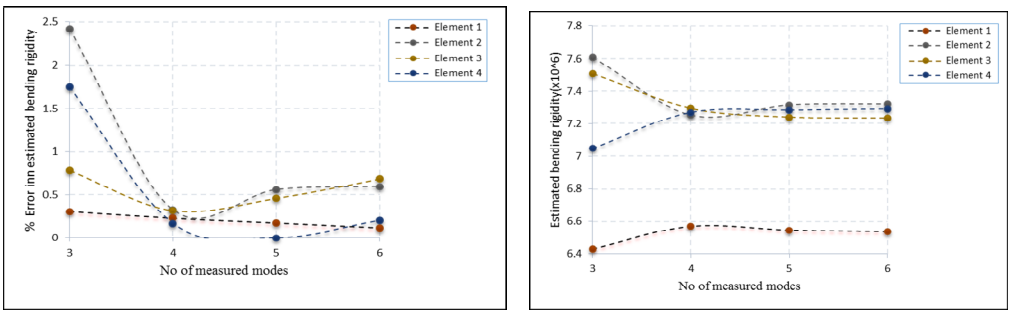

Fig 5.5.10: Error (%) and estimated bending rigidity with measured mode for 1D3 case

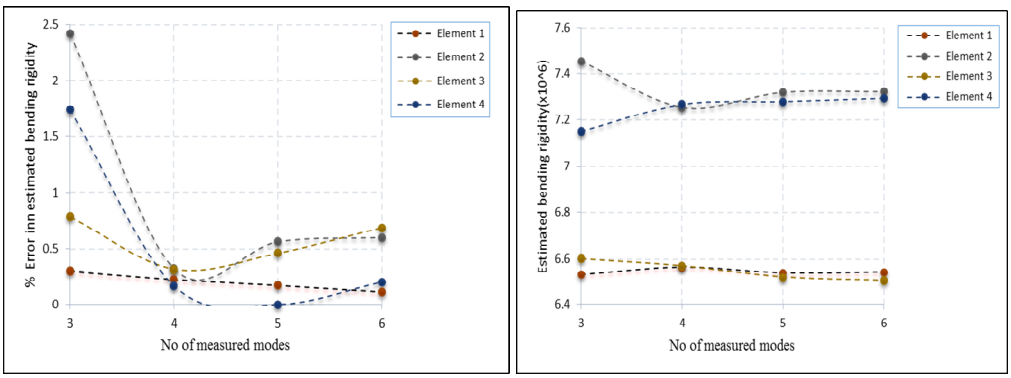

Fig 5.5.11: Error (%) and estimated bending rigidity with measured mode for 2D3, 4 case

It is noted that the % error in the estimation of the structural parameters decreases with the increase in number of measurement of modal data. The effect of measurement noise on the estimated structural parameters by this identification model is also studied.

5.6 Example VI (steel portal frame)

A Single bay two storey steel portal frame is considered for the validation of the proposed damage detection model **DMS** using experimentally measured data. The dimensions (meter) and the degrees of freedoms are shown in Fig. 5.6.1. Different undamaged structural properties are described in Table 4.2.4. Details of the % reduction in cross section is tabulated in Table 4.2.5.

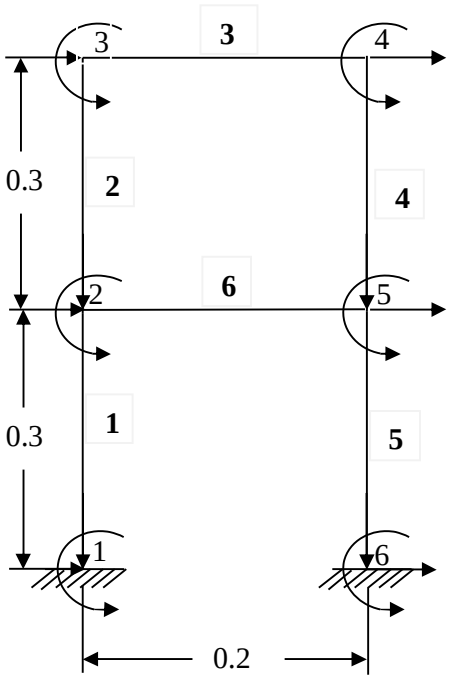

Fig. 5.6.1: Model of six element Portal Frame showing the d.o.f. (all dimensions are in meter)

Coefficient of elasticity of the material is 2.0×10^{11} kN/ sqm and mass density is 7.85×10^{3} kg/cum. Different undamaged structural properties are presented in Fig 4.2.4 Different damage scenario are graphically represented in Fig. 5.6.2.

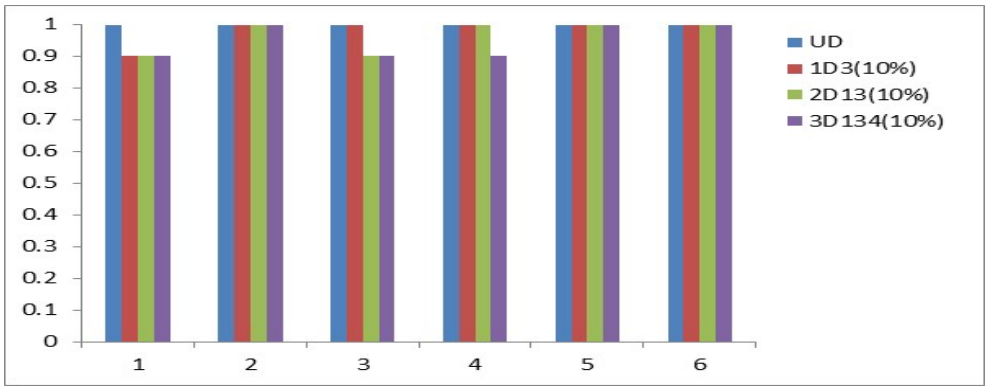

Fig. 5.6.2: Graphical representation of various case of multiple damage

The comparison of the experimental and analytical natural frequencies for UD and different damage conditions are shown in Table 5.6.1.

Table 5.6.1: Change of natural frequency for different damage cases for first few modes.

Damage Case	**1st Mode**		**2nd Mode**		**3rd Mode**	
	Experimental	**Analytical**	**Experimental**	**Analytical**	**Experimental**	**Analytical**
UD	56	57.7	189	209.16	392	398.04
1D1	55	56.54	184	204.71	390	389.33
2D13	55	55.496	182	199.01	383	381
3D134	54	55.25	174	194.926	354	373.705

It is observed that the numerical and experimental natural frequencies are close to each other if the damage extent is less. However, few variation observed for higher damage. Fig.5.6.3 and Fig.5.6.4 are developed for showing the predicted structural parameters using **DMS** model.

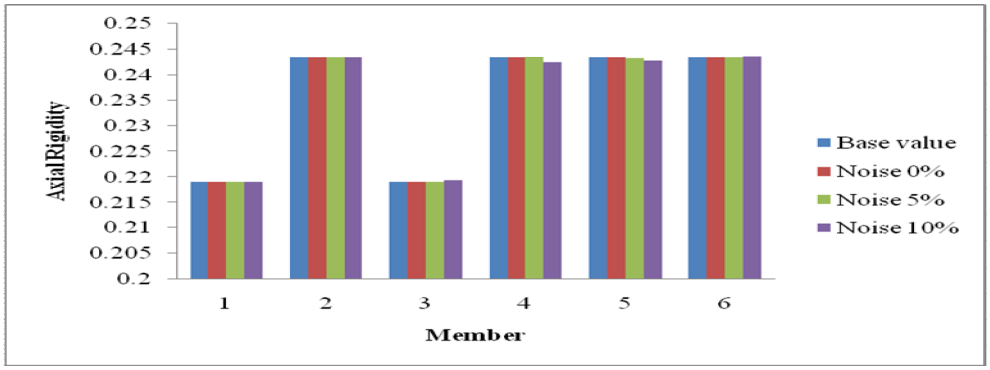

Fig. 5.6.3: Predicted axial rigidity to the member with noise and 10 (%) damage for 2D13 case

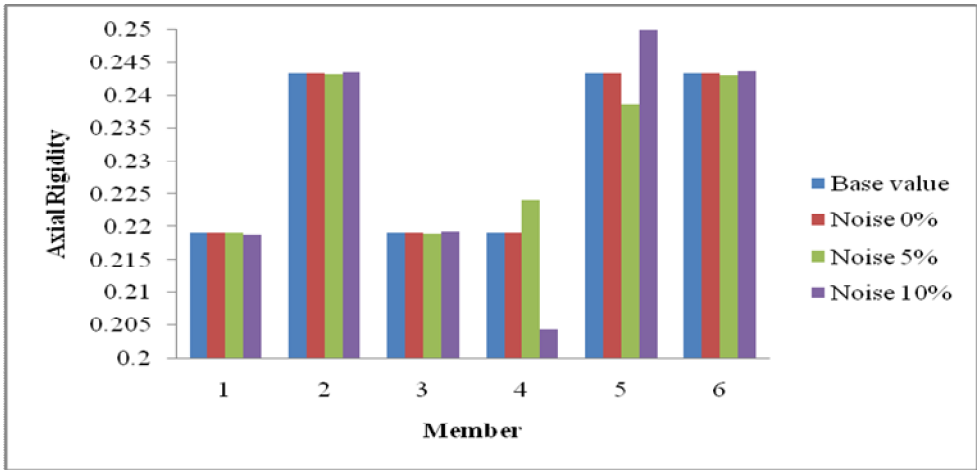

Fig. 5.6.4: Predicted axial rigidity and member with noise and 10 percentage damage for 3D134 case

It is observed from Fig.5.6.3 and Fig.5.6.4 that axial rigidity are almost truly predicted using **DMS** in presence of the noise also.

The results of various models developed and subsequent validation of those models with different examples both numerical as well as experimental problems with and without measurement random noises have been presented and discussed. Five numerical models have been developed based on inverse approach using static or dynamic responses with random noise. Several numerical examples have been studied with these identification models with incremental random noise and different numbers of measured modes. Experimentally obtained data have also used to validate these numerical models and to establish the feasibility of practical application. The maximum error (%) of axial & bending rigidity for different elements by various developed models using both numerically noisy data is also studied.

Chapter – 6

Conclusion & Future Scope of Study

6.1 Concluding remarks

Present study deals with the structural condition monitoring aspect, particularly the prediction of damage in terms of reduction of structural parameters e.g., axial rigidity, bending rigidity using limited static and dynamic responses measured at a few selected locations. Equation error approach is employed in a finite element framework adopting inverse static and dynamic technique. The uncertainty associated with the measurement is generally considered as measurement noise and it is duly considered and compared on the accuracy of the identification of parameters. Computational algorithms have developed and numerical examples are presented to establish the efficacy of the proposed method. Experimental study is also performed to have an insight on a few basic aspects of static and modal testing and subsequent extraction of the static and modal parameters. The experimental validation of the numerical models developed have been attempted with those extracted static and modal responses from measured data at few nodes. Based on the results of the examples studied, few important conclusions are as follows.

1. Inverse static identification approach seems to be simple and able to predict damage in case of simple cantilever beams. However, for complex structure, huge static data may be required for accurate prediction of the structural parameters.
2. The Experimental validation of the numerical models based on static responses shows satisfactory results of predicting bending rigidities with 6% error in SLD Model and 3% error in case SSD Model.
3. Damage identification with inverse dynamic approaches (DFS, DFC and DMS) may address the condition monitoring aspect in a much better way, with limited measurement.

4. All these models are able to predict structural parameters and identify the damages with great accuracy even with minor measurement noise in case of numerical examples.

5. The Experimental validation of the same problem considered in case of static models (Example II) by the dynamic model DFS shows further improvement on the accuracy of the identification with the error in tune of 1.5%.The error is further reduced (< 1.0%) in case of dynamic response used obtained numerically.

6. Dynamic models based on derivatives of the modal data e.g., DFC and DMS are able to identify the damage from limited noisy data with greater accuracy even at a very low damage level.

7. The proposed model DFS and DMS are able to predict damage and may be feasible for practical problem as it is able to identify the structural parameters with first few modal data measured at selected degrees of freedom experimentally obtained. The identification of the axial rigidity seems to be further improved by the DMS model incorporating Modal strain energy concept as compared to DFS model. The error seem to be < 1% and 4.4% in case of two storey portal frame example by using numerical and experimental data respectively.

8. However, much greater error is obtained in case of axial rigidities of the beam (Example II) & bending rigidity in case of portal frame (Example VI), which may be attributed to the constraints of selection of measured degree of freedom. These errors can be reduced to a minimum by using tri-axial accelerometer or by putting additional accelerometer in the orthogonal direction, in addition to the direction considered.

9. It is noted that the accuracy of the predicted parameters increases with the increase of the number of measured modes and decreases with the increase of noise level in all the models developed.

10. The condition of all the elements may be monitored continuously if the measured data are available in a continuos manner in case of practical application.
11. The experimental study even with simple structures validates the proposed numerical models and demonstrate the potential of the proposed numerical models for their practical implementation.
12. The encouraging results of the structural parameter identification by sequential improvement of the models andd subsequent validation by the experimental data may address the problem of condition monitoring for simple real life structures.

6.2 Future scope of study

The broad objective of the present investigation lies in applying the inverse static and dynamic approaches for condition monitoring of structures. In the present scope of work two-dimensional beam, frame or truss structures are considered within the linear domain. Several other important aspects may be considered for future studies, which are as follows:

i. Experimental validation of the model in case of large complex structure
ii. Consideration of non-linearity in the formulation of structural behavior.
iii. Consideration of damping parameters in the model formulation
iv. Development of statistical based damage identification algorithm considering all the uncertainties.
v. Effect of selection of sensor location and performance of the models
vi. Application and subsequent modification of the proposed model in case of real life structure

REFERENCES

Abdalla, M., Grigoriadis, K., and Zimmerman, D. (2003). An optimal hybrid expansion-reduction damage detection method. *Journal of Vibration and Control, 9*(8), 983-995. doi:10.1177/10775463030098005

Abdo, M. A. B., and Hori, M. (2002). A numerical study of structural damage detection using changes in the rotation of mode shapes. *Journal of Sound and Vibration, 251*(2), 227-239. doi:10.1006/jsvi.2001.3989

Agneni, A. (2000). On the Use of the Gauss Filter in Modal Parameter Estimation. *Mechanical Systems and Signal Processing, 14*(2), 193-204. Academic Press. doi:10.1006/mssp.1999.1253

Alampalli, S., Fu, G. K., and Dillon, E. W. (1997). Signal Versus Noise In Damage Detection By Experimental Modal Analysis. *Journal of Structural Engineering.* ASCE. doi:10.1061/(ASCE)0733-9445(1997)123:2(237).

Balageas., D., Fritzen, C.-P., and Güemes, A. (2006). *Structural health monitoring* (p. 495). London (UK) ; Newport Beach, Carlifornia (USA): John Wiley and Sons Inc.

Bani-Hani, K., Ghaboussi, J. and Schneider, S. P. (1999). "Experimental study of identification and control of structures using neural network, Part 1:identification", *Earthquake Engrg. Struct, Dyn.,* 28, 995-1018.

Barai, S. V. and Pande, P. C. (1997). "Time-delay neural networks in damage detection of railway bridges", *Adv.Engrg. Software*, 28, 1-10.

Barai, S. V. and Pande, P. C. (2000). "Integration of damage assessment paradigms of steel bridges on a blackboard architecture", *Expert Systems with Applications*, 19, 193-207.

Begg, R. D., Mackenzie, A. C., and Dodds, C. J. (1976). Structural Integrity Monitoring Using Digital Processing of Vibration Siqnals. *Proc. of 1976 Offshore Technology Conference* (p. 8). Houston, TX: Offshore Technology Conference. doi:10.4043/2549-MS

Bernal, D. (2002). Load Vectors for Damage Localization. *Journal of Engineering Mechanics, 128*(1), 7-14. Madrid.: ASCE. doi:10.1061/(ASCE)0733- 9399(2002)128:1(7)

Biswas, M., Pandey, A. K., and Samman, M. M. (1990). Diagnostic Experimental Spectral/Modal Analysis of A Highway Bridge. *The International Journal of Analytical and Experimental Modal Analysis, 5*(1), 33-42.

Carlin, R., and Garcia, E. (1996). Parameter optimization of a genetic algorithm for structural damage detection. *Proceedings of the 14th International Modal Analysis Conference (IMAC)* (pp. 1292-1298). Dearborn, MI: Society for Experimental Mechanics, Inc, Bethel.

Carlos, E. V., Brincker, R., Dascotte, E. and Andersen, P. (2001). " Fem Updating Of The Heritage Court Building Structure",

Carrasco, C. J., Osegueda, R. A., Ferregut, C. M., and Grygier, M. (1997). Damage localization in a space truss model using modal strain energy. *Proceedings of the 1997 15th International Modal Analysis Conference (IMAC) Part 2 (of 2)*.

Cawley, P., and Adams, R. D. (1979). The location of defects in structures from measurements of natural frequencies. *The Journal of Strain Analysis for Engineering Design*, *14*(2), 49-57. Professional Engineering Publishing. doi:10.1243/03093247V142049 Bibliography 189

Cempel, C., Natke, H. G., and Ziół kowski, A. (1992). Application of Transformed Normal Modes for Damage Location in Structures. In P. Stanley (Ed.), *Structrual Integrity Assessment* (pp. 246-255). London, UK: Spon Press.

Chance, J. E., Worden, K., and Tomlinson, G. R. (1994). Processing signals for damage detection in structures using neural networks. *Smart Structures and Materials*, *2191*, 187-198.

Chou, J. H., and Ghaboussi, J. (2001). Genetic algorithm in structural damage detection. *Computers and Structures*, *79*(14), 1335-1353. doi:10.1016/S0045- 7949(01)00027-X

Cobb, R. G., and Liebst, B. S. (1997). Structural damage identification using assigned partial eigenstructure. *AIAA Journal*, *35*(1), 152-158. doi:10.2514/2.77

Cornwell, P., Doebling, S. W., and Farrar, C. R. (1999). Application of the Strain Energy Damage Detection Method to Plate-Like Structures. (Anon, Ed.)*Journal of Sound and Vibration*, *224*(2), 359-374. SEM, Bethel, CT, United States. doi:10.1006/jsvi.1999.2163

Crema, L. B., and Mastroddi, F. (1998). A direct approach for updating and damage detection by using FRF data. *23rd International Conference on Noise and Vibration Engineering, ISMA* (pp. 159-166). Leuven, Belgium: Katholieke Universiteit Leuven.

De-Wen Zhang and Fu-Shang Wei, "Extracting Modes of Constrained Structure with Elastic Supports from Free Test Data", *Journal of Aerospace Engineering*, 2007, 20(1): 1-9

Diego F. Giraldo, Wei Song, Shirley J. Dyke and Juan M. Caicedo, " Modal Identification through Ambient Vibration: Comparative Study", *Journal of Engineering Mechanics*, 2009, 135(8): 759-770

Doebling, S. W., and Farrar, C. R. (1996). Computation of structural flexibility for bridge health monitoring using ambient modal data. *11th Conference on Engineering Mechanics. Part 1 (of 2)* (Vol. 2, pp. 1114-1117). Fort Lauderdale FL, USA: ASCE, New York, NY, United States.

Doebling, S. W., Farrar, C. R., and Goodman, R. S. (1997). Effects of measurement statistics on the detection of damage in the alamosa canyon bridge. *Proceedings of the 15th International Modal Analysis Conference (IMAC)* (pp. 919-929). Orlando, FL.

Doebling, S. W., Farrar, C. R. and Prime, M. B. (1998). " A summary review of vibration-based damage identification methods", *The Shock Vibration Digest*. 30(2), 91-105.

Drinkwater, B. W. and Wilcox, P. D. (2006). "Ultrasonic arrays for non-destructive evaluation: A review", NDT and E Intl, 39, 525-541.

Erbatur, F., Hasançebi, O., Tütüncü, İ ., and KilIç, H. (2000). Optimal design of planar and space structures with genetic algorithms. *Computers and Structures*, *75*(2), 209-224. doi:10.1016/S0045-7949(99)00084-X

Ewins, D. J. (2000). *Modal Testing: Theory, Practice and Application.* (J. B. Roberts, Ed.) (2nd ed., pp. 1-6). Baldock, Hertfordshire, UK: Research Studies Press.

Farrar, C. R., Doebling, S. W., and Nix, D. A. (2001). Vibration-based structural damage identification. *Philosophical Transactions of the Royal Society A: Mathematical, Physical and Engineering Sciences*, *359*(1778), 131-149. The Royal Society. doi:10.1098/rsta.2000.0717

Fox, C. H. J. (1992). The Location of Defects in Structures: A Comparison of the Use of Natural Frequency and Mode Shape Data. *Proceedings of 10th International Modal Analysis Conference (IMAC)* (Vol. 1, pp. 522-528). San Diego, CA.

Friswell, M. I., Penny, J. E. T., and Garvey, S. D. (1998). A combined genetic and eigensensitivity algorithm for the location of damage in structures. *Computers and Structures*, *69*(5), 547-556. doi:10.1016/S0045-7949(98)00125-4

Gao, Y., and Spencer, B. F. (2006). Online damage diagnosis for civil infrastructure employing a flexibility-based approach. *Smart Materials and Structures*, *15*(1), 9-19. doi:10.1088/0964-1726/15/1/030

Goldberg, D. E. (1989). *Genetic Algorithms in Search, Optimization and Machine Learning*. *AddisonWesley* (1st ed., pp. 1-432). Boston, MA: Addison-Wesley Longman Publishing Co., Inc.

Gudmundson, P. (1982). Eigenfrequency changes of structures due to cracks, notches or other geometrical changes. *Journal of the Mechanics and Physics of Solids*, *30*(5), 339-353. doi:10.1016/0022-5096(82)90004-7

Guo, H. Y., and Li, Z. L. (2009). A two-stage method to identify structural damage sites and extents by using evidence theory and micro-search genetic algorithm. *Mechanical Systems and Signal Processing*, *23*(3), 769-782. doi:10.1016/j.ymssp.2008.07.008

Hajela, P. , Soeiro, F.J. (1990), "Structural damage detection based on static and modal analysis", *AIAA Journal*, 28, 1110-1116.

Hamey, C. S., Lestari, W., Qiao, P. Z., and Song, G. B. (2004). Experimental Damage Identification of Carbon/Epoxy Composite Beams Using Curvature Mode 192

Hassiotis, S. (2000). Identification of damage using natural frequencies and Markov parameters. *Computers Structures*, *74*(3), 365-373. doi:10.1016/S0045- 7949(99)00034-6

Hassiotis, S., and Jeong, G. (1993). Assessment of structural damage from natural frequency measurements. *Computers Structures*, *49*(4), 679-691. doi:10.1016/0045-7949(93)90071-K

Hassiotis, S., and Jeong, G. D. (1995). Identification of Stiffness Reductions using Natural Frequencies. *Journal of Engineering Mechanics*, *121*(10), 1106-1113. doi:10.1061/(ASCE)0733-9399(1995)121:10(1106)

He, J. M., and Fu, Z. F. (2001). *Modal Analysis* (Vol. 117, pp. 1-291). Oxford, UK: Butterworth-Heinemann.

Hejll, A. (2004). *Structural Health of Bridges: Monitor, Assess and Retrofit*. *Luleå University of Technology*. Luleå University of Technology, luleå.

Hjelmstad, K.D. and Shin, S. (1997). Damage Detection And Assessment Of Structures From Static Response. *Journal of Engineering Mechanics*, ASCE, 123(6):568-576.

Hsu, T. Y., Huang, S. K., Lu, K. C., and Loh, C. H. (2011). A damage detection algorithm integrated with a wireless sensing system. *Journal of Physics: Conference Series*, *305*(1), 1-12. doi:10.1088/1742-6596/305/1/012042

Huth, O., Feltrin, G., Maeck, J., Kilic, N., and Motavalli, M. (2005). Damage identification using modal data: Experiences on a prestressed concrete bridge. *Journal of Structural Engineering*, *131*(12), 1898-1910. doi:10.1061/(ASCE)0733-9445(2005)131:12(1898)

J.C. Asmussen and R.Brincker.(1996). "Estimation of Frequency Response Function by Random Decrement *", Department of Building Technology and Structural Engineering Aalborg University*,
Jaishi, B., Ren, W. X., Zong, Z. H., and Maskey, P. N. (2003). Dynamic and seismic performance of old multi-tiered temples in Nepal. *Engineering Structures*, *25*(14), 1827-1839. doi:10.1016/j.engstruct.2003.08.006

Jang, S.A., Sim, S.-H., Spencer Jr., B.F., Department of Civil and Environmental Engineering, University of Illinois at Urbana Champaign, Illinois, U.S.A. (2002)"*Structural Damage Detection using static strain data"*.

Jiang, S. F., Zhang, C. M., and Zhang, S. (2011). Two-stage structural damage detection using fuzzy neural networks and data fusion techniques. *Expert Systems with Applications*, *38*(1), 511-519. doi:10.1016/j.eswa.2010.06.093

Juneja, V., Haftka, R. T., and Cudney, H. H. (1997). Damage Detection and Damage Detectability - Analysis and Experiments. *Journal of Aerospace Engineering*, *10*(4), 135-142. doi:10.1061/(ASCE)0893-1321(1997)10:4(135)

Kanazawa, K. (2006). Structural damage detection from natural frequency eliminated by temperature effect. *Proc. IMAC-XXIV:IMAC-XXIV: A Conference on Structural Dynamics*. Bethel, CT: Society for Experimental Mechanics.

Kawiecki, G. (2001). Modal damping measurement for damage detection. *Smart Materials and Structures*, *10*(3), 466-471. doi:10.1088/0964-1726/10/3/307

Kennedy, C. C., and Pancu, C. D. P. (1947). Use of vectors in vibration measurement and analysis. *Journal of The Aeronautical Sciences*, *14*(11), 603-625.

Kim, B. S., and Kwak, H. K. (2001). A study of crack detection in plates using strain mode shapes. *Proceedings of the International Modal Analysis Conference (IMAC)* (Vol. 2, pp. 1212-1218).

Kitada, Y. (1998). "Identification of non-linear structural dynamic systems using wavelets", *J. Struct. Mech. ASCE*, 124(10), 1059-1066

Ko, J. M., Wong, C. W., and Lam, H. F. (1994). Damage detection in steel framed structures by vibration measurement approach. *Proceedings of the 12th International Modal Analysis Conference (IMAC)* (Vol. 2251, pp. 280-286). Bethel: SPIE.

Koh, B. H. H., and Dyke, S. J. J. (2007). Structural health monitoring for flexible bridge structures using correlation and sensitivity of modal data. *Computers and Structures*, *85*(3-4), 117-130. doi:10.1016/j.compstruc.2006.09.005

Kourehli, Seyed Sina, Amiri, Golamreza Ghodrati, Ghafory-Ashtiany, Mohsen, and Bagheri Abbdollah (2012). Structural damage detection based on imperfect static responses by means of pattern search algorithm. *15 WCEE, LISBA.*

Kullaa, J. (2003). "Damage detection of the Z24 bridge using control charts", *Mech.. Sys. Signal Processing*, 17(1), 163-170.

Kyriazoglou, C., Lepage, B., and Guild, F. (2004). Vibration damping for crack detection in composite laminates. *Composites Part A Applied Science and Manufacturing*, *35*(7-8), 945-953. doi:10.1016/j.compositesa.2004.01.003

Lagaros, N. D., Papadrakakis, M., and Kokossalakis, G. (2002). Structural optimization using evolutionary algorithms. *Computers and Structures*, *80*(7-8), 571-589. doi:10.1016/s0045-7949(02)00027-5

Lestari, W., and Qiao, P. Z. (2005). Damage detection of fiber-reinforced polymer honeycomb sandwich beams. *Composite Structures*, *67*(3), 365-373. doi:10.1016/j.compstruct.2004.01.023

Lestari, W., Qiao, P. Z., and Hanagud, S. (2006). Curvature Mode Shape-based Damage Assessment of Carbon/Epoxy Composite Beams. *Journal of Intelligen Material Systems and Structures*, *18*(3), 189-208. doi:10.1177/1045389X06064355

Lew, J. S. (1995). Using transfer function parameter changes for damage detection of structures. *AIAA Journal*, *33*(11), 2189-2193. doi:10.2514/3.12965

Li, Z. S., Swanson, J. A., Helmicki, A. J., and Hunt, V. J. (2005). Modal Contribution Coefficients in Bridge Condition Evaluation. *Journal of Bridge Engineering*, *10*(2), 169-178. doi:10.1061/(ASCE)1084-0702(2005)10:2(169)

Lieven, N. A. J., and Ewins, D. J. (1988). Spatial correlation of mode shapes: the coordinate modal assurance criterion (COMAC). *Proceedings of the 6th International Modal Analysis Conference (IMAC)* (pp. 690-695). Bethel: Society for Experimental Mechanics.

Lifshitz, J. M., and Rotem, A. (1969). Determination of Reinforcement Unbonding of Composites by a Vibration Technique. *Journal of Composite Materials*, *3*(3), 412-423. doi:10.1177/002199836900300305

Lim, T. W., and Kashangaki, T. A. (1994). Structural damage detection of space truss structures using best achievable eigenvectors. *AIAA Journal*, *32*(5), 1049-1057. doi:10.2514/3.12093

Lingmi Zhang, Rune Brincker and Palle Andersen.(2002). "An Unified Approach For Two -Stage Time Domain Modal Identification",
Liu, Pei-Ling, and Chian, chung-chi (1997). Parametric identification of truss structures using static strain. *Journal of Structural Engineering, ASCE*, 123(7):927-933.

Luber, W. (1997). Structural damage localization using optimization method. In Anon (Ed.), *Proceedings of the International Modal Analysis Conference IMAC* (pp. 1088-1095). SEM, Bethel, CT, United States.

Maeck, J., and De Roeck, G. (1999). Dynamic bending and torsion stiffness derivation from modal curvatures and torsion rates. *Journal of Sound and Vibration, 225*(1), 153-170. doi:10.1006/jsvi.1999.2228

Maia, N. M. M., Silva, J. M. M., and Almas, E. A. M. (2003). Damage Detection in Structures: From Mode Shape To Frequency Response Function Methods. 196 Bibliography

Maia, N. M. M., Silva, J. M. M., and Sampaio, R. P. C. (1997). Localization of damage using curvature of the frequency-response-functions. In Anon (Ed.), *Proceedings of the International Modal Analysis Conference (IMAC)* (Vol. 1, pp. 942-946). SEM, Bethel, CT, United States.

Maia, N.M.M., Silva,J.M.M., Almas, E.A.M. and Sampaio,R.P.C. (2003). " Damage detection in structures :from mode shape to frequency response function methods" *Mech. Sys. Signal Processing*, 17(3), 489-498

Mares, C., Mottershead, J. E., and Friswell, M. I. (1999). Damage location in beams by using rigid-body constraints. *Proceedings of the DAMAS 99, Damage Assessment of Structures.* (Vol. 167–168, pp. 381-390). Dublin, Ireland: Trans Tech Publications, Switzerland.

Messina, A., Williams, E. J., and Contursi, T. (1998). Structural Damage Detection by A Sensitivity and Statistical-Based Method. *Journal of Sound and Vibration, 216*(5), 791-808. doi:10.1006/jsvi.1998.1728

Moller N., Brincker R., Herlufsen H. and Andersen P. (2001) .*Modal Testing of Mechanical Structures Subject to Operational Excitation Forces.*

Muthumani, K., Lakshmanan, N., Gopalakrishnan N., Sathishkumar, K., Sreekala, R. and Rao G.V.Rama (2010). Damage Identification of Beam-Like Structure through Static Defection and Natural Frequency as Damage Indicators. *Indo-U.S Forensic Engineering Workshops, ASCE.*

Ndambi, J. M., Vantomme, J., and Harri, K. (2002). Damage assessment in reinforced concrete beams using eigenfrequencies and mode shape derivatives. *Engineering Structures, 24*(4), 501-515. doi:10.1016/S0141-0296(01)00117-1

Oh, B. H. and Jung, B. S. (1998). "Structural damage assessment with combined data of static and modal test", *J. Struct. Engrg. ASCE,* 124(8), 0956-0965.

P.H. Kirkegaard, P.Anderson and R. Brincker.(1997)"Structural Time Domain Identification (STDI) Toolbox for use with Matlab", *Department of Building Technology and Structural Engineering Aalborg University,*

Pandey, A. K., and Biswas, M. (1994). Damage detection in structures using changes in flexibility. *Journal of Sound and Vibration*, *169*(1), 3-17. doi:10.1006/jsvi.1994.1002

Pandey, A. K., and Biswas, M. (1995). Experimental verification of flexibility difference method for locating damage in structures. *Journal of Sound and Vibration*, *184*(2), 311-328. doi:10.1006/jsvi.1995.0319

Pandey, A. K., Biswas, M., and Samman, M. M. (1991). Damage detection from changes in curvature mode shapes. *Journal of Sound and Vibration*, *145*(2), 321-332. doi:10.1016/0022-460X(91)90595-B Bibliography 197

Park, S. Y., Stubbs, N., Bolton, R., Choi, S. H., and Sikorsky, C. (2001). Field verification of the damage index method in a concrete box-girder bridge via visual inspection. *Computer-Aided Civil and Infrastructure Engineering*, *16*(1), 58-70. doi:10.1111/0885-9507.00213

Parloo, E., Guillaume, P., and Van Overmeire, M. (2003). Damage Assessment Using Mode Shape Sensitivities. *Mechanical Systems and Signal Processing*, *17*(3), 499-518. doi:10.1006/mssp.2001.1429

Paul J. Fanning and E. Peter Carden "Experimentally Validated Added Mass Identification Algorithm Based on Frequency Response Functions", *Journal of Engineering Mechanics*., 2004, 130(9): 1045-1051

Perera, R., Ruiz, A., and Manzano, C. (2009). Performance assessment of multicriteria damage identification genetic algorithms. *Computers and Structures*, *87*(1-2), 120-127. doi:DOI: 10.1016/j.compstruc.2008.07.003

Pothisiri, T., and Hjelmstad, K. D. (2003). Structural damage detection and assessment from modal response. *Journal of Engineering Mechanics*, *129*(2), 135-145. American Society of Civil Engineers. doi:10.1061/(ASCE)0733- 9399(2003)129:2(135)

Qiao, P., Lu, K., Lestari, W., and Wang, J. L. (2007). Curvature mode shape-based damage detection in composite laminated plates. *Composite Structures*, *80*(3), 409-428. doi:10.1016/j.compstruct.2006.05.026

R.B.Randall, G. Zurita and T. Wardrop ," Extraction of Modal Parameters from Response Measurements" , *Investigation and Desarrollo ,* No. 4:5 – 12(2004) ISSN 1814-6333, 2004

R.Brincker and Palle Andersen, "A Way of Getting Scaled Mode Shapes in Output Only Modal Testing"

R.Brincker, A. De Stefano and B.Piombo , "Ambient Data to Analyse the Dynamic Behaviour of Bridges: A First Comparison Between Different Techniques", 1996

R.Brincker, L. Zhang and Palle Andersen " Modal Identification from Ambient Responses using Frequency Domain Decomposition"

R.Brincker, L. Zhang, Palle Andersen " Output-Only Modal Analysis by Frequency Domain Decomposition" , *Proceedings of ISMA* 25, 2000 – Volume 2, 2000

R.Brincker, Palle Andersen, R. Cantieni,(2001) "Identification and Level 1 Damage Detection of the Z24 Highway Bridge by Frequency Domain Decomposition",
Rahai, A., Bakhtiari-Nejad, F., and Esfandiari, A. (2006). Damage Assessment of Structure using Incomplete Measured Mode Shapes. *Structural Control and Health Monitoring, 14*(5), 808-829. doi:10.1002/stc.183

Ratcliffe, C. P. (1997). Damage Detection Using a Modified Laplacian Operator on Mode Shape Data. *Journal of Sound and Vibration, 204*(3), 505-517. doi:10.1006/jsvi.1997.0961

100 Reich, G. W., and Park, K. C. (2000). Experimental application of a structural health monitoring methodology. *Proceedings of SPIE - The International Society for* 198 Bibliography *Optical Engineering, 3988*, 143-153. Newport Beach, CA, USA: Society of Photo-Optical Instrumentation Engineers, Bellingham, WA, USA. doi:10.1117/12.383135

Reza, D., Nayeri.,Tasbihgoo,F.,Wahbeh,M.,Caffrey,J.P.,Masri,S.F.,Conte,J.P. and Elgamal,A. "Study of Time-Domain Techniques for Modal Parameter Identification of a Long Suspension Bridge with Dense Sensor Arrays", *Journal of Engineering Mechanics*, 2009, 135(7): 669-683

Ruotolo, R. and Surace, C. (1997). "Damage assessment of multiple cracked beams: Numerical and experimental validation", J.Sound Vib, 206(4), 567-588.

Rytter A. (1993). *Vibration based inspection of civil engineering structures. Department of Building Technology and Structural Engineering*. University of Aalborg, Denmark, Aalborg.

Sampaio, R. P. C., Maia, N. M. M., and Silva, J. M. M. (1999). Damage Detection Using the Frequency-Response-Function Curvature Method. *Journal of Sound and Vibration, 226*(5), 1029-1042. doi:10.1006/jsvi.1999.2340

Sanayei, Masoud, Bell, Erin Santini and Javdekar, Chitra N. (2005). Bridge Deck Finite Element Model Updating using Multi-Response NDT data. *Structures Congress, ASCE.*

Sanayei, Masoud. and J. Saletnik, Michael. (1996*).* Parameter estimation of structures from static strain measurements. II: Error sensitivity analysis. *Journal Structural Engineering, 122(5): 563-572.*

Sanayei, Masoud., Imbaro., Gregory, R., McClain., Jennifer, A.S. and Brown, Linfield C. (1997), " Structural Model Updating Using Experimental Static Measurements", *Journal Of Structural Engineering, ASCE, 123(6):792798.*

Sanayei, Masoud , Onepede , O. (1991), "Damage assessment of structures using static test data", *AIAA Journal*, 29, 1174-1179.

Sau-Lon James Hu, Ping Li, Harold T. Vincent and Huajun Li, "Modal Parameter Estimation for Jacket-Type Platforms Using Free-Vibration Data", *Journal of Waterway, Port, Coastal, and Ocean Engineering*, 2011, 137(5): 234-245

Sazonov, E. S., Klinkhachorn, P., GangaRao, H. V. S., and Halabe, U. B. (2003). Non- Baseline Damage Detection from Changes in Strain Energy Mode Shapes Experiments on Armored Vehicle Launched Bridge. *Proceedings of 29th Annual Review of Progress in Quantitative Nondestructive Evaluation (QNDE)* (pp. 1415-1422). Bellingham, WA. doi:10.1063/1.1570297

Shama, A. A., Mander, J. B., Chen, S. S., and Aref, A. J. (2001). Ambient vibration and seismic evaluation of a cantilever truss bridge. *Engineering Structures*, *23*(10), 1281-1292. doi:10.1016/S0141-0296(01)00027-X

Shi, Z. Y., Law, S. S., and Zhang, L. M. (1998). Structural Damage Localization from Modal Strain Energy Change. *Journal of Sound and Vibration*, *218*(5), 825-844. doi:10.1006/jsvi.1998.1878

Shi, Z. Y., Law, S. S., and Zhang, L. M. (2000). Damage Localization by Directly Using Incomplete Mode Shapes. *Journal of Engineering Mechanics*, *126*(6), 656-660. doi:10.1061/(ASCE)0733-9399(2000)126:6(656)

Skjaerbaek, P. S., Nielsen, S. R. K., and Çakmak, A. Ş . (1996). Identification of damage in reinforced concrete structures from earthquake records – optimal location of sensors. *Soil Dynamics and Earthquake*, *15*(6), 347-358. doi:10.1016/0267-7261(96)00018-8

Staszewski, W. J. (1998). "Structural and Mechanical Damage Detection using Wavelets", *The Shock and Vibration Digest*, 36(6), 457-472

Stubbs, N., Kim, J. T., and Topole, K. (1992). An efficient and robust algorithm for damage location in offshore platforms. *Proceedings of the ASCE 10th Structures Congress* (pp. 543-546).

Tee, A. B., Bowman, M. D. and Sinha, K. C. (1990). "Application of fuzzy logic to condition assessment of concrete slab bridges", *Transportation Research Record* 1184, 22-30

Tomaszewska, A. (2010). Influence of statistical errors on damage detection based on structural flexibility and mode shape curvature. *Computers and Structures*, *88*(3- 4), 154-164. doi:10.1016/j.compstruc.2009.08.017

Tsai, T., Yang, J. C. S., and Chen, R. Z. (1985). Detection of damages in structures by the cross random decrement method. *Proceedings of the International Modal Analysis Conference Exhibit* (Vol. 2, pp. 691-700).

Vandiver, J. K., and Hole, W. (1976). Detection of Structural Failure on Fixed Platforms By Measurement of Dynamic Response. *Proceedings of 1976 Offshore Technology Conference* (p. 10). Houston, TX: Offshore Technology Conference.

Wang, J. Y., Ko, J. M., and Ni, Y. Q. (2000). Modal sensitivity analysis of Tsing Ma Bridge for structural damage detection. *Proceedings of SPIE - The International Society for Optical Engineering: Nondestructive Evaluation of Highways, Utilities, and Pipelines IV* (Vol. 3995, pp. 300-311). Newport Beach, CA, USA: Society of Photo-Optical Instrumentation Engineers, Bellingham, WA, USA.

Wang, L., Chan, T. H. T., Thambiratnam, D. P., and Tan, A. C. C. (2010b). Improved correlation-based modal strain energy method for global damage detection of truss bridge structures. In J. R. Zhang and C. S. Cai (Eds.), *Proceedings of the International Symposium on Life-Cycle Performance of Bridge and Structures* (pp. 145-154). Changsha, China: Science Press (China).

Wang, X., Hu, N., Fukunaga, H., and Yao, Z. H. (2001). Structural damage identification using static test data and changes in frequencies. *Engineering Structures*, *23*(6), 610-621. doi:10.1016/S0141-0296(00)00086-9

Wen, C. M., Hung, S. L., Huang, C. S., and Jan, J. C. (2007). Unsupervised fuzzy neural networks for damage detection of structures. *Structural Control and Health Monitoring*, *14*(1), 144-161. doi:10.1002/stc.116

West, W. M. (1984). Illustration of the use of modal assurance criterion to detect structural changes in an orbiter test specimen. *Proceedings of the Air Force Conference on Aircraft Structural Integrity* (pp. 1-6). Los Angles.

Williams, C., and Salawu, O. S. (1997). Damping as a damage indication parameter. (Anon, Ed.)*Proceedings of the International Modal Analysis Conference (IMAC) (SPIE Vol. 3089)*. SEM, Bethel, CT, United States.

Wolff, T., and Richardson, M. (1989). Fault Detection in Structures from Changes in their Modal Parameters. *Proceedings of the 7th International Modal Analysis Conference (IMAC)* (pp. 87-94). Las Vegas, NV, USA. 202

Worden, K. (1997). Structural Fault Detection Using a Novelty Measure. *Journal of Sound and Vibration*, *201*(1), 85-101. doi:10.1006/jsvi.1996.0747

Wu, X., Ghaboussi, J., and Garret, J. H. (1992). Use of Neural Networks in Detection of Structural Damage. *Computers and Structures* (Vol. 42, pp. 649-659). doi:10.1016/0045-7949(92)90132-J

Wu, Z. S., and Xu, Z. D. (2006). Acceleration Response Energy Method for Damage Identification of Bridge Structures (pp. 689-690). Porto, Portugal: Taylor and Francis/Balkema.

Xingyu Song, Hongwei Ma, Kun Wang , " A new Developed Modal Parameter Identification Method Based on Empirical Mode Decomposition and Natural Excitation Technique", *Procedia Engineering* ,199 (2017) 1020–1025, 2017

Xu, H., and Humar, J. (2005). Application of artificial neural networks in vibration based damage detection. In P. J. Shull, A. L. Gyekenyesi, and A. A. Mufti (Eds.), *Proceedings of the SPIE, Volume 5767* (1st ed., Vol. 5767, pp. 120-131). USA: SPIE-Int. Soc. Opt. Eng. doi:10.1117/12.597758

Xu, H., and Humar, J. (2006). Damage detection in a girder bridge by artificial neural network technique. *Computer-Aided Civil and Infrastructure Engineering*, *21*(6), 450-464. Malden, MA 02148, United States: Blackwell Publishing Inc.

Xu, Z. D., and Wu, Z. S. (2007). Energy damage detection strategy based on acceleration responses for long-span bridge structures. *Engineering Structures*, *29*(4), 609-617. doi:10.1016/j.engstruct.2006.06.004

Yan, A.-M., Kerschen, G., Boe, P. D. and Golinval, J.-C. (2005). "Structural damage diagnosis under varying environmental conditions – Part II: Local PCA for nonlinear cases", *Mech. Sys. Signal. Processing*, 19, 865-880.

Yeo, Inho, Shin, Soobong, Sung. Lee, Hea and Chang, Sung-Pil (2000). "Statistical Damage Assessment of Framed Structures from Static Responses". *Journal of Engineering Mechanics, ASCE, 126(4):414-421.*

Yoon, M. K., Heider, D., Gillespie, J. W., Ratcliffe, C. P., and Crane, R. M. (2009). Local Damage Detection with the Global Fitting Method Using Mode Shape Data in Notched Beams. *Journal of Nondestructive Evaluation*, *28*(2), 63-74. doi:10.1007/s10921-009-0048-6 Bibliography 203

Yoon, M. K., Heider, D., Gillespie, J. W., Ratcliffe, C. P., and Crane, R. M. (2010). Local Damage Detection with the Global Fitting Method Using Operating Deflection Shape Data. *Journal of Nondestructive Evaluation*, *29*(1), 25-37. doi:10.1007/s10921-010-0062-8

Zabel, V. (2005). "An application of discrete wavelet analysis and correction coefficient to parametric system identification", *Struct. Health Monitoring*, 4(1), 0005-0018.

Zang, C., and Imregun, M. (2001). Structural Damage Detection using Artificial Neural Networks and Measured FRF Data Reduced via Principal Component Projection. *Journal of Sound and Vibration*, *242*(5), 813-827. doi:10.1006/jsvi.2000.3390

Zapico, J. L., Worden, K., and Molina, F. J. (2001). Vibration-based damage assessment in steel frames using neural networks. *Smart Materials Structures*, *10*(3), 553-559. doi:10.1088/0964-1726/10/3/319

Zhang, U. K., and Kumar, A. V. (2011). Inverse Method for Estimating Resistivity of Carbon Fiber Composite Structures. *Journal of Engineering Materials and Technology*, *133*(1), 011009-1 - 011009-6. doi:10.1115/1.4002627